

**Investigation of the function and control of Dia2, a regulator of
genomic stability in budding yeast**

A DISSERTATION
SUBMITTED TO THE FACULTY OF THE GRADUATE SCHOOL
OF THE UNIVERSITY OF MINNESOTA
BY

Andrew Craig Kile

IN PARTIAL FULFILLMENT OF THE REQUIREMENTS
FOR THE DEGREE OF
DOCTOR OF PHILOSOPHY

Deanna M. Koepp, Ph.D.
Advisor

November 2009

© Andrew Craig Kile 2009

Acknowledgements

I would first like to thank Deanna for welcoming me into her lab as one of her first graduate students. In establishing a new laboratory, she has invested a significant amount of trust in me as a person and a scientist, and I am grateful for the opportunity. I am very appreciative of the flexibility I have been afforded in my graduate projects, as well as the guidance and encouragement for me to think critically. I am truly a better scientist because of it. The members of the Koepp lab have also made it my home for many years, and I have enjoyed their company and scientific insight.

The greater yeast community during my studies has continually been very helpful. They have always been willing to share reagents, equipment, and wisdom.

I would also like to acknowledge my friends and family. Their unwavering support has been instrumental during my graduate career. They are truly a great resource.

The following individuals for help providing reagents, technical assistance, insightful discussion, or critical review of manuscripts for publication:

Anja Katrin-Bielinsky – University of Minnesota
Rodney Rothstein - Columbia University
Mike Tyers - University of Toronto
Steve Elledge - Harvard Medical School
Wade Harper - Harvard Medical School
Ed Hurt - University of Heidelberg
Jun Qin - Baylor College of Medicine
Françoise Stutz - University of Geneva
Christine Guthrie – UCSF
Yolanda Sanchez – Dartmouth Medical School

Individual contributions to experimental data in Chapters II-IV are indicated in the section “List of Experimental Contributions through Chapters II-IV”

Abstract

Maintenance of genomic integrity can be particularly challenged during DNA replication, which is critical for cellular viability and proliferation. Cancer cells exhibit loss of genomic integrity, thus it is critical to understand the pathways involved in genome maintenance. We have identified the F-box protein Dia2 as a novel and previously unappreciated mediator of genome stability. F-box proteins are substrate specificity subunits of SCF ubiquitin ligases for ubiquitin mediated proteolysis, although most remain uncharacterized in their function or targets. Deletion of the *DIA2* gene in *Saccharomyces cerevisiae* leads to genomic integrity defects, and the Dia2 protein associates with chromatin and origins of replication, indicating it performs a chromatin-associated role in DNA replication. Interestingly, the Yra1 protein was identified to physically interact with Dia2 and promotes Dia2 binding to replication origins yet is not a proteolytic substrate of SCF^{Dia2}. The Dia2 protein itself is subject to proteolysis, but is stabilized by the activation of the replication checkpoint and this suggests it plays a role during periods of replication stress and DNA damage during S phase. Surprisingly, Dia2 turnover is not controlled by an autocatalytic mechanism involving its F-box domain, but instead relies on a region upstream of its F-box that controls both its stability and nuclear localization. Replication checkpoint activation leads to inhibition of late-firing origins, stabilization of replication forks, as well as stabilization of the Dia2 protein. Our observations indicate that SCF^{Dia2} activity performs ubiquitin ligase activity at one or both of these sites that are regulated by the checkpoint. These studies establish a novel link between DNA replication and genomic integrity to the SCF ubiquitin ligase via Dia2.

TABLE OF CONTENTS

Acknowledgements	i
Abstract	ii
Table of Contents	iii
List of Tables	v
List of Figures	vi
List of Abbreviations	ix
List of Experimental Contributions through Chapters II-IV	xi
Chapter I: Introduction to DNA replication, Genome Maintenance, and the SCF Pathway for Protein Ubiquitination	1
Molecular components of DNA replication	3
The S-phase checkpoint	11
The Ubiquitin-Proteasome System and SCF Ubiquitin Ligases	18
Chapter II: The F-box protein regulates DNA replication	37
Chapter Summary	37
Chapter Introduction	38
Materials and Methods	40
Results	43
Discussion	51
Supplemental Material	70
Chapter III: Yra1 is required for S phase entry and affects Dia2 binding to replication origins	74
Chapter Summary	74
Chapter Introduction	75
Materials and Methods	78
Results	85
Discussion	94

Chapter IV: Activation of the S phase checkpoint inhibits degradation of the F-box protein Dia2	118
Chapter Summary	118
Chapter Introduction	119
Materials and Methods	122
Results	126
Discussion	135
Supplemental Material	155
Chapter V: Summary and Discussion	159
Bibliography	171
Appendix	
Reprint Permissions	185

LIST OF TABLES

Chapter II:	The F-box protein Dia2 regulates DNA replication	
	Table 1: Strains used in this study	54
	Table 2: The <i>dia2</i> mutant interacts genetically with checkpoint mutants	55
	Supplemental Table 1: Primers used in this study	71
Chapter III:	Yra1 is required for S phase entry and affects Dia2 binding to replication origins	
	Table 1: Strains used in this study	99-100
	Table 2: Primers used in this study	101
Chapter IV:	Activation of the S phase checkpoint inhibits degradation of the F-box protein Dia2	
	Table 1: Strains used in this study	137
	Table 2: Plasmids used in this study	138
	Table 3: Oligonucleotides used in this study	139

LIST OF FIGURES

Chapter I:	Introduction to DNA replication, Genome Maintenance, and the SCF Pathway for Protein Ubiquitination	
	Figure 1: Illustration of proteins and steps involved in DNA replication	31
	Figure 2: The replication and DNA damage checkpoint pathway	33
	Figure 3: The SCF pathway in protein ubiquitination	35
Chapter II:	The F-box protein regulates DNA replication	
	Figure 1: Dia2 is an F-box protein required for normal growth	56
	Figure 2: The <i>dia2</i> mutant exhibits S-phase defect	58
	Figure 3: The <i>dia2</i> Δ F-box mutant exhibits growth and S-phase defects	60
	Figure 4: The Dia2 protein binds replication origins	62
	Figure 5: <i>dia2</i> mutants are hypersensitive to DNA damage	64
	Figure 6: The <i>dia2</i> mutant accumulates Rad52-YFP foci	66
	Figure 7: Deletion of <i>CLB5</i> and <i>CLB6</i> alleviates the premature S-phase in <i>dia2</i> cells and leads to decreased S-phase damage	68
	Supplemental Figure S1: The 18Xmyc-tagged Dia2 allele is functional	72
	Supplemental Figure S2: Overexpression of <i>CLB5</i> and <i>CLB6</i> is toxic to <i>dia2</i> cells	73
	Supplemental Figure S3: Skp1 associates with <i>ARS603</i> in nocodazole-arrested cells	73

Chapter III: Yra1 is required for S phase entry and affects Dia2 binding to replication origins	
Figure 1: Dia2 binds Yra1	102
Figure 2: Dia2 interacts genetically with Yra1	104
Figure 3: Yra1 and Dia2 associate with chromatin	106
Figure 4: Yra1 associates with replication origins	108
Figure 5: Yra1 interacts with Hys2	110
Figure 6: <i>yra1</i> mutants are defective for S phase entry	112
Figure 7: <i>sub2</i> mutants are competent in S phase entry	114
Figure 8: Binding to Yra1 is important for Dia2 origin Association	116
Chapter IV: Activation of the S phase checkpoint inhibits degradation of the F-box protein Dia2	
Figure 1: Dia2 ^{Myc} protein abundance fluctuates throughout the cell cycle	140
Figure 2: Analysis of Dia2 mutants	143
Figure 3: Dia2 protein turnover is not controlled by the SCF pathway	145
Figure 4: Dia2 degradation requires an NLS-containing domain	147
Figure 5: An N-terminal domain required for Dia2 protein turnover overlaps the NLS region	149
Figure 6: Checkpoint proteins inhibit Dia2 turnover in response to replication stress	151
Figure 7: Model for S-phase checkpoint regulation of Dia2	153
Supplemental Figure S1: <i>9MYC-DIA2</i> behaves as wildtype	155
Supplemental Figure S2: The SCF substrate Sic1 is stabilized in SCF mutants	157

Supplemental Figure S3: During G1, Dia2 shows turnover rates comparable to wildtype in checkpoint mutants

158

LIST OF ABBREVIATIONS

α F = alpha-factor pheromone peptide
APC = Anaphase Promoting Complex
ARS = Autonomously Replicating Sequence
ATP = Adenosine Triphosphate
ATR = ATM and Rad3-related
Bp = Base pairs
Cdc = Cell Division Cycle
CDK = Cyclin-Dependent Kinase
ChIP = Chromatin Immunoprecipitation
Chk = Checkpoint
CHX = Cycloheximide
Clb = Cyclin B
Cln = Cyclin
CRL = Cullin-RING ubiquitin Ligase
Cul = Cullin
DAPI = 4',6'-diamidino-2-phenylindole
DIA = Digs Into Agar
DNA = Deoxyribonucleic Acid
dNTP = deoxyribonucleotide triphosphate
DSB = Double Strand Break
dsDNA = Double Stranded DNA
FACS = Fluorescence Activated Cell Sorting
Fbx = F-box Protein
FITC = Fluorescein Isothiocyanate
G1 = Gap Phase 1
G2 = Gap Phase 2
Grr = Glucose Repression Resistant
HU = Hydroxyurea
IP = Immunoprecipitation
LRR = Leucine-rich Repeat
M = Mitosis
Mcm = Minichromosome Maintenance
Mdm = Mitochondrial Distribution and Morphology
Mec = Mitosis Entry Checkpoint
MET = Methionine Requiring
MMS = Methyl Methanesulfonate
MRC = Mediator of Replication Checkpoint
Nedd8 = Neural precursor cell-expressed developmentally down-regulated
NLS = Nuclear Localization Signal
Noc = Nocodazole
ORC = Origin of Replication Complex
PCNA = Proliferating Cell Nuclear Antigen
PCR = Polymerase Chain Reaction

Pof = Pombe F-box
Pol = Polymerase
Pre-RC = Pre-replicative Complex
Psf = Partner of Sld Five
RFC = Replication Factor C
RPA = Replication Protein A
Rad = Radiation sensitive
Rbx = RING Box
RING = Really Interesting New Gene
RNA = Ribonucleic Acid
Roc = Regulator of Cullins
RT-PCR = Reverse Transcriptase PCR
Rub = Regulator of ubiquitination
S = Synthesis
SCF = Skp1, Cdc53/Cul1/F-box
Skp = Suppressor/Subunit of Kinetochoe Protein mutant
Sld = Synthetically lethal with Dpb11
ssDNA = Single Stranded DNA
SDS-PAGE = Sodium Dodecyl Sulfate Polyacrylamide Gel Electrophoresis
TCA = Trichloroacetic Acid
TPR = Tetratricopeptide-repeat
UV = Ultraviolet
WCE = Whole Cell Extract
WT = Wildtype
YFP = Yellow Fluorescent Protein
YRA = Yeast RNA Annealing Protein

LIST OF EXPERIMENTAL CONTRIBUTIONS IN CHAPTERS II-IV

Chapter II: The F-box protein regulates DNA replication

- **Figure 1 A,B,D:** Dia2 assembles with SCF components in yeast cells. **D. Koeppe** generated data and figure.
- **Figure 1C:** Dia2 assembles with SCF components in yeast cells. **A. Kile** generated data and figure.
- **Figure 2A and 2C:** The *dia2* mutant enters S phase earlier than WT. **D. Koeppe** plated cells onto media and collected and calculated budding indexes
- **Figure 2B:** The *dia2* mutant enters S phase earlier than WT. **A. Kile** Generated flow cytometry data, figure, and calculated S-phase percentages.
- **Figure 3A and 3C:** The Δ F-box mutant enters S phase earlier than WT. **D. Koeppe** plated cells onto media and collected and calculated budding indexes
- **Figure 3B:** The Δ F-box mutant enters S phase earlier than WT. **A. Kile** Generated flow cytometry data, figure, and calculated S-phase percentages.
- **Figure 4:** The Dia2 protein binds replication origins: **D. Koeppe, S. Swaminathan,** and **V. Rodriguez-Rivera** performed experiments.
- **Table 2:** The *dia2* mutant interacts genetically with checkpoint mutants. **D. Koeppe** performed experimental analysis.
- **Figure 5:** *dia2* mutants are hypersensitive to DNA damage. **D. Koeppe** performed experiments.
- **Figure 6:** The *dia2* mutant accumulates Rad52-YFP foci. **D. Koeppe** performed experiments and calculated percentages.
- **Figure 7:** Deletion of *CLB5* and *CLB6* alleviates the premature S-phase in *dia2* cells and leads to decreased S-phase damage. **D. Koeppe** performed experiments and analysis.
- **Figure S1B:** Expression of the 18Xmyc-tagged Dia2 protein. **A. Kile** Generated data and figure.
- **Figure S1C:** The Dia2 F-box deletion mutant does not bind Skp1. **A. Kile** Generated 18xM- Δ F strain, data, and figure.

Chapter III: Yra1 is required for S phase entry and affects Dia2 binding to replication origins

- **Figure 1:** Yra1 is a stable protein, and its stability is unchanged in *dia2* Δ cells. A) **D. Koeppe** carried out biochemical procedure and protein identification B,C,E) **S. Swaminathan** performed experiments. D) **A. Kile** and **S. Swaminathan** contributed equally to experimental data.
- **Figure 2:** Dia2 interacts genetically with Yra1. B) **D. Koeppe** generated strains and tested genetic interactions. C) **A. Kile** generated strains and tested overexpression.
- **Figure 3:** Yra1 and Dia2 associate with chromatin. 1) **S. Swaminathan** performed histone association assay. B) **A. Kile** generated strain and carried out chromatin

fractionation assay.

- **Figure 4:** Yra1 associates with replication origins. A-D) **S. Swaminathan** carried out chromatin immunoprecipitation experiments. C) **A. Kile** helped in quantifying *RPL8B* abundance.
- **Figure 5:** Yra1 interacts with Hys2. A-C) **D. Koepp** and **S. Swaminathan** generated experimental data.
- **Figure 6:** *yra1* mutants are defective for S phase entry. A and B) **D. Koepp** and **A. Kile** performed experiments and flow cytometry.
- **Figure 7:** *sub2* mutants are competent in S phase entry. A) **A. Kile** generated strains and carried out experiment. B and C) **D. Koepp** and **A. Kile** performed experiments and flow cytometry.
- **Figure 8:** Binding to Yra1 is important for Dia2 origin association. A-C) **S. Swaminathan** performed all immunoprecipitation and chromatin-immunoprecipitation experiments.

Chapter IV: Activation of the S phase checkpoint inhibits degradation of the F-box protein Dia2

- **A. Kile** Constructed all 9myc-tagged Dia2 strains and plasmids, performed all experiments, generated data and figures.
- **D. Koepp** helped with image presentation of stability quantification present in figures.

CHAPTER I

**Introduction to DNA replication, Genome Maintenance,
and
the SCF Pathway for Protein Ubiquitination**

Accurate DNA replication

All organisms begin life as a single cell. To mature into an adult or propagate the species, that cell must duplicate itself and its genome. This process is called mitotic cell division, and is highly ordered to ensure that each resulting daughter cell resembles that of the parent cell with equivalent genetic content. In eukaryotes from yeast to human, the mitotic cell cycle is composed of distinct and conserved linear stages; Gap Phase 1 (G1), where the cell synthesizes organelles and prepares for the cell cycle; Synthesis Phase (S), the stage in which the critical events of DNA replication occur; Gap Phase 2 (G2), where further cell growth occurs and prepares for division; and finally Mitosis (M), where the replicated chromosomes are condensed, aligned, and separated followed by cytokinesis, the physical division of the cell into equal daughter cells.

Duplication and faithful segregation of the genome occur in Synthesis Phase (S) and Mitosis (M) of the Cell Division Cycle, respectively. Numerous molecular pathways control the linear, unidirectional, and accurate progression through S phase, as well as monitor problems that may occur (17, 112, 123). The critical process of DNA replication is perhaps the most genetically vulnerable time of cellular life. Loss of genome maintenance occurs by accumulation of mutations, chromosomal rearrangements, double stranded breaks (DSBs) or abnormal gain or loss of genetic material (34, 60). During DNA replication, these problems can occur more readily due to the inherent risks of manipulation of DNA during duplication of the genome. Fortunately, DNA replication has evolved to be highly regulated and monitored to promote genomic integrity, which is essential to the organism. However, flaws in proper genome duplication, segregation, or control of genome integrity can lead to developmental defects and disease such as cancer

(60, 123). By investigating the molecular pathways that function during such critical processes, it is possible to gain insight into how such disease states arise. Utilizing the model organism *S. cerevisiae* can elucidate the pathways that control DNA replication and genome maintenance.

Molecular Components of DNA Replication

Replication Origin Licensing

DNA replication is initiated from many origins of replication distributed throughout the chromosomes. In *S. cerevisiae*, conserved ARS elements (Autonomously Replicating Sequences) have been identified as fulfilling this purpose. These sequences were initially found by their ability to promote replication of plasmid DNA in *cis*, and indicate defined eukaryotic origins of replication (11, 21). Although these ARS sequences promote DNA replication and plasmid retention, at the time it was unclear how they were recognized. Later experiments showed ARS elements are recognized and bound by a complex of conserved Orc1-Orc6 (Origin of Replication Complex) proteins (13, 152).

The ORC complex appears to constitutively bind ARS elements throughout the *S. cerevisiae* cell cycle (5, 12). However, several studies indicate this may not be the case in higher organisms. In *Xenopus* cells, ORC appears to be removed in metaphase as determined by immunofluorescence, and in mammalian cells ORC is also diminished in mitosis (12, 27, 120). ORC promotes the assembly of the pre-RC (pre-Replication Complex) onto origins, which is temporally regulated during late M and early G1 and is

often called “licensing”. Proper formation of the pre-RC at origins is essential for DNA replication to occur.

In addition to ORC, the pre-RC contains Cdc6 (Cell Division Cycle-6) and Cdt1 (Cdc10-dependent Transcript-1), which together recruit the presumptive heterohexamer Mcm2-7 DNA helicase complex (MCM, Figure 1) (17). In all organisms studied, including *S. cerevisiae*, it has been found that pre-RCs only form in late mitosis when the Anaphase Promoting Complex (APC) activity is high, and Clb-CDK (Cyclin-B-Cyclin-Dependent Kinase) is low (12, 152). Consistent with this separation of biochemical states, inactivation of CDK by overexpression of the CDK inhibitor Sic1 during G2 causes pre-RC formation at origin DNA and rereplication (39, 45). Conversely, ectopic mitotic Clb-CDK activity in early G1 is sufficient to inhibit pre-RC assembly (12, 41). Taken together, these suggest that Clb-CDK activity coordinates the separation of pre-RC formation and replication states (12).

Cdc6 is a protein that binds ORC, displays ATPase activity, and is essential for DNA replication and viability in budding yeast (12). The current model suggests that Cdc6 and ORC ATPase activity is responsible for recruitment and loading of the proposed DNA helicase MCM complex (17). Consistent with this, *cdc6* mutants fail to assemble functional pre-RCs leading to the loss of DNA replication in budding yeast, as well as low levels of DNA unwinding (35). One pathway controlling pre-RC assembly in budding yeast is the regulated proteolysis of Cdc6. Measurements of Cdc6 protein abundance during the cell cycle have shown that it is an unstable protein from late G1 to late M phase and governed by SCF^{Cdc4} (44, 135). Upon S-phase entry Clb-CDK phosphorylates Cdc6, which triggers its recognition and destruction in budding yeast. As

mentioned previously, Clb-CDK is absent in late M phase upon activation of the APC ubiquitin ligase, which allows Cdc6 to accumulate and help recruit the Mcm2-7 complex to chromatin-bound ORC. Interestingly, mutants that are stabilized for Cdc6 or Cdc6 overexpression still do not result in rereplication of DNA in a single cell cycle. Pre-RC formation is proposed to be regulated by multiple mechanisms to control origin licensing and firing (12, 122, 152). Many of these appear to be redundant, and controlled centrally by CDK activity (122).

Mcm2-7 proteins act as a complex (MCM) thought to encircle double stranded DNA, and loss of any of the MCM components results in inviability in budding yeast (17, 45). MCM is proposed to be loaded onto DNA at origins facilitated by the activity of ORC and Cdc6, as stated above. *MCM* genes were initially discovered in genetic screens for the maintenance of extrachromosomal plasmids or progression of the cell cycle in *S. cerevisiae* (45, 105, 113, 152). Mcm2-7 proteins were subsequently shown to be a family of related proteins, have ATPase domains, and structurally form a hexameric ring (152). Temperature sensitive *mcm* mutants in budding yeast indicate that loss of MCM activity results in defective replication initiation, as well as elongation (45, 91). Also in support of this genetic evidence, ChIP (chromatin immunoprecipitation) experiments show MCM association with replication origins as well as movement with the replication fork (5, 17). Together, these observations suggest that MCM is required for both replication initiation and elongation activities during S phase for duplication of the genome.

MCM (with Cdt) accumulation in the nucleus in late M phase is also tightly controlled with similar timing of Cdc6 stabilization and dependent on low CDK activity. Free MCM binds with Cdt1 and this interaction is required for nuclear localization of

Mcm proteins and Cdt1 (122, 172). The role of Cdt1 appears to be recruitment of MCM to origins and facilitating loading MCM onto DNA (17, 172). During late M phase, these pre-RC components localize to the nucleus, and are then recruited to chromatin by Cdc6 and ORC (42). Upon the transition to replication at START, Mcm proteins and Cdt1 accumulate in the cytoplasm as S-phase progresses (172). Available evidence indicates that CDK also controls the timing of MCM with Cdt1 localization in the nucleus. *cdc28* temperature sensitive mutants in yeast arrested at G2 show reaccumulation of MCM in the nucleus, and overexpression of the mitotic cyclin Clb2 in G1 display distribution of MCM to the cytoplasm (89, 121). This pattern of pre-RC subunit localization mirrors that of Cdc6 stability, and has been shown to also be dependent on Clb-Cdk kinase activity as well (12, 45). In higher eukaryotes, a protein called Geminin interacts with Cdt1 and inhibits association with MCM, however a Geminin homolog in *S. cerevisiae* has not been identified.

Together, the regulation of pre-RC assembly at replication origins is a process called licensing and is responsible for limiting the potential of replication initiation to only once per S phase (Figure 1). Two states exist; low CDK activity promotes pre-RC formation, whereas high CDK activity leads to replication initiation and disassembly of the pre-RC. The post-RC (ORC) remains until reassembled beginning at the end of mitosis, when Cdk activity is once again low. Redundant mechanisms controlling formation exist, as “firing” of any replication origin more than once per cell cycle can lead to rereplication and abnormal DNA content. Anaphase entry under these situations can lead to a severe loss of genome integrity. Cellular systems that monitor genome integrity during the cell cycle will be discussed in “Checkpoints”. Successful origin

licensing is primed for replication firing, where the activities of replication initiation and elongation take place in S phase.

Replication Initiation and Elongation

For DNA synthesis to occur the MCM helicase must be activated and the “replisome” containing the components of the replication fork are loaded onto DNA (Figure 1) (152). DNA polymerases and many other factors must become associated with the pre-RC to initiate DNA replication. Current evidence suggest these components of the Pre-RC include Sld2/Sld3, Cdc45, Mcm10, polymerase α (Pol α), polymerase ϵ (Pol ϵ), and the GINS complex (54, 90, 152, 200). Assembly of these components onto pre-RCs is dependent on the kinase activity of Clb-CDK as well Cdc7-Dbf4 (also referred to as DDK, Dbf4-dependent Kinase, see below).

At START, CDK and DDK facilitate replication initiation and activation of the replisome. As cells enter S-phase, Clb5 and Clb6 B-type cyclins associate and activate the CDK Cdc28, in *S. cerevisiae* (112). While deletion of either *CLB5*, *CLB6*, or *CLB5 CLB6* together is viable, DNA replication initiation is slowed providing evidence for their role in S-phase. Additionally, *CLB5* mutants show defects in activation of late origins of replication, and Clb5 is regulated by APC-mediated ubiquitination and destruction (68, 156). It is also likely that Clb5 is the preferred cyclin for S-phase CDK activity (119). The other important S-phase kinase DDK is composed of the kinase Cdc7 with its activator Dbf4, and is also regulated by the APC ubiquitin ligase. Not surprisingly, deletions of *CDC7* or *DBF4* are both inviable in *S. cerevisiae* and conditional mutants arrest at replication initiation (57, 62). Interestingly, by ChIP analysis, DDK associates

with origins as they fire, whereas there is little or no evidence of this association with CDK (43, 152). This suggests that DDK associates and controls origins for individual and temporal control during S phase, but CDK is a more global activator of DNA replication.

At START, both Clb-CDK and DDK become active by APC inactivation. Sld2 and Sld3 (Synthetically Lethal with *dpb11-1*) are phosphorylated by CDK, which then recruit the initiation/elongation factors Dpb11 and Cdc45 to origins (Figure 1)(173, 193). This appears to be the essential CDK function in replication initiation, as phosphomimics of Sld2 in the presence of a Dpb11-Sld3 fusion protein OR a special allele of *CDC45* with high-copy Dpb11 bypasses the requirement for CDK activity (173, 193).

DDK phosphorylates several of the MCM subunits, which is also necessary for recruitment and stable association of Cdc45, especially during elongation (152, 154). An allele of *MCM5*, *mcm5-bob1* partially suppresses the critical role for DDK (59, 154). This provides evidence that Mcms are targets of DDK for DNA replication initiation. It was later reported that DDK promotes assembly of a stable MCM-Cdc45 complex on S-phase chromatin (154). Prior to this finding, it was determined that Cdc45 is also an essential protein required for DNA replication, however its exact role continues to be elusive (58, 152). While CDK and DDK are necessary for this assembly, the exact order of kinase function and assembly of these factors have yet to be elucidated, and are likely interdependent. The DNA polymerase Pol ϵ and Dpb11 are both required for each other's association at replication origins, yet Pol ϵ is part of the replisome while Dpb11 is not (152). This indicates that both proteins function at replication initiation, but only Pol ϵ travels with the replication fork and it functions in elongation. Mcm10 was identified

in the same genetic screen as the other MCM genes, it is not homologous to the Mcm2-7 subunits and its exact biochemical function has yet to be determined (105, 113, 152).

Mcm10 has been shown to be required for Cdc45 loading and stabilizing the catalytic Polymerase α (Pol α) subunit, Cdc17 (141). *MCM10* is essential in budding yeast, and inactivation of the Mcm10 protein by the degron system shows parallel destabilization of Cdc17, with defects in replication initiation as well as ongoing fork progression (141, 152). CHIP experiments also indicate Mcm10 protein is found at replication origins and travels with the replication fork. These findings suggest it is necessary for both initiation and elongation processes of DNA replication.

The more recently discovered GINS complex is required for both initiation and progression of the DNA replication fork (73, 87, 90, 170). GINS (Go-Ichi-Ni-San) represent budding yeast Sld5, Psf1, Psf2, and Psf3 and are all essential for viability (170). Additionally, it's been found that conditional *psf1* or *sld5* mutants have reduced efficiency of origin firing even at permissive conditions (170). GINS is recruited to origins and MCM at initiation by Dpb11-Sld2-Sld3-Cdc45 (90, 170). GINS has also been shown to physically interact with MCM, and studies suggest it is required for Dpb11 origin association and vice versa, further indicating the interdependence of initiation events (170). While the exact mechanism and sequence of association have yet to be determined, the overall theme is the collaborative assembly of factors promotes replication initiation and progression of the replisome (90, 152). Successful formation of this initiation complex, which is likely rapid, activates DNA unwinding by the MCM helicase and movement of the replication fork away from origins.

Replication elongation is the coordinated DNA unwinding and synthesis activity provided by the replisome (Figure 1). The MCM helicase is presumed to be responsible for the DNA unwinding ahead of the polymerases. Mcm2-7, Cdc45, Mcm10, GINS, Pol α , and Pol ϵ all move with the replication fork and are part of the replisome, as evidenced by the collection of ChIP data from many research findings (5, 12, 23, 141, 152, 170, 184). Dpb11, Sld2, and Sld3 have not been observed to move with the replication fork, and are considered to be necessary for initiation only (90, 152). Once the replication fork is initiated, DNA unwinding occurs and additional factors associate with the replisome for propagation of the fork. Interestingly, previous *in vitro* experiments of intact MCM alone has failed to show robust DNA unwinding. However, a recently purified *D. melanogaster* GINS-Cdc45-MCM complex exhibits helicase activity, suggesting these proteins function together for DNA unwinding (114).

Different polymerases are thought to be responsible for replicating the leading and lagging DNA strands (Figure 1) (54, 90). The unwinding of DNA by the helicase leads to single stranded DNA, which is coated by RPA proteins (Replication Protein A) (184). Pol α , with the help of the MCM and Cdc45 proteins, is loaded onto RPA-coated ssDNA and then synthesizes a short RNA primer by the Pri2 subunit, which is used for a small amount of DNA synthesis by the Cdc17 subunit (23, 54). Pol α is currently the only known polymerase in *S. cerevisiae* for *de novo* synthesis of DNA, however it is not a processive polymerase (23, 116). The synthesis of DNA leads to the loading of the sliding clamp PCNA (Proliferating Cell Nuclear Antigen) by the RFC (Replication Factor C) clamp loader (23, 54, 184). PCNA then loads Pol δ in place of Pol α and continues as a more processive DNA polymerase that contains proofreading activity (184). Pol δ has

been implicated as the lagging strand polymerase by genetic interaction with other lagging strand proteins (23). This polymerase switch takes place many times on the lagging strand due to the 5'→3' nature of DNA polymerases and results in the production of Okazaki fragments, that are later ligated together by Cdc9 (DNA ligase I in mammals) (54, 184).

On the leading strand of replication fork, Pol ϵ takes over DNA synthesis for processive elongation and is also associated with PCNA. Strong evidence for Pol ϵ as the leading strand polymerase came from determining which DNA strand accumulates mutations using a special active-site Pol ϵ mutant (23, 138). However, complete mutation of the catalytic domain is dispensable for growth in *S. cerevisiae*, and this observation needs to be resolved (23, 78). The 5'→3' uninterrupted synthesis of DNA on the leading strand moves in the direction of DNA unwinding. Replication forks move bidirectionally away from origins of replication. As S phase progresses, replication forks fired from the many origins eventually fuse to end in the complete replication of the genome.

The S-phase checkpoint regulation of DNA replication

Eukaryotic cells have evolved mechanisms to promote the accurate completion of cell cycle events, such as S phase, called checkpoints. The presence of DNA damage by endogenous or exogenous means does not cause a robust G1 arrest or apoptosis in budding yeast as it does in mammalian cells, but induces a system for response to DNA damage and replication stress (61, 123).

Checkpoints are signal transduction pathways that halt or stall progression of the cell cycle with the ultimate goal of maintaining genome integrity (34, 61, 123). S phase is a very genetically susceptible phase of the cell cycle for mutation. Checkpoint activation during replication slows S-phase progression, prevents activation of late-firing origins, stabilizes replication forks, and inhibits anaphase entry (101, 123, 174). Defects in this system leads to a high rate of genomic instability and concomitant decrease in cell viability. In human cells, loss of checkpoints correlate with the loss of stable genomes, a prominent hallmark of cancer cells (60).

S-phase checkpoint: Sensing replication stress

During S-phase, problems with DNA replication by endogenous or exogenous stress lead to activation of the S-phase checkpoint (Figure 2) (18, 20). In this regard, replication stress will be generally used to describe replication fork pausing by intrinsic or extrinsic factors. These may include normal DNA-protein structures that obstruct progression, abnormal DNA structures, DNA damage lesions or DNA adducts, problems with the replisome itself, or replication block by the depletion of dNTP pools.

Strong evidence suggests RPA (Replication Protein A)-coated single-stranded DNA (ssDNA) is the recognized signal for the S-phase checkpoint pathway (20, 60, 61). Several groups have demonstrated that collision of the replication fork with many forms of stress halts fork progression, but the MCM helicase continues to unwind double-stranded DNA resulting in long tracts of unreplicated ssDNA (24, 175). RPA rapidly coats the ssDNA, like normal replication, but with greatly increased lengths. *In vitro*, if DNA replication is inhibited in the presence of replication stress, downstream S-phase

checkpoint signaling does not occur and RPA does not accumulate (102). This indicates that the active process of DNA replication is required to generate ssDNA for RPA association. Similarly, it was found that an RPA allele (*rfa1-t11*) in budding yeast supports replication but is compromised to induce a checkpoint response in the presence of DNA damage (61, 198, 199). These observations indicate that RPA coating of ssDNA is important for checkpoint signaling, and is dependent on DNA unwinding at the site of stress. Not surprisingly, the length of ssDNA (with RPA) correlates with the intensity of checkpoint activation (24, 102, 104). These findings are consistent with the suggestion that “uncoupling” of MCM and the replication fork is caused by replication stress and leads to the accumulation of ssDNA-RPA, recognized as the S-phase checkpoint signal (60).

Independent protein complexes recognize ssDNA-RPA, the 9-1-1 clamp and Mec1-Ddc2, but are thought to work together to activate the S-phase checkpoint (Figure 2). RPA-coated ssDNA adjacent to double stranded DNA is recognized by the “9-1-1” clamp (*S. cerevisiae* Rad17-Mec3-Ddc1) (34, 61, 106, 181, 199). Studies on these proteins indicate they form a heterotrimeric ring structure, similar to PCNA (130). In *Xenopus* extracts, *in vitro* depletion of the 9-1-1 clamp compromises checkpoint activation (103). In budding yeast, evidence indicates that strains deleted for any component of the 9-1-1 complex are viable, but checkpoint signaling is defective, leading to decreased genome integrity and cell viability.

While PCNA is loaded onto DNA with the pentameric RFC complex, Rad24 associated with the Rfc2-5 subunits is required to load the 9-1-1 clamp in response to replication stress (14, 46, 55, 199). Genetically, deletion of *RAD24* in *S. cerevisiae* is

viable, but when exposed to replication stress, cell viability dramatically decreases similar to other checkpoint mutants (47, 61). Biochemically, data indicate that Rad24-RFC interacts with components of 9-1-1 *in vitro* and *in vivo*, and load the clamp on to sites of ssDNA-RPA (61). These data provide evidence that both the 9-1-1 clamp and the clamp loader are required for downstream checkpoint activation. However, what is the 9-1-1 actually required for? Some evidence suggests polymerases and other factors become associated with the 9-1-1 complex to mediate checkpoint functions and coordinate repair (123). This activity is likely to be important, but this role is largely uncharacterized. However, strong evidence supports that its main role is to help recruit and activate Mec1 (Mitosis Entry Checkpoint-1), a central transducer kinase of the checkpoint and a PI3K-like kinase family member (34, 61).

The 9-1-1 complex is critical in the activation of Mec1, the budding yeast homolog of mammalian ATR (Ataxia-Telangiectasia Mutated and Rad3-Related). Mec1 has been found to physically interact with RPA, and *MEC1* deletion strains in yeast are inviable (198). At least part of its essential role in normal growth is regulation of dNTP pools; deletion of an inhibitor of ribonucleotide reductase *SML1* (Suppressor of Mec1 Lethality-1) suppresses this *mec1Δ* lethality [Zhao, 1998]. It was later determined that Mec1 depends on Ddc2 (DNA Damage Checkpoint-2, ATRIP in mammals) for recognition of ssDNA-RPA (22 2003, 126, 145, 185).

Loss of *DDC2* or its homologs in any organism have the same defects as loss of *MEC1* (61, 126). Mec1 and Ddc2 form a complex independent of DNA damage or replication stress, and are now considered obligate partners (34, 61). Mec1-Ddc2 localizes with ssDNA-RPA, independently of the 9-1-1 clamp, but this is not sufficient

for Mec1 activation (19, 34). Indeed, recent observations indicate co-overexpression and co-localization of the 9-1-1 clamp and Ddc2 in *S. cerevisiae* lead to checkpoint activation in the absence of DNA damage or replication stress (19). In summary, the sensor for activation of the S-phase checkpoint (and later the G2/M checkpoint) is ssDNA-RPA that has colocalized the 9-1-1 complex and Mec1-Ddc2 (ATR-ATRIP). Mec1 kinase activation thus transduces the checkpoint signal for cellular responses such as cell cycle progression, maintenance of stalled forks, and coordinating repair.

Checkpoint kinases, downstream effectors, and targets

Upon Mec1 kinase activation, downstream effectors are phosphorylated to coordinate response to DNA damage and replication stress. Recently, several large proteomic screens have identified many Mec1 targets, but most are not yet characterized (111, 115, 161, 164). In budding yeast, one primary target substrate is a central downstream kinase, Rad53 (Radiation sensitive-53, Chk2 in mammalian cells), however in metazoan systems Chk1 is the central downstream substrate for the S-phase checkpoint (61). Nonetheless, it has been found that *RAD53* deletion is lethal for budding yeast cells, however this is suppressed with the *sml1Δ* mutant similar to *mec1Δ* [Zhao, 1998].

Rad53 requires the Rad9 (Radiation sensitive-9) or Mrc1 (Mediator of Replication Checkpoint-1) adaptor proteins for activation. Rad9 is thought to be required to activate Rad53 in response to DNA damage, however, Mrc1 is required to activate Rad53 from stalled replication forks by collision with DNA damage or dNTP depletion (2, 61, 123, 146). In budding yeast, deletion of *RAD9* or *MRC1* is viable, yet Rad53 activation under stress is defective and further supports their role as checkpoint proteins (61, 146). In *mrc1*

deletion mutants in *S. cerevisiae*, upon replication fork stalling by depleting dNTPs, replication forks collapse (77, 101). This evidence suggests that Mrc1 interacts with and stabilizes the replication fork to prevent collapse under conditions of fork stalling (123).

The main downstream activities that Rad53 (or Chk1 in mammals) facilitates are the inhibition of replication initiation at late firing origins, stabilization of stalled replication forks, and inhibition of anaphase entry (Figure 2) (20, 123). Identification of proteins that are targets of Mec1 and Rad53 are underway, and not surprisingly include components of the replication and cell cycle machinery (60). Blocking of late origins likely occurs through Rad53-dependent phosphorylation of Dbf4-Cdc7, required for replication initiation, although the exact mechanism of inhibition remains unclear (152). DDK interacts with and promotes replication initiation at each individual origin, as opposed to the more global role of CDK, and is therefore a point of replication control after replication has already begun (152). However, it has been argued that the most critical function of Rad53 in the S-phase checkpoint is the maintenance of the replication fork to prevent fork collapse; While other checkpoint mutants can recover from fork stalling by HU, *rad53* mutants display irreversible fork collapse and loss of viability (61, 101, 123, 152). Replication fork collapse causes DSBs and recombinagenic structures that cause loss of genome integrity. As previously stated, one response of the S-phase checkpoint is to inhibit anaphase which is another checkpoint that promotes maintenance of the genome.

G2/M DNA damage Checkpoint

Activation of the S-phase checkpoint leads to the G2/M checkpoint to arrest cell cycle progression at the metaphase to anaphase transition. This allows time for the cell to repair and recover from genomic stress prior to the segregation of chromosomes, and is also critical for genome integrity. Segregation of incompletely replicated or damaged DNA is associated with high rates of genome instability (61, 123). The G2/M checkpoint is activated by the same sensing mechanisms and signal transduction pathway as the S-phase checkpoint (34, 61, 123). However, DNA damage post replication or outside of regions of active replication can also trigger the checkpoint, such as DSBs (9, 61, 123).

The principle role of this checkpoint is to arrest the cell at G2/M by inhibiting anaphase entry by maintaining Pds1 abundance (an inhibitor of the separase enzyme that cleaves the cohesin proteins which hold sister chromatids together), like the spindle assembly checkpoint (61). While Rad53 is the main transducer of the S-phase checkpoint response, both Rad53 and Chk1 directly control the cell cycle machinery (146). Pds1 becomes hyperphosphorylated after DNA damage dependent on Chk1, which blocks its ubiquitination by the APC (36). Rad53 also regulates Pds1 stabilization, but instead it is thought that inhibitory phosphorylation of the APC activator Cdc20 prevents APC activation and Pds1 ubiquitination (61, 146 2003). However, the exact mechanism of this has not been elucidated. Rad53 has also been shown to regulate mitotic exit by maintaining CDK activity, likely through inhibition of Cdc5 (30, 146).

Failure of the cell to activate the S-phase checkpoint also results in the loss of the G2/M arrest that follows. Although DNA damage and other forms of replication stress persist, the cell cycle machinery is not halted and transition to anaphase is engaged (61).

The most critical and sensitive events during the cell division cycle are accurate duplication and segregation of the genome. Transmission of mutated and unrepaired genetic material causes high rates of genome instability and thus results in the loss of viability (34, 60, 61). Perturbations in the processes involved in replication, monitoring the state of the genome, or control of the cell cycle machinery are highly deleterious for cellular life.

The Ubiquitin-Proteasome System

One critical mechanism for specific proteolytic control of proteins is known as the ubiquitin-proteasome system (85, 189). It involves the conjugation of a polyubiquitin chain via a cascade of enzymatic reactions to a specific substrate protein, followed by recognition and destruction by the 26S proteasome (see Figure 3 for a diagram of this pathway with SCF as an example E3 ligase) (85, 136, 189). Typically, lysine-48 (K48) linked chains are thought to be the primary chain-topology for targeting to the 26S proteasome, a large and multisubunit protease that recognizes and degrades polyubiquitinated substrates in an ATP-dependent manner (81, 85, 189). Although the minimum K48-linked chain length *in vivo* is not known, *in vitro* four K48-linked ubiquitins are sufficient for degradation (176, 189).

The ubiquitin-proteasome system is highly conserved and exists throughout eukaryotes. However, ubiquitin conjugation to a substrate does not only lead to degradation. Monoubiquitination, multi-monoubiquitination, and polyubiquitin-chains leading to non-proteolytic roles have all been described (29, 64).

Ubiquitin conjugation and the 26S Proteasome

The conserved 76 amino acid protein ubiquitin (approximately 8 kDa), is covalently linked to the ϵ -amino group of lysine residues of a substrate or another ubiquitin molecule (136). This process is called ubiquitination. Ubiquitin is conjugated to the substrate by a sequential cascade of enzymatic reactions, and begins with the E1. The E1 enzyme, also known as the ubiquitin-activating enzyme, forms a thioester linkage with the carboxy-terminal glycine (G76) of ubiquitin in an ATP-dependent reaction. A catalytic cysteine residue within the E1 is responsible for this linkage (136).

In the second step of the cascade, the E2 ubiquitin-conjugating enzyme temporarily accepts the ubiquitin protein from E1 by its catalytic cysteine and thus also forms a thioester intermediate (136). The last and arguably the most pivotal step require the ubiquitin ligase, or E3 (136, 189).

Ubiquitin ligases interact directly with a substrate protein, and therefore provide the primary specificity for the ubiquitin pathway (Figure 3) (85, 136). There is usually only one E1 enzyme in most organisms, but several more E2s. However, E3s represent the most diverse and numerous component of the general ubiquitination pathway (85, 136). This 3-step sequential enzymatic cascade is responsible for all ubiquitin reactions, regardless of the specific fate of the ubiquitinated substrate. While it is thought that one E2 enzyme interacts with one E3 at a time, some E3s have been shown to interact with multiple E2s. This may represent further specificity and designation of ubiquitin chain topology (189). Repetitions of the conjugation pathway can lead to processive

ubiquitination of a substrate (176, 189). A chain of K48-linked ubiquitin can then be recognized for degradation by the 26S proteasome (Figure 3) (176).

The 26S proteasome is a large multisubunit cellular protease that predominantly recognizes and destroys substrates with K48 ubiquitin linkages (81). It is composed of the barrel-shaped 20S catalytic core, and a regulatory 19S “cap” on one or both ends of the 20S core. The enzymatic activity of the proteasome resides in the 20S core, which cleaves proteins into ~15 residue peptides (81, 189). The function of the 19S core is primarily to recognize ubiquitinated proteins and help unfold and channel them into the 20S core for proteolysis. The last step of the ubiquitin pathway is catalyzed by the ubiquitin ligases, which are a very diverse class of enzymes.

The SCF family of ubiquitin ligases

One of the best-characterized and most understood multisubunit E3s is the highly conserved SCF (Skp1, Cdc53/Cul1, F-box) ligase (Figure 3). The SCF ubiquitin ligase plays a fundamental role in regulating the stability of critical proteins involved in cell cycle control (26, 40, 118, 139). Within *S. cerevisiae* the *CDC53*, *CDC34*, and *CDC4* components of SCF complexes were initially discovered through the classic genetic screen that displayed loss of cell division cycle progression (62). Consistent with this classification, temperature-sensitive mutations in these *CDC* (Cell Division Cycle) genes display cell cycle arrest at the G1/S transitions and *CDC53*, *CDC34*, and *CDC4* all encode essential genes required for viability (62, 110, 150). It was later shown that cell cycle arrest is caused by defective ubiquitination and degradation of critical cell cycle

regulators, primarily the B-type cyclin/Cdk inhibitor Sic1 (Substrate Inhibitor of Cyclin-dependent protein kinase-1) at G1/S (7, 110, 150, 192).

The protein Cdc53 (Cell Division Cycle 53) in budding yeast is the rigid Cul1 scaffold of the SCF complex (132, 134). Cdc53/Cul1 recruits the small protein Rbx1 (RING-Box protein 1) by a C-terminal cullin homology (CH) domain (40, 72, 124, 153). Rbx1, the RING subunit, was discovered simultaneously by several groups and was determined to be an essential gene and obligate component of SCF complexes (72, 124, 153). In budding yeast, deletion of *RBX1* is lethal, and omission of Rbx1 protein fails to robustly ubiquitinate substrates such as Sic1 *in vitro* which suggest an important function (72, 124, 153). Rbx1 was shown to dock the only currently recognized E2 enzyme for the SCF, Cdc34 (Cell Division Cycle protein 34), which is responsible for ubiquitination of substrates (134, 153). While Rbx1 associates with Cdc53 at the C-terminus, the adaptor subunit Skp1 interacts at the N-terminal region (40, 134).

The human Skp1 (S-phase Kinase-associated Protein-1) subunit was first isolated from the Cyclin A-Cdk2 (Cyclin-Dependent Kinase-2) complex from mammalian cells (192, 196). Additionally, genetic evidence showed that Skp1 overexpression led to suppression of the temperature sensitive arrest of *cdc4-1* (described below) mutants, which cause high levels of the inhibitor Sic1 (7, 150). In *S. cerevisiae*, *SKP1* (known as Suppressor/Subunit of Kinetochore Protein mutant-1) is an essential gene like the other SCF components (7, 37). Temperature-sensitive mutants *skp1-11* and *skp1-12* arrest at the restrictive temperature at G1 and G2/M transitions, respectively (7). Skp1 is characterized as an “adaptor” subunit of the SCF and is required for the association of

one of many variable F-box proteins, the substrate receptor subunits of the SCF (7, 132, 192).

F-box proteins are specificity subunits for SCF E3 ligases

F-box proteins directly interact with substrates; therefore they provide selectivity for the entire SCF complex, the archetype being yeast Cdc4 (7, 50, 159). F-box proteins were determined to be the substrate specificity subunits of SCF complexes by several lines of research. Skp2, a human F-box protein, was found in a complex with Cyclin A-Cdk2 and Skp1 (196). It was genetically shown that overexpression of *SKP1* in *cdc4-1* mutants exhibited suppression of temperature sensitivity (7), and indicated that *SKP1* and *CDC4* interact within the same pathway. Temperature sensitive mutants in *skp1* or *cdc4* displayed Sic1 stabilization *in vivo*, and *SKP1* overexpression in *cdc4-1* mutants showed that Sic1 proteolysis was restored.

The F-box family of proteins was recognized upon sequence alignments of Skp1-interacting proteins and identified the F-box domain, a structural motif found in many proteins and throughout eukaryotic evolution (7). The F-box domain is a conserved sequence of approximately 40 amino acids and is required for its interaction with the rest of the SCF complex via Skp1 (7, 131, 159). Not surprisingly, it was also shown that mutation in conserved residues in the F-box domain show loss of interaction with Skp1 (7). Furthermore, several studies indicate that the F-box is required to destabilize substrates (7, 48, 52, 79). Additional protein-protein interaction domains were also

identified within several F-box protein family members, however many do not have common domains (7, 40, 132, 192).

Direct evidence of F-box proteins as specificity subunits came with the *in vitro* reconstitution of SCF ligase complexes and their ubiquitination of predicted substrates (50, 159). It was shown that *S. cerevisiae* Cdc4 1) formed a complex of Cdc4-Skp1-Cdc53-Cdc34 dependent on Skp1 2) Bound directly to both Skp1 and Sic1 3) Sic1 interaction with the SCF complex was dependent on Cdc4 4) Disruption of the WD40 repeats in Cdc4 abrogated interaction with Sic1 and 5) All subunits of the complex were required for ubiquitinating phosphorylated Sic1 *in vitro* (159).

It was also shown that another F-box protein, Grr1, could not substitute for Sic1 ubiquitination, and Cdc4 could not substitute for Grr1 in Cln1 (a Grr1 target) ubiquitination *in vitro* (159). Thus, the idea that SCF complexes are distinct ubiquitin ligase complexes whose substrate specificity was dependent on the associated F-box protein is often termed the “F-box Hypothesis” (50, 131, 132, 159). Nomenclature suggests identity of individual complexes be designated in superscript by their associated F-box protein, such as SCF^{Cdc4}, SCF^{Grr1}, etc.

Database searches of F-box family members have indicated up to 21 in *S. cerevisiae*, 110 in humans, 320 in *C. elegans*, and 700 in *A. thaliana* (26, 134). While it is currently unknown how many of these actually form SCF complexes or are bona-fide F-box proteins *in vivo*, the regulatory potential of such a modular ligase is immense.

Investigation of SCF complexes and F-box protein biology has shown a number of interesting trends and a growing number of substrates have been identified in several model systems.

Common themes in F-box proteins

As a general observation, the F-box domain is typically found near the amino-terminal end of the protein (40, 71, 132, 192). F-box proteins identified by database searches have also indicated an array of known protein-protein interaction domains within family members. While the F-box usually resides near the N-terminus, additional protein interaction domains are typically found in the C-terminal region (40, 71). As previously mentioned, and discussed further below, these additional domains are now thought to comprise the substrate interaction motifs necessary for recognition and specificity (26, 134, 192).

Two large classes of protein-protein interaction domains found in F-box proteins contain WD40-repeats or Leucine-rich repeats (LRR), suggesting common types of interaction motifs (26, 70, 192). Two of the initially characterized F-box proteins contain such domains; Cdc4 has 7 WD40 repeats, and Grr1 has 12 leucine-rich repeats. However, many F-box proteins do not contain any recognizable protein interaction domains, but many of which have not been characterized and may not form *bona fide* SCF complexes.

F-box proteins often recognize phosphoproteins as substrates. Characterization of Grr1 and Cdc4 has shown an obligate requirement for substrate phosphorylation, described as a “phospho-degron”, for recognition by the F-box protein (134, 153, 159, 192). During the initial genetic analysis of the cell cycle defects of the temperature sensitive *cdc4*, *cdc34*, and *cdc53* mutants, it was determined that the B-type cyclin inhibitor Sic1 was stabilized (150). Upon further investigation, Sic1 ubiquitination and

turnover required phosphorylation by the G1 cyclins Cln1/Cln2 (50, 159, 182). In several studies it has been shown that mutation of phosphorylation sites in Sic1 or deactivation of CDK exhibit stabilization of Sic1 (50, 134, 150, 182). Further analyses of many F-box protein-substrate interactions in several systems have suggested this may be a common requirement for many F-box protein-substrate interactions (26, 132, 134, 192). It also raises the possibility that other protein modifications such as acetylation, methylation, etc., may also act as “triggers” for interaction. Due to observed phosphorylation requirements of substrates for recognition by F-box proteins, this provides a model in how individual interaction and targeting is regulated. This likely explains the observation that individual F-box proteins have multiple substrates, however control on the ligase side of the interaction can also occur.

Regulation of SCF complexes and F-box receptors

Activity of individual SCF complexes can be regulated through several different mechanisms (134, 192). One mechanism that seems universal to all cullin family members (E3 ligase scaffolds) is Nedd8/Rub1 conjugation (71, 92, 134, 192). Interestingly, Rub1 conjugation to cullin proteins occurs by a similar E1-E2-E3 pathway, yet specific for the small ubiquitin-like protein Nedd8 (human) or Rub1 (*S. cerevisiae*) (67, 92, 97). In higher organisms and *S. pombe*, Nedd8 modification is essential and its loss leads to a decrease in SCF activity *in vivo* (129, 187). Cdc53 of the SCF complex in budding yeast is also Rub1-conjugated, but is not essential for viability. However, Rub1 is essential in combination with conditional alleles in SCF components suggesting it does play a role in SCF activity in budding yeast. It has been proposed that reversible cycling

of Nedd8/Rub1 modification of Cullins regulates individual complexes by controlling subunit assembly (38, 71, 134, 192). This is thought to allow the Cullin-RING ubiquitin ligases to disassemble and reassemble to increase the modularity of the substrate receptor subunits, such as F-box proteins.

Another point of SCF ligase regulation is through control of the substrate-receptor itself, the F-box protein. Early in the characterization of F-box proteins it was recognized that the receptors are unstable proteins themselves (52, 197). Deletion of the F-box domain in Cdc4, Grr1, and Met30 all stabilize the proteins. It has also been shown that stabilization of these occur in SCF pathway mutants; Temperature sensitive *skp1-11*, *skp1-12*, *cdc53-1*, and *cdc34-2* strains show loss of turnover of these F-box proteins (52, 197). SCF complex assembly is thought to facilitate an “autoubiquitination” mechanism, which also occurs in vitro (88). It is not understood why this occurs, whether it be a byproduct of the catalytic ubiquitin cycle involving the SCF or a specific mechanism of F-box protein regulation. Although this mechanism of control is conserved in several F-box proteins, it may not be universal; the F-box protein Rcy1 is not stabilized by deletion of the F-box or in SCF mutants, but also does not assemble into an SCF complex (53).

Interestingly, the human F-box protein Skp2 is regulated by another multisubunit ubiquitin ligase, the Anaphase Promoting Complex (APC) (10, 26, 188). SCF^{Skp2} function in mammalian cells primarily controls p27, an S-phase CDK inhibitor (28, 117, 180). APC^{Cdh1} activity during G0/G1 of the cell cycle leads to an inverse relationship of low Skp2 abundance and high p27 levels, which inhibits S-phase CDK activity. APC^{Cdh1} inactivation allows SCF^{Skp2} accumulation for p27 ubiquitination and destruction (10, 188). This is an elegant cellular mechanism of E3 ligase crosstalk that helps coordinate

cell cycle events as a circuit. While Skp2 is currently the only F-box protein that has been shown to be a target of the APC, it stands to reason that other examples may also emerge. Interestingly, in budding yeast SCF^{Cdc4} controls the stability of the F-box protein Ctf13 (74). However, Ctf13 is unlinked to SCF function and instead is thought to play a role in kinetochores (40, 71). These observations suggest it is possible other individual ligases control SCF function by regulation of the F-box protein receptors.

Subcellular localization of F-box proteins can also play a role in proper SCF function toward their substrates. In *S. cerevisiae*, SCF^{Cdc4} targets the CDK inhibitor Far1 for destruction in the absence of mating pheromone. Far1 translocates between cytoplasm and nucleus, but is much more stable in the cytoplasm (16). Cdc4 is normally localized in the nucleus and mislocalized Cdc4 causes cytoplasmic turnover of Far1 (16). This suggests that regulation of subcellular localization of F-box proteins is also required for proper SCF complex formation and cellular homeostasis.

Early Evidence of *DIA2* function in *S. cerevisiae*

With the sequencing of the *Saccharomyces cerevisiae* genome completed, database searches for F-box domains have revealed approximately 20 putative F-box proteins (26, 71, 134, 192). Some of these have been well characterized (Cdc4, Grr1, Met30), however the cellular roles of the other possible F-box proteins are only beginning to be understood (71, 192). The unstudied ORF YOR080W was identified as one of the genes encoding tetratricopeptide repeats (TPR), followed by an F-box domain, followed by leucine-rich repeats (LRR). YOR080w was subsequently named *DIA2* (Digs Into Agar-2) as its deletion was identified in a genetic screen for haploid invasive growth

phenotypes (127). However, the *dia2Δ* mutant phenotype was relatively weak in this regard.

The F-box protein Pof3 in the fission yeast *S. pombe* was later found to play a role in genome maintenance and telomere function (76). This F-box protein has a similar domain organization as Dia2, with N-terminal TPR repeats and C-terminal LRR repeats flanking the F-box (76). Indeed Dia2 was identified as the proposed budding yeast homolog of Pof3. The Pof3 protein formed an SCF complex, and gene disruption of *pof3*⁺ showed it was viable, but grew slow due to a cell cycle delay. Genetic evidence also showed synthetic interaction with a number of checkpoint genes, and *Δpof3* mutants were sensitive to DNA damaging agents.

A role for *DIA2* was also independently identified in a screen for novel mutants that affect the cell cycle (148). This group sensitized budding yeast to internal damage by utilizing the *pds1Δ* mutant, which is unable to block metaphase to anaphase upon DNA damage checkpoint activation. In this study *dia2Δ pds1Δ* cells were found to be synthetically lethal, which indicated that *DIA2* normally plays a role in genome maintenance. Loss of *DIA2* was hypothesized to cause higher amounts of endogenous damage, which required an intact checkpoint response for viability (148). Similarly to fission yeast *Δpof3* mutants, *dia2Δ* mutants showed an accumulation of G2/M cells, possibly due to an active G2/M DNA damage checkpoint. This seemed likely, since *Δpof3* mutants in *S. pombe* showed constitutively phosphorylated Chk1, a marker of checkpoint activation (76).

Dia2 was previously found to interact with several components of the replisome by a large-scale mass spectrometry screen of protein complexes in *S. cerevisiae* (66).

Although the significance of this was not known, Dia2 was found to be physically associated with Mcm2, Mcm3, Mcm5, and Ctf4. Additionally, Skp1 and Cdc53 co-purified with Dia2, indicating the first evidence of *bona fide* SCF^{Dia2} formation in vivo (66). *In vitro* experiments of purified components also suggested SCF^{Dia2} formation, as well as activity measured by autoubiquitination (84,88).

Whole genome analyses have further identified genetic interaction of *DIA2* with a number of pathways related to DNA replication and genome maintenance (15, 128, 177). However, while these studies genetically link *DIA2* function in genome maintenance, a specific physiological role has not yet been described.

Overview of Thesis Research

This dissertation is a collection of thesis research on the initial characterization of *DIA2* in *Saccharomyces cerevisiae*. I present primary work that I've completed in whole, or in part, toward the understanding of the cellular role(s) of Dia2. Combinations of approaches have been used in studying Dia2 including genetic, biochemical, and cell biological analyses. These findings now support a function for Dia2 in DNA replication and genome maintenance, and further our knowledge of F-box protein biology. Chapter II provides the initial evidence that Dia2 is a functional F-box protein in vivo and plays a role in DNA replication and promotes genome maintenance in *S. cerevisiae*. Evidence suggests that Dia2 is a chromatin-bound protein that can interact with origins of replication. Chapter III highlights findings of genetic and physical interaction of the Yra1 protein with Dia2. Yra1 has been previously described as involved in mRNA processing and nuclear export; however, we find it performs a novel role outside of this activity.

Yra1 helps recruit Dia2 to replication origins and interacts with Dia2 biochemically and genetically which suggests a dual role for the Yra1 protein. Finally, Chapter IV presents evidence concerning control of Dia2 protein abundance by a proteolytic mechanism. This chapter describes observations of this control by testing domain mutants of Dia2, pathways, and nuclear localization for control and function of the Dia2 protein. Turnover is blocked during periods of replication stress dependent on checkpoint proteins. Although the physiological role for control of Dia2 protein abundance is not yet clear, the data indicate that it may promote Dia2 activity in the cell for proper genome maintenance.

Figure 1

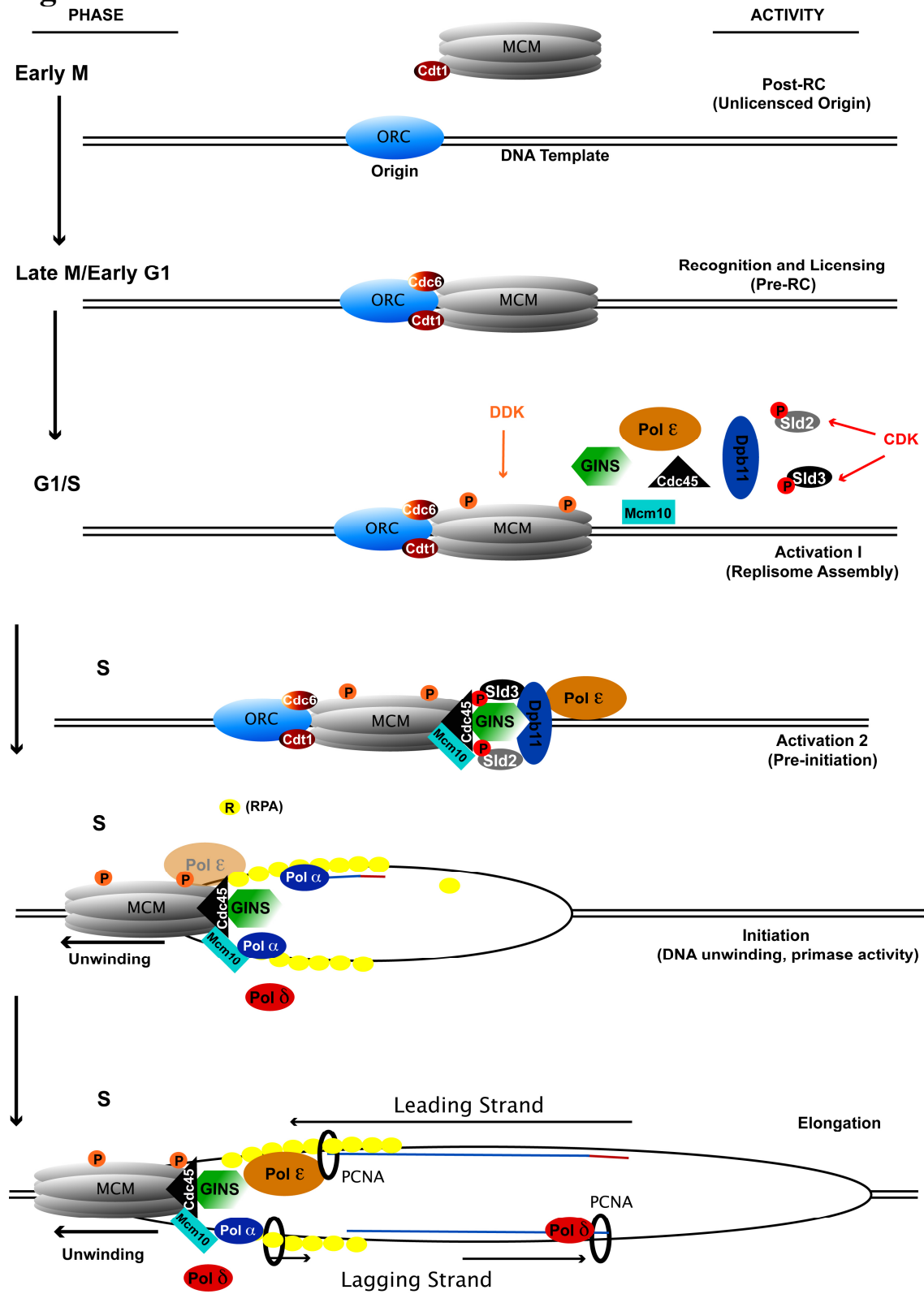


Figure 1: Stages of DNA replication in budding yeast. Only one side of replication bubble is shown for simplicity. Early M) Following a previous cycle of DNA replication, origins are bound only by ORC and represent an unlicensed state. Replication cannot reoccur again at a fired origin during a single S phase and remains in this state through early M phase. Late M/Early G1) In late M phase Cdc6 accumulates and binds to ORC, which recruits Cdt1-bound MCM to origins after these complexes have re-entered the nucleus. G1/S) Transition into S phase activates DDK and CDK, which phosphorylate MCM and Sld2/Sld3 respectively. S) Following phosphorylation of Sld2 and Sld3 by CDK, replisome components Cdc45, Dpb11, Mcm10, GINS, and Pol ϵ interdependently assemble at the licensed origin to form the pre-initiated complex. S: Initiation) Assembly of the replisome activates DNA unwinding by MCM and binding of RPA to ssDNA. Pol α synthesizes short RNA primer followed by DNA synthesis. S: Elongation) Replication fork progresses by DNA unwinding. Pol ϵ with PCNA is responsible for leading strand DNA synthesis. Lagging strand synthesis is carried out by reiterations of Pol α to Pol δ polymerase switch. Pol δ synthesizes DNA with the help of PCNA.

Figure 2

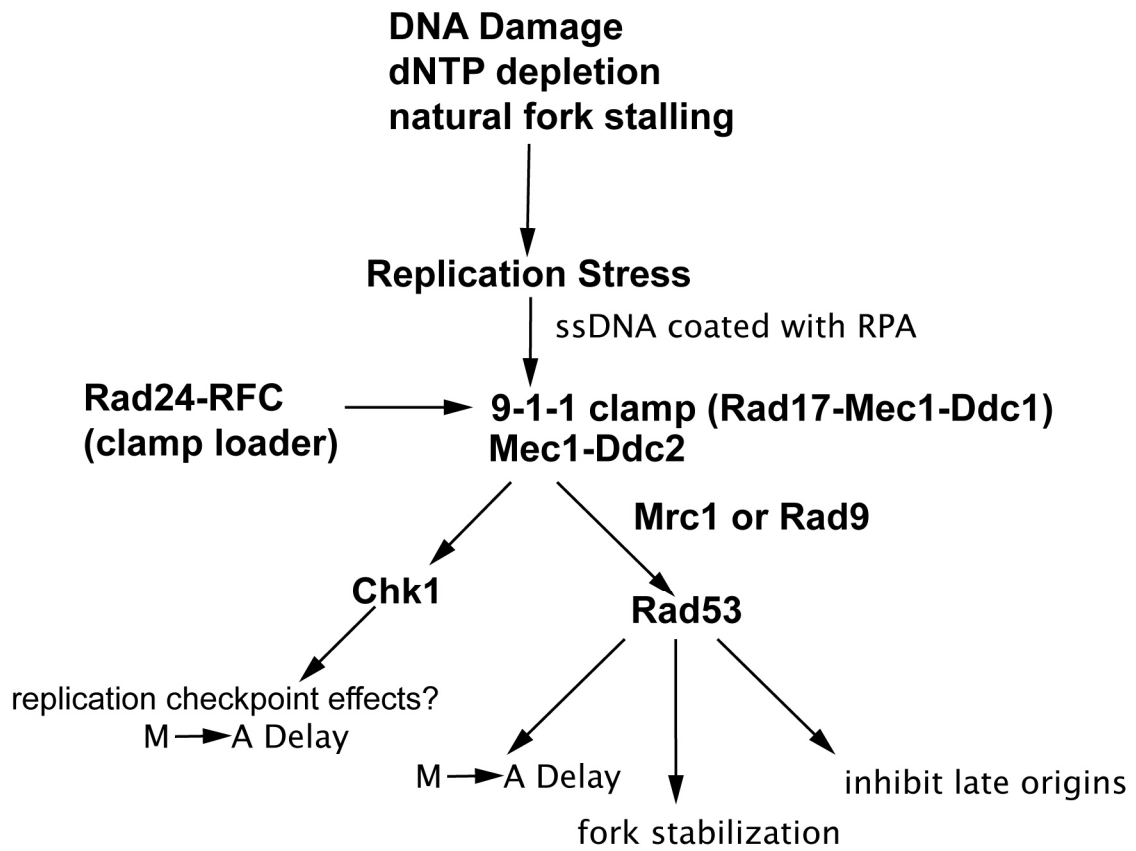


Figure 2: Pathway for activation of the S-phase checkpoint by DNA damage or replication stress. Problems during DNA synthesis such as DNA damage replication fork stalling lead to replication stress. ssDNA accumulates via uncoupling of DNA unwinding and DNA synthesis. Long tracts of ssDNA are coated by RPA and are recognized independently by the 9-1-1 ring-like clamp and the Mec1-Ddc2 kinase. The 9-1-1 clamp is loaded at the ssDNA-dsDNA junction by the Rad24-RFC clamp loader. The colocalization of the 9-1-1 clamp and Mec1-Ddc2 is necessary for proper activation of the checkpoint. Mec1 kinase activates Rad53 with the help of the adaptor protein Rad9 in the presence of DNA damage, or the adaptor Mrc1 in the presence of replication fork stalling. Rad53 kinase then signals to downstream pathways to inhibit late origin firing, mediate fork stabilization, and inhibit the metaphase to anaphase transition. Chk1's role in replication checkpoint signaling is less established, but may be minor. However, both Chk1 and Rad53 block the metaphase to anaphase transition by similar mechanisms in the G2/M DNA damage checkpoint. This occurs if the replication checkpoint is insufficient to address the problems associated with replication stress such as DNA damage or fork collapse.

Figure 3

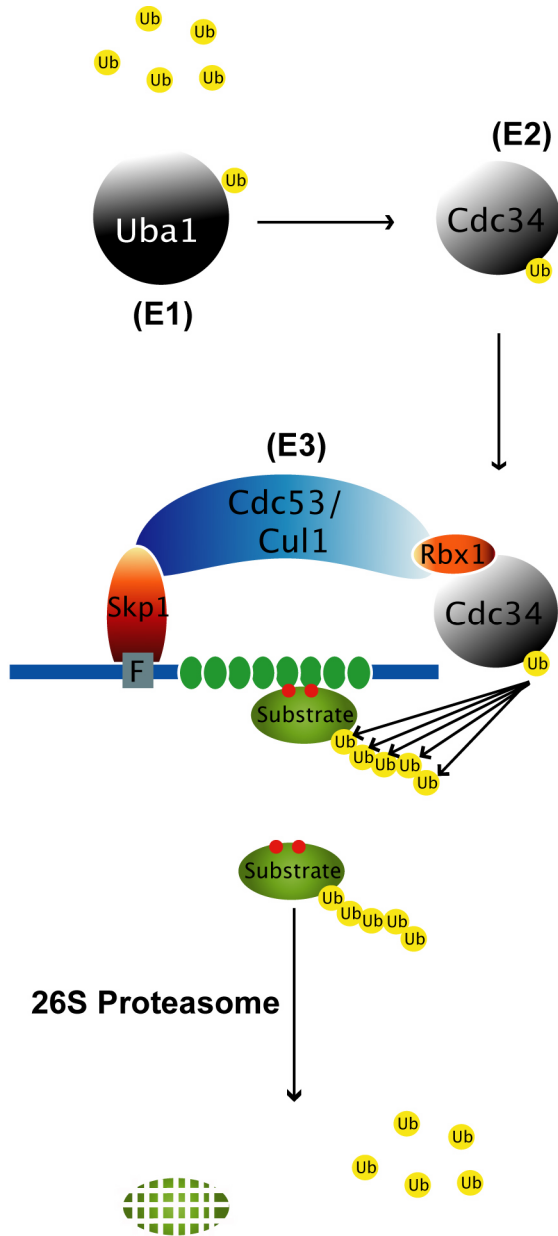


Figure 3: The SCF pathway in protein ubiquitination for targeting substrates to 26S proteasome for degradation. Ubiquitin (Ub) is activated by Ubiquitin activating enzyme (E1, Uba1 in *S. cerevisiae*) and forms a thioester intermediate. Ubiquitin is then transferred and forms a thioester with the E2 enzyme (Cdc34 for SCF pathway in *S. cerevisiae*). The multisubunit SCF ubiquitin ligase (E3) recruits Cdc34 by the RING-containing protein Rbx1, which interacts with the Cdc53 scaffold protein C-terminus. The linker protein Skp1 interacts at the Cdc53 N-terminus and recruits a variable F-box substrate adaptor protein by interaction with the conserved F-box domain (F). Additional protein-protein interactions in the F-box protein recruit a substrate, which is then conjugated to a ubiquitin molecule by Cdc34. Repetitions of this cascade lead to polyubiquitinated forms of a substrate. A polyubiquitin chain with K48 linkages leads to targeting to the 26S proteasome for destruction. Ubiquitin is recycled for additional use.

CHAPTER II

The F-box protein Dia2 regulates DNA replication

Chapter Summary

Ubiquitin-mediated proteolysis plays a key role in many pathways inside the cell and is particularly important in regulating cell cycle transitions. SCF (Skp1/Cul1/F-box protein) complexes are modular ubiquitin ligases whose specificity is determined by a substrate-binding F-box protein. Dia2 is a *Saccharomyces cerevisiae* F-box protein previously described to play a role in invasive growth and pheromone response pathways. We find that deletion of *DIA2* renders cells cold-sensitive and subject to defects in cell cycle progression, including premature S-phase entry. Consistent with a role in regulating DNA replication, the Dia2 protein binds replication origins. Furthermore, the *dia2* mutant accumulates DNA damage in both S and G2/M phases of the cell cycle. These defects are likely a result of the absence of SCF^{Dia2} activity, as a Dia2 Δ F-box mutant shows similar phenotypes. Interestingly, prolonging G1 phase in *dia2* cells prevents the accumulation of DNA damage in S-phase. We propose that Dia2 is an origin-binding protein that plays a role in regulating DNA replication.

Introduction

The duplication of a single cell requires multiple complex regulatory networks controlled by cyclin/CDK (cyclin-dependent kinase) complexes responsible for cell cycle transitions. It is clear that the ubiquitin-proteasome system is also important for the regulation of cell cycle progression, most notably in regulating the degradation of cyclins and cyclin-dependent kinase inhibitors (40, 82). In the ubiquitin-proteasome pathway, substrate proteins are covalently attached to the small polypeptide ubiquitin in an enzymatic cascade. The addition of long chains of ubiquitin polymers, linked using lysine 48 of each ubiquitin monomer, to substrate proteins leads to destruction of the substrate protein via the 26S proteasome (137). The primary means of specificity in the ubiquitination reaction is accomplished by the E3 ubiquitin ligase, as this enzyme is responsible for recruiting substrate proteins (33, 63).

Members of the highly conserved SCF (Skp1/Cdc53/E-box protein) ubiquitin ligase family have been shown to control cell proliferation by regulating the ubiquitin-mediated proteolysis of key cell cycle regulators (28, 50, 84, 110, 159, 160, 167, 180, 191). SCF complexes are modular ubiquitin ligases whose specificity is determined by a substrate-binding F-box protein (50, 159). The 40-50 amino acid F-box motif is required for binding to Skp1. Thus, mutation of the F-box motif renders F-box proteins incapable of targeting their substrate proteins for ubiquitination (7). Many F-box proteins have been identified in both humans and model eukaryotic systems, suggesting that SCF pathways reflect a highly conserved mechanism for controlling protein function. In *Saccharomyces cerevisiae*, at least 17 F-box proteins have been identified, but many of these proteins have not been well characterized (40, 132).

The F-box protein Dia2 was initially described as a mutant that exhibits a switch from apical to bipolar budding pattern and is hyperinvasive (127). Dia2 has recently been proposed to target a transcription factor in the pheromone-response pathway for ubiquitination (8), although this conclusion is controversial (32). Other evidence suggests that Dia2 plays a role in cell cycle progression. The *dia2* deletion mutant accumulates large-budded cells, indicative of a block in mitotic progression, and has been found to be synthetically lethal with a *pds1* mutant, which exhibits sister chromatid segregation defects at anaphase (148). In addition, Dia2 is related to the *Schizosaccharomyces pombe* F-box protein Pof3, which has been shown to be important for maintaining genomic stability (76).

To maintain genomic integrity, the timing of S-phase initiation is linked with growth control mechanisms in the G1 phase of the cell cycle. In budding yeast, the S-phase cyclins Clb5 and Clb6 are required for proper entry into S-phase from G1 (151). The control of the G1 to S phase transition is particularly important, as genes involved in this pathway are often mutated in tumor cells. DNA replication initiates at replication origins, called autonomously replicating sequences (ARSs) in *S. cerevisiae*. Activation, or firing, of origins is precisely controlled to ensure that each chromosome is only replicated once per cell cycle (12). Here we present evidence that Dia2 has a role in cell cycle regulation by demonstrating that Dia2 binds replication origins and is involved in regulating the timing of the G1 to S phase transition of the cell cycle.

Materials and Methods

Media and cell culture. Yeast were maintained and cultured according to standard methods (143). Yeast strains used in this study are listed in Table 1.

Strain construction. *CLB5* and *CLB6* deletion strains were constructed by standard PCR replacement method using the primers DK133, DK134, DK142, DK143. Double and triple mutant strains were generated using standard *S. cerevisiae* genetics (143). To generate the 18Xmyc tagged *Dia2* allele, a fragment of the *DIA2* gene was amplified using the primers DK176 and DK359, cloned in frame with 18 copies of the myc epitope using Xho I and Nco I sites in plasmid pJBN130. After linearization with Eco RV, the DNA was transformed into Y80 cells and transformants were selected on media lacking histidine. Primer sequences are listed in Supplemental Table 1.

Plasmid construction. The *DIA2* gene was amplified in fragments using primers DK97, DK98, DK99 and DK100. The fragments were cloned into the Bam HI and Xho I sites of pRS316 to generate pDMK465. The Δ F-box mutant was generated using a two-step PCR method with the primers DK97, DK9100, DK148 and DK149 and cloned into Bam HI and Xho I sites of pRS406 to generate pDMK289. An Eco RI fragment containing the F-box deletion was swapped with the Eco RI fragment of pDMK465 to generate pDMK736. The *DIA2* open reading frame was amplified using the primers DK95 and DK96 and cloned in frame with the lox site of pUNI-10 using Nde I and Bam HI restriction sites to generate pDMK107. This construct was then recombined with the host vector p1210 to generate an HA3-tagged baculovirus expression construct (pDMK109) using recombinant Cre (New England Biolabs, Beverly, MA) as described by Liu et al., 1998. Primer sequences are listed in Supplemental Table 1.

Baculovirus production and protein expression. Baculovirus was produced in Sf9 cells using Baculogold Baculovirus DNA (BD Pharmingen, San Diego, CA) and Lipofectin reagent (Invitrogen, Carlsbad, CA) according to the manufacturer's instructions. Sf9 cells were cultured in Insect-Xpress (Cambrex, distributed by Fisher Scientific, Pittsburgh, PA) with 10% heat-inactivated fetal calf serum at 27°C. Baculovirus protein expression experiments were performed in HI-Five cells (Invitrogen, Carlsbad, CA). Cells were cultured in Excell 405 media (JRH Biosciences, Lenexa, KS) without serum at 27°C. 40 hrs after infection, insect cells were collected and lysed in NETN buffer (20 mM Tris pH 8.0, 100 mM NaCl, 1 mM EDTA, 0.5% Igepal, 10 mM NaF, 25 mM β -glycerophosphate plus Complete Protease inhibitor cocktail (Roche Applied Science, Indianapolis, IN)). Proteins were immunoprecipitated with anti-Flag antibodies (Sigma, St. Louis, MO) or anti-Myc (9E10) antibodies (Covance Research Products, Inc., Berkeley, CA) and ProtA/G plus agarose (Santa Cruz Biotechnology, Santa Cruz, CA). Anti-HA (HA.11) antibodies (Covance Research Products, Inc., Berkeley, CA) were used for immunoblotting. HRP-conjugated secondary antibodies were from Jackson Immunoresearch, Inc. (West Grove, PA).

Immunoprecipitation of yeast proteins. Cells were harvested at O.D.₆₀₀ = 1.0 and treated with 1% formaldehyde for 15 minutes at room temperature to cross-link proteins. Lysates were prepared as for chromatin immunoprecipitation (141). Proteins were immunoprecipitated with anti-Skp1 antibodies (159) and ProtA/G plus agarose (Santa Cruz Biotechnology, Santa Cruz, CA). Samples were boiled for 30 minutes prior to SDS-PAGE to reverse cross-links. Anti-myc (9E10) antibodies (Covance Research

Products, Inc., Berkeley, CA) were used for immunoblotting. HRP-conjugated secondary antibodies were from Jackson ImmunoResearch, Inc. (West Grove, PA).

Flow cytometry. Cells were collected and fixed in 70% ethanol for at least 30 minutes and then resuspended in PBS (140 mM NaCl, 3 mM KCl, 5 mM Na₂HPO₄, 2 mM KH₂PO₄, pH7.4) + 0.02% sodium azide. To prepare for flow cytometry, fixed cells were treated with FACS buffer (200 mM Tris-HCl, 20 mM EDTA + 0.1% RNase A) overnight at 37°C and then stained in 50 mg/ml propidium iodide in PBS. Prior to analysis, cells were diluted 10-fold in PBS and sonicated for 5 sec at 15% efficiency using a Sonic Dismembrator (Fisher Scientific, Pittsburgh, PA). Data analysis was performed with the FlowJo v6.3.3 software and graphs generated using Deltagraph 4.0.

Chromatin Immunoprecipitation. All assays followed the procedure of Ricke and Bielinsky, 2004. ARS305 and ARS603 primers are described (4). ATP11 primers are listed in Supplemental Table 1. Anti-Myc (9E10) antibodies were from Covance Research Products, Inc., Berkeley, CA and anti-Skp1 antibodies were a gift from J. Wade Harper (159).

Fluorescence microscopy. Cells were sonicated briefly as described for Flow cytometry prior to observation. YFP signals were observed using a Zeiss Axioscop 2 microscope equipped with a Zeiss AxioCam R2 digital camera and 100X objective with DIC filter. Images were captured using Zeiss Axiovision software release 3.1 (Carl Zeiss, Inc., Thornwood, NY).

Results

Dia2 assembles with SCF components and is required for normal growth

Dia2 is an F-box protein with TPR repeats in the N-terminus and leucine-rich repeats in the C-terminus (Figure 1A). It has previously been shown that recombinant Dia2 can assemble with SCF components (88) and that overexpressed Dia2 assembles with Skp1 and Cdc53 in yeast cells (66). We also observed Dia2 assembly with SCF components using an HA₃-tagged Dia2 baculovirus for expression in insect cells. As shown in Figure 1B, HA₃-Dia2 co-immunoprecipitates with both Flag-tagged Skp1 and Myc-tagged Cdc53 when coexpressed in insect cells. We examined whether Dia2 associates with SCF components under endogenous expression levels in yeast. To facilitate this experiment, we generated a strain that expressed a Dia2 fusion protein tagged at the C-terminus with 18 copies of the myc (9E10) epitope. The Dia2 18Xmyc-tagged strain complements a deletion strain (Supplemental Figure 1), indicating that the tagged protein is functional. We observe two major forms of Dia2; the larger form migrates at the predicted size for full-length Dia2. The larger form of Dia2 preferentially co-precipitates with Skp1 (Figure 1C). We also observe Cdc53 co-precipitating with Skp1 when a myc-tagged version of Cdc53 is expressed in the Dia2 18Xmyc-tagged strain. Consistent with what has been previously observed, we find that Cdc53 exists as two forms in yeast cells (110, 191); presumably the larger form that we observe in Figure 1C is modified by Rub1 as it preferentially interacts with Skp1 (92). We conclude that Dia2 is a *bona fide* F-box protein and assembles into an SCF complex in yeast cells.

The *dia2* null mutant grows slower at low temperatures. When individual spores from a dissection of a *dia2* null heterozygous diploid are grown on rich media at room

temperature, a pattern of 2 slow-growing to 2 fast-growing colonies is seen (Figure 1D).

The slow-growing colonies are resistant to G418, indicating that they are deletions of *DIA2* as the *kanMX* gene (183), which confers G418 resistance, was used to replace the *DIA2* gene in the genome (84). The slow growth defect of *dia2* mutant is rescued by introducing a *CEN* plasmid carrying the *DIA2* gene (Figure 3A). Thus, Dia2 is required for normal cell growth in *S. cerevisiae*.

dia2 mutants enter S-phase prematurely

Previous work has established a role for Dia2 in G2/M progression as a significant fraction of *dia2* cells accumulate as large-budded cells with the nucleus at the bud neck (148). However, we also observed defects that hinted at a role for *DIA2* in S-phase. As shown in Figure 2A, *dia2* mutants are sensitive to hydroxyurea (HU) as are *skp1-11* and *cdc53-1* mutants. In addition, overexpression of the S-phase cyclins Clb5 and Clb6 from a galactose-inducible promoter is toxic to *dia2* cells but not wildtype cells (Supplemental Figure 2).

To test whether *DIA2* might have role in S-phase, we synchronized *dia2* and wildtype (WT) cells in G1 with alpha factor, released them from arrest at 25°C and prepared samples at 10-minute intervals for flow cytometry. We observed that the *dia2* mutant cells entered S-phase 10 minutes earlier than wildtype cells under these conditions (Figure 2B, compare the 40 and 50 minute timepoints). We calculated the percentage of cells in S-phase for both strains at the 30, 40 and 50 minute time points; these numbers are shown next to the profiles in Figure 2B. Similar premature S-phase entry was

observed in *dia2* cells when we counted bud emergence as a measure for S-phase entry (Figure 2C).

To determine if the S-phase defects associated with the *dia2* deletion mutant were a result of the absence of an SCF^{Dia2} complex, we generated an in-frame deletion of the F-box domain in Dia2 (Δ F-box) to prevent association with SCF components. This mutant was placed under the control of the *DIA2* promoter on a *CEN* plasmid and transformed into the *dia2* deletion strain. As shown in Figure 3A, the Δ F-box mutant exhibits a growth defect and HU-sensitivity similar to the *dia2* deletion mutant covered by an empty vector. In addition, the *dia2* cells covered by the Δ F-box mutant show an early S-phase entry phenotype when cells are synchronized in G1, released at 25°C and then examined for DNA content and bud emergence (Figures 3B and C). We calculated the percentage of cells in S-phase for both strains at the 35, 40, 45 and 50 minute timepoints in the samples analyzed by flow cytometry; these numbers are listed next to the profiles in Figure 3B. As shown, the defect in the Δ F-box mutant is not as dramatic as the *dia2* deletion strain, but a significant fraction of the cells do reproducibly enter S-phase earlier. A smaller fraction of the *dia2* cells covered by the *DIA2* plasmid also enter S-phase early. We speculate that the null strain covered by the *DIA2* plasmid is not entirely equivalent to wildtype cells; this may be because Dia2 protein levels are tightly regulated (A.C. Kile and D.M. Koepp, unpublished observations). Nevertheless, the Δ F-box mutant clearly exhibits S-phase defects. Taken together, these data indicate that Dia2 plays a role in S-phase timing and that this role is dependent on its function as a component of an SCF ubiquitin ligase.

Dia2 binds replication origins

A large-scale proteomic screen determined that a number of DNA replication proteins copurified with the Dia2 protein (66). Given this observation and the links to S-phase with the *dia2* mutant, we wanted to determine if the Dia2 protein might be localized to origins of replication. To test this possibility, we used chromatin immunoprecipitation to assay for Dia2 binding to both an early and a late-firing origin. To facilitate this experiment, we used the Dia2 18Xmyc-tagged strain.

We observed that the Dia2 protein binds both *ARS305* (early-firing) and *ARS603* (late-firing) sequences (4) but not to the non-origin DNA near *ATP11*, which is 20 kb away from an origin in both directions (Figure 4, lanes 1-4). This binding is dependent on the addition of the cross-linker formaldehyde and is not observed in immunoprecipitations with a strain lacking the epitope-tagged Dia2 fusion (Figure 4, lanes 5-8). We conclude that Dia2 is an origin-binding protein, which is capable of binding both early and late-firing origins.

To test whether other SCF components localized to origins, we performed chromatin immunoprecipitations using anti-Skp1 antibodies (159) and a myc-tagged version of Cdc53 (191). As shown in Figure 4B, both Skp1 and Cdc53 co-precipitated with *ARS305* and *ARS603* DNA in a cross-linker dependent manner. These results strongly suggest that an SCF^{Dia2} complex is present at replication origins.

We next examined the association of Dia2 with origins throughout the cell cycle using cells that had been arrested in G1-, S- and M-phases by treatment with alpha factor, HU and nocodazole, respectively. We observe specific association of Dia2 with both *ARS305* and *ARS603* only in nocodazole-arrested cells (Figure 4C), indicating that Dia2

likely binds origins after origin firing. In addition, Skp1 also associates with *ARS603* in nocodazole-arrested cells (Supplemental Figure 3), consistent with the assembly of an SCF^{Dia2} complex at origins at this time during the cell cycle.

dia2 mutants accumulate DNA damage in S and G2/M

To better understand the role of Dia2 during the cell cycle and because *S. pombe pof3* exhibits synthetic lethality with several checkpoint mutants, we tested for genetic interactions between the *dia2* mutant and checkpoint mutants. We observed synthetic interactions between the *dia2* mutant and checkpoint mutants. We observed synthetic interactions between the *dia2* deletion mutant and a number of DNA damage and DNA replication checkpoint mutants, including *mec1*, *mrc1*, *chk1*, *rad9*, *rad17*, *rad24*, *pds1* and *cdc20-1* (Table 2). The synthetic lethal interactions with *rad9* and *pds1* have been previously identified (148). These interactions suggest that the *dia2* mutant accumulates damaged DNA and requires functional checkpoint pathways for viability.

Consistent with this possibility, we found that the *dia2* mutant is hypersensitive to both exogenous and endogenous DNA damage. To test the ability of *dia2* cells to respond to endogenous DNA damage, we used the temperature-sensitive *cdc13-1* strain, which accumulates single-stranded DNA at the non-permissive temperature. As shown in Figure 5A, the *dia2 cdc13-1* double mutant exhibits a faster loss of viability after exposure to 37°C than the *cdc13-1* mutant does. We observed no significant loss of viability in either the *dia2* or wildtype strains after incubation at 37°C. To examine the ability of *dia2* cells to an exogenous DNA damaging agent, we used MMS (methyl methanesulfonate), a DNA methylating agent. As shown in Figure 5B, both the *dia2* null

and ΔF -box mutants are sensitive to 0.005% MMS while *dia2* cells expressing *DIA2* are not.

To examine the possibility that *dia2* cells accumulate spontaneous DNA damage, we used a Rad52-YFP reporter strain. Rad52 is involved in recombinational repair and has been shown to localize to discrete nuclear foci when cells are treated with DNA damaging agents (99). We generated a *dia2* Rad52-YFP strain and examined the cells using fluorescence microscopy. A deletion mutant of the checkpoint kinase Mec1 (suppressed by deletion of the ribonucleotide reductase inhibitor Sml1) was used as a positive control (99). The *dia2* mutant showed an increased number of Rad52-YFP foci over wildtype. Strikingly, the *dia2* mutant showed nearly as many Rad52-YFP foci as the *mec1 sml1* mutant. Representative examples are shown in Figure 6A.

We correlated the number of cells exhibiting Rad52-YFP foci with bud morphology as a measure of cell cycle stage. Approximately 40% of both small-budded (S-phase) and large-budded (G2/M phase) *dia2* cells exhibit Rad52-YFP foci while only a small number are seen in unbudded (G1 phase) cells (Figure 6B). The percentage of *dia2* cells showing Rad52-YFP foci was similar to the percentage of *mec1 sml1* cells exhibiting foci. As expected, a small fraction of wildtype cells exhibit Rad52-YFP foci in S-phase, but almost none in G1 and G2/M phases (99).

To confirm that the formation of Rad52-YFP foci resulted from a defect in an SCF-dependent role of Dia2, we repeated these experiments with the *dia2* Rad52-YFP strain covered by an empty vector, a plasmid expressing the ΔF -box mutant or wildtype *DIA2* (Figure 6C). Both the empty vector and ΔF -box samples showed a high percentage of S and G2/M cells with Rad52-YFP foci while the strain covered with the *DIA2*

plasmid showed nearly wildtype levels of foci formation. From these data, we conclude that the *dia2* mutant accumulates DNA damage in S and G2/M phases of the cell cycle. Furthermore, this damage is a result of the absence of SCF^{Dia2} activity.

Delaying S-phase entry alleviates S-phase DNA damage in dia2 cells

One possible explanation for the accumulation of DNA damage in *dia2* cells is that it is a result of the premature entry into S-phase. Similar precocious S-phase defects linked to DNA damage and chromosomal instability have been observed in *sic1* mutants as well as in cells overexpressing members of the Swi/Snf family of transcription factors (96, 158). To address this possibility, we generated a *dia2 clb5 clb6* triple deletion mutant. Deletion of *CLB5* and *CLB6* has been shown to prolong G1 phase (151) and we reasoned that the premature S-phase entry in *dia2* cells might be dependent on the presence of S-phase cyclins. As predicted, the early S-phase entry from an alpha factor-induced G1 arrest in *dia2* cells is abolished in the *dia2 clb5 clb6* mutant (Figure 7A).

We then examined the formation of Rad52-YFP foci in the *dia2 clb5 clb6* background. As a control, the *clb5 clb6* Rad52-YFP strain showed a slightly elevated percentage of S-phase cells with foci compared to wildtype (Figure 7B). Strikingly, we found that deletion of *CLB5* and *CLB6* in the *dia2* strain decreased the percentage of S-phase cells showing Rad52-YFP foci to nearly the same levels as the *clb5 clb6* strain. However, the percentage of G2/M *dia2 clb5 clb6* cells exhibiting foci was not significantly different than *dia2* cells alone. These results suggest that prolonging G1

phase in *dia2* cells can prevent most of the S-phase specific DNA damage that occurs in these cells.

Discussion

A role for Dia2 in regulating DNA replication

We propose that Dia2 is an origin-binding protein that plays a role in regulating DNA replication. This is supported by the premature S-phase entry in *dia2* cells as well as the rescue of S-phase DNA damage in *dia2* cells by deletion of *CLB5* and *CLB6*. The role of Dia2 in the regulation of DNA replication is most likely the result of its function as part of an SCF complex. Dia2 assembles with Skp1 and Cdc53 in yeast cells and the Dia2 DF-box mutant shows phenotypes similar to complete deletion of the *DIA2* gene. Furthermore, Dia2, Skp1 and Cdc53 all associate with replication origins as measured by chromatin immunoprecipitation. A simple model then would be that an SCF^{Dia2} complex targets an unknown factor that promotes DNA replication. The ubiquitination of this substrate prevents premature S-phase entry and likely leads to the substrate's degradation via the proteasome.

Since Dia2 assembles at origins of replication, one intriguing possibility is that Dia2 regulates DNA replication by facilitating the ubiquitination of another origin-binding protein. In this way, Dia2 might influence the make-up and/or activity of replication components found at origins. Our chromatin immunoprecipitation results suggest that Dia2 associates with replication origins after origin firing. Consistent with this, we observe Dia2 association with origins only after bud emergence in cells that have been released from a G0/G1 arrest (S. Swaminathan and D.M.Koepp, unpublished observations). One possibility is that Dia2 targets an origin-binding protein for ubiquitination after origins fire and in this way, helps to “re-set” the origins for use in the next S-phase. In the absence of Dia2, this substrate protein promotes premature onset of

S-phase in the next cell cycle. Examining in more detail how Dia2 associates with origins and determining which other proteins are found at origins at the same time will provide additional insight into the functional consequences of SCF^{Dia2} activity.

Precocious S-phase entry has been linked to genomic instability in a number of mutants that affect the cell cycle (157). Our results are consistent with these observations, in that the premature S-phase entry in *dia2* mutants leads to at least some of the DNA damage observed in these cells. Our results predict that the pathway that leads to premature S-phase in *dia2* cells is dependent on Clb5 and Clb6 activity, although whether they act upstream or downstream of the SCF^{Dia2} substrate is unclear. A straightforward explanation for the rescue of DNA damage in *dia2* cells by the *clb5 clb6* mutant might be that Clb5 and Clb6 are themselves the targets of an SCF^{Dia2} complex. However, we have not observed any changes in the protein stability of either Clb5 or Clb6 in *dia2* cells (D. M. Koepf and S. J. Elledge, unpublished observations), making this scenario unlikely. Taken together, the results presented here provide an important link between SCF-mediated ubiquitination and S-phase entry that has implications for understanding genomic stability.

Other roles for SCF^{Dia2}

There are almost certainly other pathways in addition to DNA replication in which the SCF^{Dia2} complex acts. For example, the *dia2 clb5 clb6* mutant still accumulates DNA damage foci in large-budded cells, indicating that there is a Clb5 and Clb6-independent pathway that is disrupted in *dia2* cells, which also causes DNA damage. Like *pof3* cells, the *dia2* mutant exhibits a chromosome loss phenotype (76)

(note that Fcl1 is an alternate name for Dia2). However, this phenotype is not rescued in the *dia2 clb5 clb6* mutant (D. M. Koepp and S. J. Elledge, unpublished observations), further suggesting that there is also a Clb5 and Clb6-independent role for Dia2.

The *dia2* mutant was initially identified because it exhibits elongated cells with a bipolar budding pattern with enhanced invasiveness (127). It has recently been proposed that Tec1, a pheromone-responsive transcription factor involved in the filamentous growth pathway, is a substrate of SCF^{Dia2} (8). While it is formally possible that the role of Dia2 in the filamentation pathway is linked to the DNA replication timing defects in *dia2* mutants, we think these pathways are independent as the *dia2 clb5 clb6* mutant still exhibits the elongated cell/bipolar budding pattern phenotype. Furthermore, the *dia2 tec1* double mutant exhibits the same growth and S-phase defects as the *dia2* mutant (A.C. Kile, P. Midthun and D. M. Koepp, unpublished observations). If Tec1 were the substrate responsible for the premature S-phase entry in *dia2* cells, we would expect the *dia2 tec1* strain to exhibit normal S-phase timing.

The most likely explanation for the pleiotropic phenotypes in the *dia2* deletion is that the SCF^{Dia2} complex controls the ubiquitination of more than one substrate. Many F-box proteins regulate the turnover multiple substrates. Thus it is possible that one SCF^{Dia2} substrate is involved in DNA replication while another is important for filamentous growth. Future studies identifying SCF^{Dia2} substrates will shed light on the interplay between these pathways. The results presented here are an essential step in providing a biological framework in which the role of any Dia2 substrate may be assessed.

Koepp et al. Table 1

Table 1. Strains used in this study

Strain	Genotype	Source
Y80 (wildtype)	<i>MATa can1-100 ade2-1 his3-11,15 leu2-3,112 trp1-1 ura3-1</i>	Bai et al., 1996
DKY194 (<i>dia2</i>)	As Y80 but <i>dia2Δ::kanMX</i>	Koepp et al., 2001
Y552 (<i>skp1-11</i>)	As Y80 but <i>skp1-11</i>	Bai et al., 1996
YMT741 (<i>cdc53-1</i>)	<i>MATa cdc53-1 can1-100 ade2-1 his3-11,15 leu2-3,112 trp1-1 ura3-1</i>	M. Tyers
DKY408 (<i>DIA2-18Xmyc</i>)	As Y80 but <i>DIA2::DIA2-18Xmyc-HIS3</i>	This study
W2297-4A (<i>RAD52-YFP</i>)	<i>MATa trp1-1 bar1::LEU2 leu2-3,112 can1-100 ura3-1 his3-11,15 RAD52-YFP</i>	Lisby et al., 2001
W2381-10B (<i>mec1 sml1 RAD52-YFP</i>)	As W2297-4A but <i>mec1Δ::TRP1 sml1Δ::HIS3</i>	Lisby et al., 2001
DKY443 (<i>dia2 RAD52-YFP</i>)	<i>MATa RAD52-YFP dia2Δ::kanMX ura3-1 his3-11,15 trp1-1 ade2-1 leu2-3,112</i>	This study
DKY399 (<i>clb5 clb6</i>)	As Y80 but <i>clb5Δ::HIS3 clb6Δ::LEU2</i>	This study
DKY444 (<i>clb5 clb6 RAD52-YFP</i>)	<i>MATa RAD52-YFP clb5Δ::HIS3 clb6Δ::LEU2 ade2-1 ura3-1 his3-11,15 trp1-1 leu2-3,112</i>	This study
DKY403 (<i>dia2 clb5 clb6</i>)	As Y80 but <i>dia2Δ::kanMX clb5Δ::HIS3 clb6Δ::LEU2</i>	This study
DKY445 (<i>dia2 clb5 clb6 RAD52-YFP</i>)	<i>MATa RAD52-YFP dia2Δ::kanMX clb5Δ::HIS3 clb6Δ::LEU2 ade2-1 ura3-1 his3-11,15 trp1-1 leu2-3,112</i>	This study
DKY405 (<i>dia2 mrc1</i>)	As Y80 but <i>dia2Δ::kanMX mrc1Δ::HIS3</i>	This study
DKY404 (<i>dia2 chk1</i>)	As Y80 but <i>dia2Δ::kanMX chk1Δ::HIS3</i>	This study
DKY448 (<i>dia2 rad9</i>)	As Y80 but <i>dia2Δ::kanMX rad9Δ::HIS3</i>	This study
DKY449 (<i>dia2 rad17</i>)	As Y80 but <i>dia2Δ::kanMX rad17Δ::kanMX</i>	This study
DKY450 (<i>dia2 rad24</i>)	As Y80 but <i>dia2Δ::kanMX rad24Δ::kanMX</i>	This study
JBY257 (<i>cdc13-1</i>)	As Y80 but <i>cdc13-1</i>	Sanchez et al., 1999
DKY396 (<i>dia2 cdc13-1</i>)	As Y80 but <i>dia2Δ::kanMX cdc13-1</i>	This study

Koepp et al. Table 2

Table 2. The *dia2* mutant interacts genetically with checkpoint mutants

dia2 Double mutants	Role	Phenotype
	<i>DNA damage</i>	
<i>rad9</i>	Adaptor	slower growth at 16°C and 25°C
<i>rad17</i>	Clamp loader	slower growth at 30°C
<i>rad24</i>	Clamp loader	slower growth at 30°C
	<i>Kinases</i>	
<i>mec1 sml1</i>	Transducer kinase	inviable
<i>chk1</i>	Transducer kinase	slower growth at 25°C
	<i>DNA replication</i>	
<i>mrc1</i>	Adaptor	slower growth at 25°C, inviable at 37°C
	<i>Targets</i>	
<i>pds1</i>	Cohesin	inviable
<i>cdc20-1</i>	APC activator	inviable

Koepp et al., Figure 1

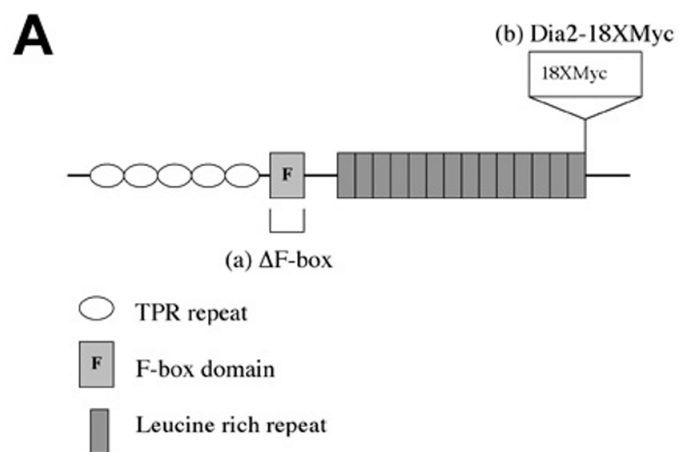
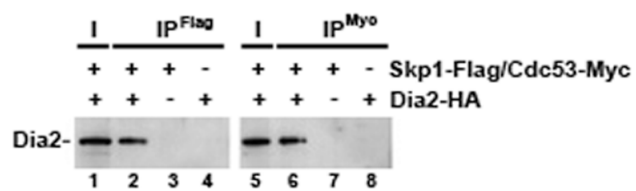
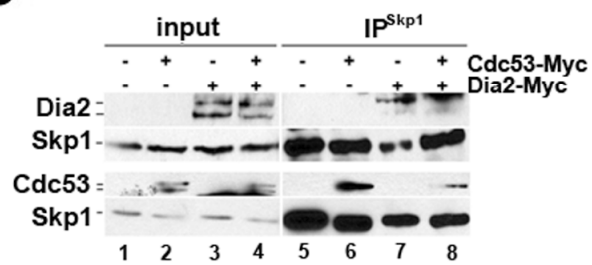
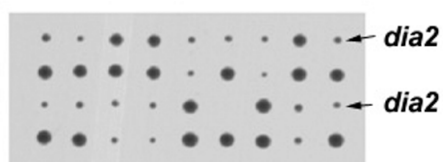
**B****C****D**

Figure 1. Dia2 is an F-box protein required for normal growth. A) Diagram of Dia2 domain structure. Structure adapted from (76, 132). Modified forms described in the text are shown in (a) and (b). B) Recombinant Dia2 assembles with SCF components. Insect cells were co-infected with HA₃-tagged Dia2 baculovirus and Flag-tagged Skp1 or Myc-tagged Cdc53 baculoviruses. After 40 hrs, cells were harvested and lysates subjected to immunoprecipitation with anti-Flag or anti-myc antibodies. Immunoblots were probed with anti-HA antibodies. I = input, IP = immunoprecipitate. C) Dia2 assembles with SCF components in yeast cells. Skp1 was immunoprecipitated using anti-Skp1 antibodies (159) from the indicated strains. Immunoblots were probed with anti-myc and anti-Skp1 antibodies. Due to significant differences in signal intensity between Dia2 and Cdc53, two separate blots are shown. D) The *dia2* deletion exhibits a slow growth phenotype at room temperature. Colonies from tetrad dissection of *DIA2/dia2* diploid induced to undergo meiosis are shown. Arrows point to representative small *dia2* colonies, while large colonies are *DIA2*.

Koepp et al., Figure 2

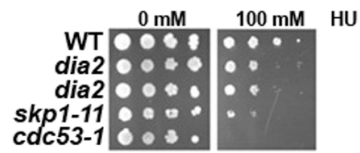
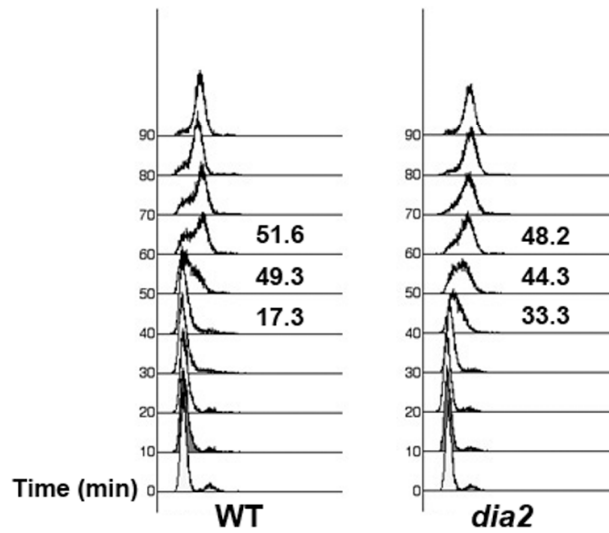
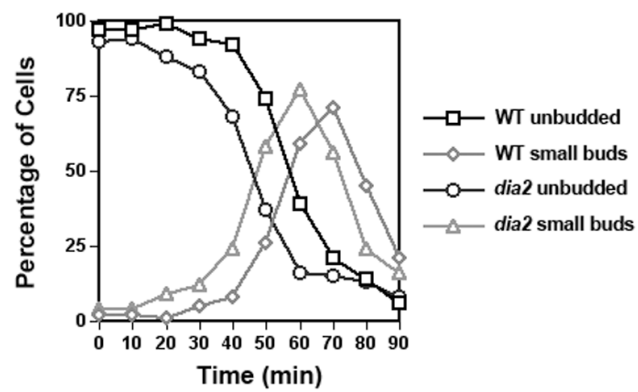
A**B****C**

Figure 2. The *dia2* mutant exhibits S-phase defects. A) SCF mutants are HU-sensitive. Serial dilutions of WT, *dia2*, *skp1-11* and *cdc53-1* strains were spotted onto rich media containing indicated amounts of HU and grown at 30°C. B) The *dia2* mutant enters S-phase earlier than wildtype. WT and *dia2* cells were arrested in G1 with alpha factor and then released from arrest at 25°C. Samples were taken at the indicated time points and used for flow cytometry. The percentage of S-phase cells was calculated for the 30, 40, and 50 minute time points using FlowJo software and is shown next to the profile for each strain. C) The *dia2* mutants exhibit early bud emergence. Cells were treated as in (B) and budding morphology was assayed by light microscopy. At least 100 cells were counted per time point and the experiment was repeated three times. Representative results from a single experiment are shown. The identity of each strain and bud stage is indicated next to the graph.

Koepp et al., Figure 3

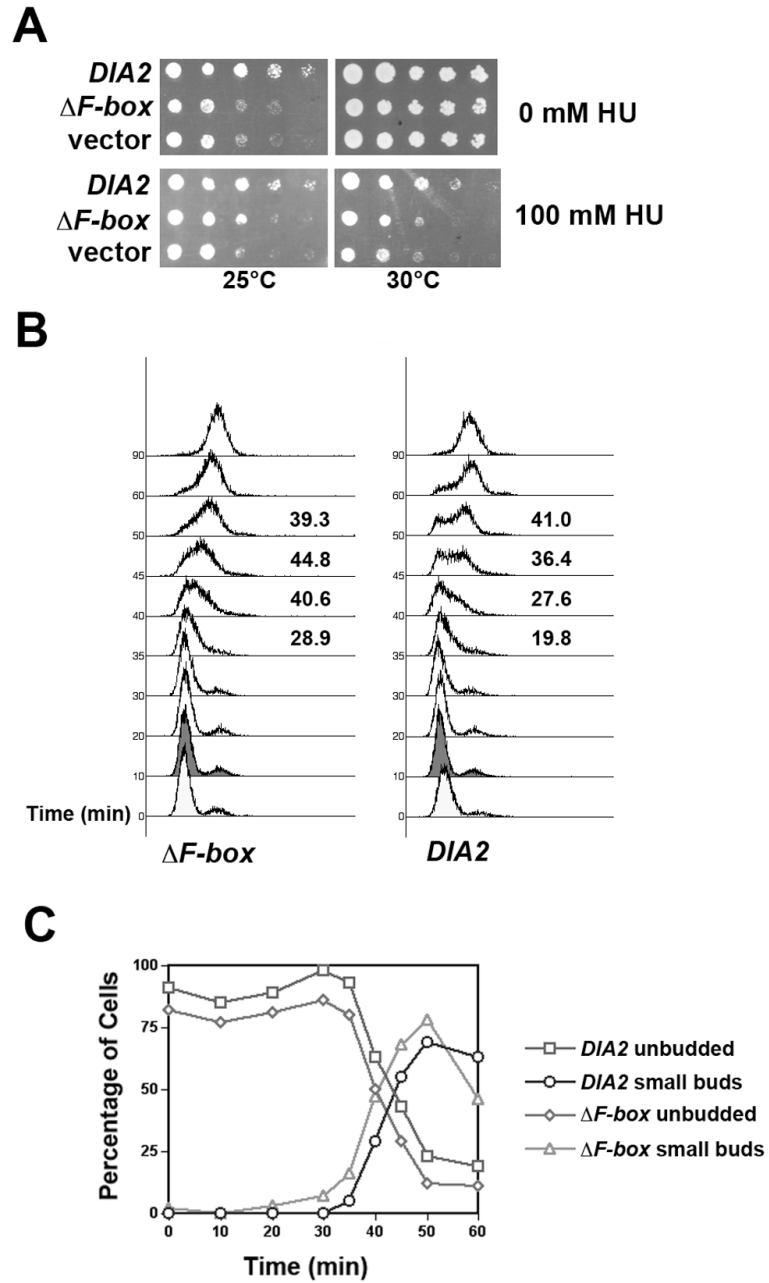


Figure 3. The *dia2* Δ F-box mutant exhibits growth and S-phase defects. A) The Δ F-box mutant is cold-sensitive and HU-sensitive. The *dia2* strain was transformed with *DIA2*, Δ F-box and empty vector DNA. Serial dilutions of each were then spotted on rich media containing the indicated amount of HU and incubated at either 25°C or 30°C. B) The Δ F-box mutant enters S-phase earlier than WT cells. WT and *dia2* Δ F-box cells were arrested in G1 with alpha factor and then released from arrest at 25°C. Samples were taken at the indicated time points and used for flow cytometry. The percentage of S-phase cells was calculated for the 35, 40, 45 and 50 minute time points using FlowJo software and is shown next to the profile for each strain. C) The *dia2* Δ F-box mutants exhibit early bud emergence. Cells were treated as in (B) and budding morphology was assayed by light microscopy. At least 100 cells were counted per time point and the experiment was repeated three times. Representative results from a single experiment are shown. The identity of each strain and bud stage is indicated next to the graph.

Koepp et al., Figure 4

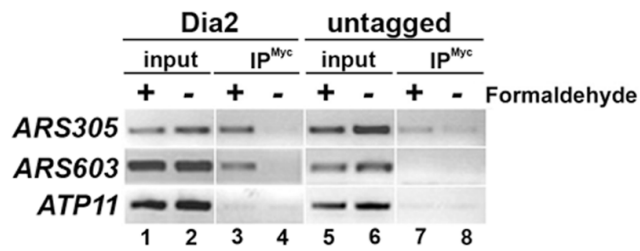
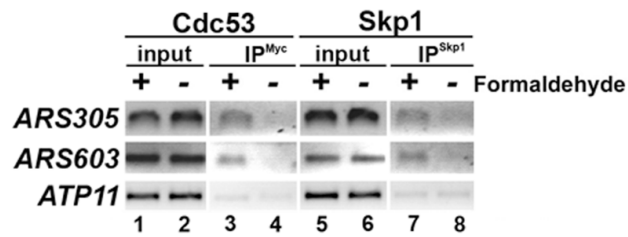
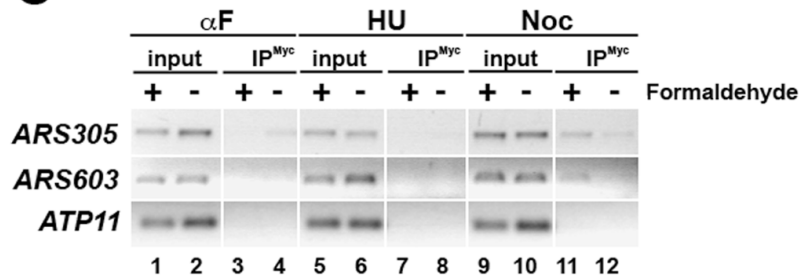
A**B****C**

Figure 4. The Dia2 protein binds replication origins. A) Chromatin immunoprecipitation was performed on the Dia2-18Xmyc tagged strain and an untagged strain. After formaldehyde crosslinking, cells were harvested and lysates prepared. Equal amounts of total protein were subjected to immunoprecipitation with anti-myc antibodies. Chromatin bound during the reaction was isolated and crosslinks were reversed prior to PCR analysis. Primers specific to *ARS305* (an early-firing origin), *ARS603* (a late-firing origin) and *ATP11* (a non-origin control) were used for PCR. B) Skp1 and Cdc53 bind origins. Chromatin immunoprecipitation was performed as in (A) using anti-Skp1 and anti-myc antibodies in a wildtype strain carrying a Cdc53-myc tagged vector. C) Dia2 binds replication origins in a cell cycle dependent manner. Chromatin immunoprecipitation was performed as in (A) except that cells were arrested in G1-, S- and M-phase by treatment with alpha factor, HU and nocodazole, respectively.

Koepp et al., Figure 5

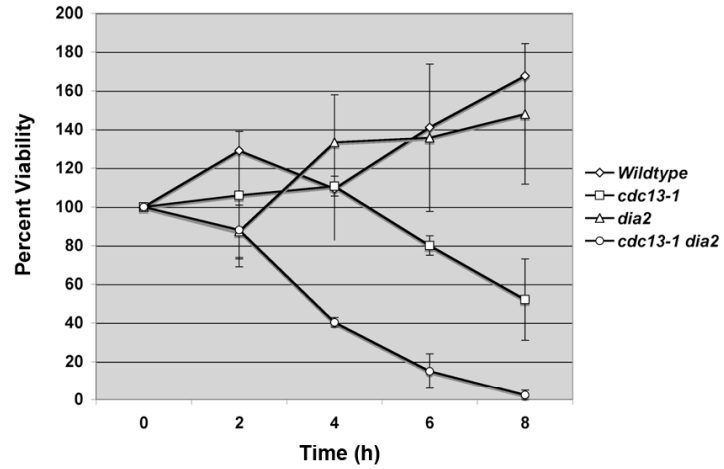
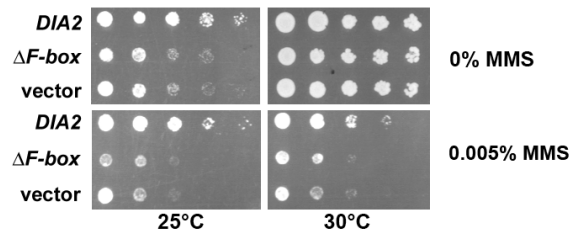
A**B**

Figure 5. *dia2* mutants are hypersensitive to DNA damage. A) The *dia2 cdc13-1* strain exhibits greater loss of viability than the *cdc13-1* strain. The indicated strains were incubated at 37°C for the indicated times. Cells were then plated on rich media and incubated at room temperature until colonies formed. Colony counts are expressed as a percentage using the 0 time point as 100%. Error bars indicate the standard deviation of at least 3 experiments. B) *dia2* mutants are sensitive to MMS. Serial dilutions of the indicated strains were spotted onto selective media containing the indicated amounts of MMS and incubated at either 25°C or 30°C.

Koepp et al., Figure 6

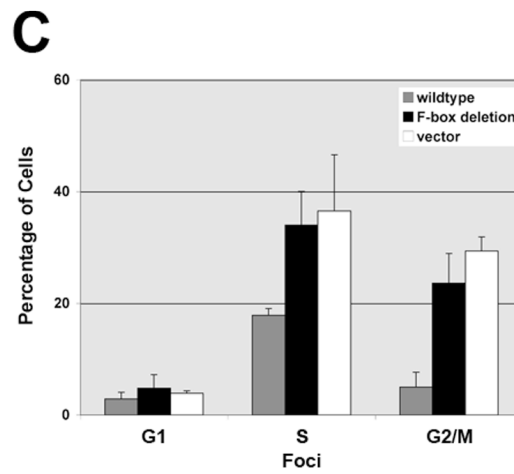
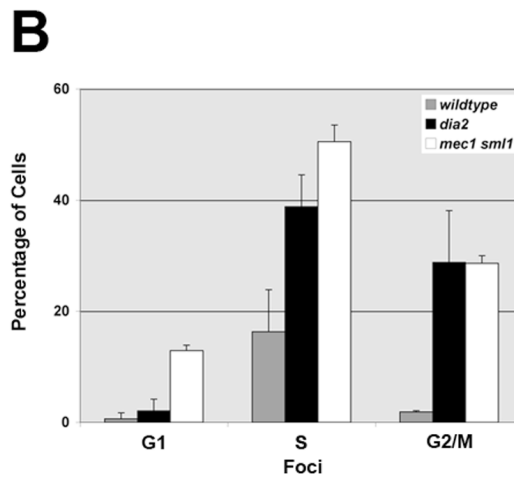
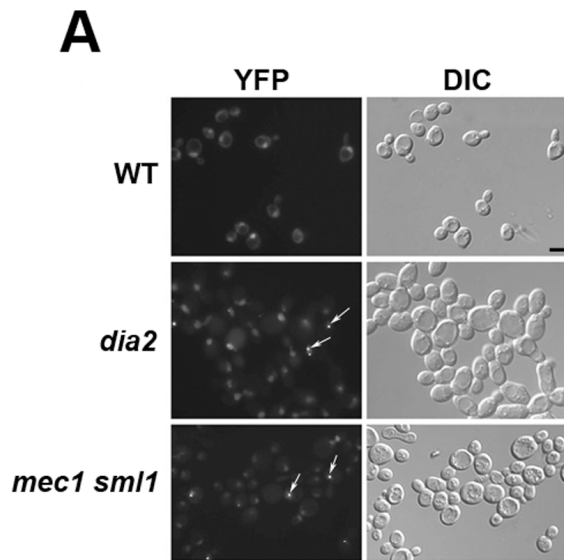


Figure 6. The *dia2* mutant accumulates Rad52-YFP foci. A) WT, *dia2* and *mec1 sml1* strains containing Rad52-YFP were grown to log phase in rich media and then examined by fluorescence and DIC (differential interference contrast) microscopy. Arrows point to examples of foci. Equal exposure times were used for all strains. The scale bar indicates 5 μ m. B) The *dia2* mutant accumulates Rad52-YFP foci in S and M phases. The number of Rad52 foci and bud morphology as a measure of cell cycle stage were counted in cells treated as in A. At least 150 cells were counted per strain. Error bars indicate the standard deviation of at least 3 experiments. C) The Δ F-box mutant accumulates Rad52 foci in S and G2/M phases. The number of Rad52 foci and bud morphology as a measure of cell cycle stage were counted in cells treated as in (A) except that the cells were grown in selective media to maintain the appropriate plasmid. At least 150 cells were counted per strain. Error bars indicate the standard deviation of at least 3 experiments.

Koepp et al., Figure 7

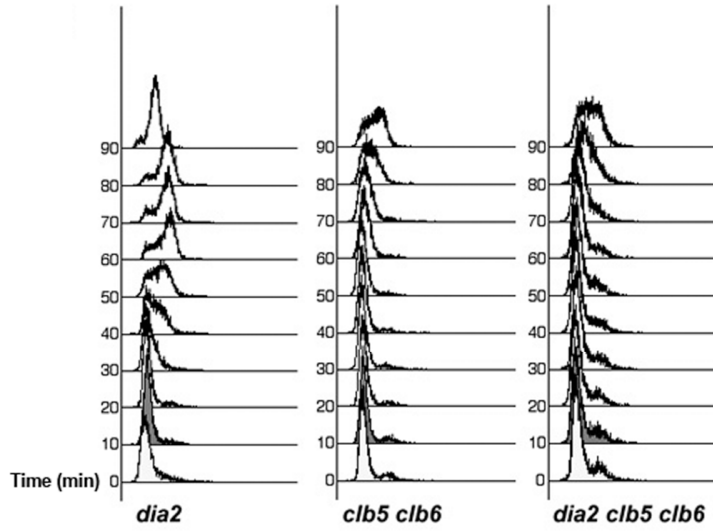
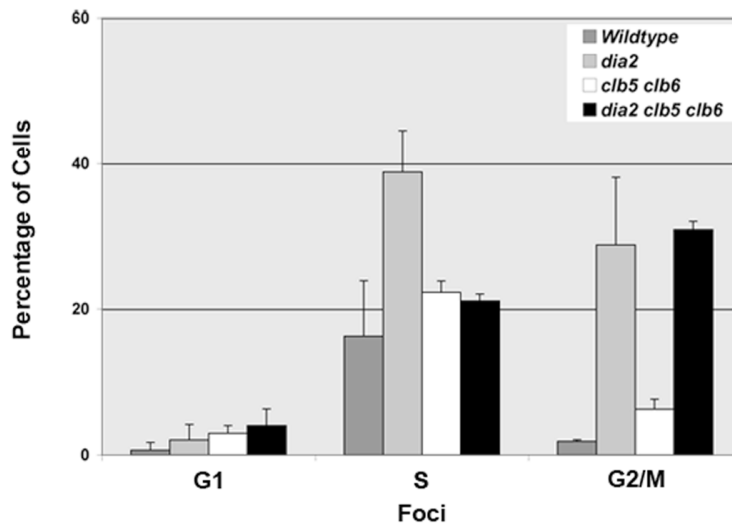
A**B**

Figure 7. Deletion of *CLB5* and *CLB6* alleviates the premature S-phase in *dia2* cells and leads to decreased S-phase damage. A) The early S-phase entry in *dia2* is dependent on Clb5 and Clb6. *dia2*, *clb5 clb6* and *dia2 clb5 clb6* cells were arrested in G1 with alpha factor and then released from arrest at 25°C. Samples were taken at the indicated time points and used for flow cytometry. B) The S-phase damage in *dia2* cells is dependent on Clb5 and Clb6. The number of Rad52 foci and bud morphology as a measure of cell cycle stage were counted in cells treated as in Figure 6. At least 150 cells were counted per strain. Error bars indicate the standard deviation of at least 3 experiments.

Supplemental Material

Materials and Methods

Overexpression studies. The galactose-inducible *CLB4* and *CLB5* constructs were gifts from S.J. Elledge (Harvard Medical School) and M. Tyers (U. Toronto), respectively. The galactose-inducible *CLB6* construct was generated by amplification of the *CLB6* gene from genomic DNA using primers DK140 and DK141. The resulting fragment was cloned into the Nde I and Bam HI sites of pUNI-10 to generate pDMK90.

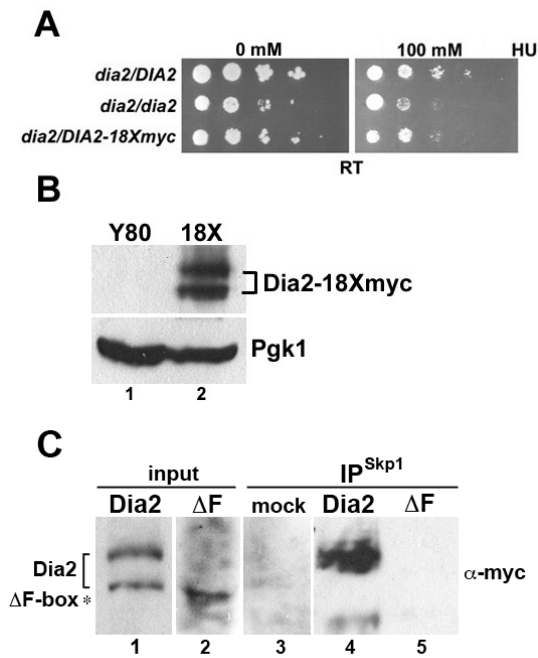
Protein expression. Extracts were prepared using a TCA extraction method. Cells were resuspended in 20% TCA and vortexed with glass beads. Precipitated proteins were resuspended in Laemmli buffer and boiled prior to resolving by SDS-PAGE.

Immunoblotting was performed with anti-myc (9E10) antibodies (Covance Research Products, Berkeley, CA) and anti-Pgk1 antibodies (Invitrogen Molecular Probes, Carlsbad, CA).

Koepp et al. Supplemental Table 1

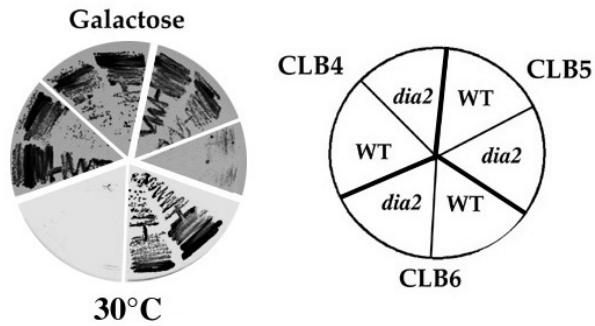
Supplemental Material Table 1. Primers used in this study

Name	Restriction site	Sequence (5'-3')
DK95	Nde I	CGCCATATGTCGTATAAATTTATTACC
DK96	Bam HI	CGGGATCCCTATGAGTATGAATATGA
DK97	Bam HI	CGGGATCCGTAAAACGACTTCTGTTC
DK98	Pst I	GAGATACTGCAGACTTGT
DK99	Pst I	ACAAGTCTGCAGTATCTC
DK100	Xho I	CCCTCGAGCGATCTATCAATGGTTGG
DK119B	Nde I	CCGCATATGGGAGAGAACCACGAC
DK120	Bam HI	GCGGGATCCCTACTTAAGATTAATAG
DK133		GCGCTTTTCCCTGTATTTAAAGCCGCTGAACACCTTTACTGAACAGGCCTCCTCTAGTACACTC
DK134		AAAATGTAAAGAGTATGCGAATTCATGAGCATTACTAGTACTAATGCGCGCCTCGTTCAGAATG
DK140	Nde I	CCGCCATATGAATTGTATCCCTAGTCC
DK141	Bam HI	CCGGATCCTCAACGTTTTTGTTTACAC
DK142		TTGAAAATTATTATTCTCTGATATTCTCTCCCTCCTTTTAAATTTTTAAACTCAGGTATCGTAAGATGCA
DK143		ATGATATTTAAGATGCAGGGGGTTAGCTGGCTATAATTTTGATCTATGTTTCACGTTGAGCCATTAGTATC
DK148		TGGTGCCAAGTTGAATTCATTGCCAACTAAATGAGTTTT
DK149		ACTGATTTAGTTGGCAATGAATTCACTTGGCACCAATA
DK176	Xho I	CTCGAGTTGCCGATAGAATACTACC
DK359	Nco I	CCATGGATGAGTATGAATATGAATTA
ATP11-1		CATTATGCGCTGTGATTCCTGTC
ATP11-2		GTGGCCTTGCAAATTCCTGGTGTAG



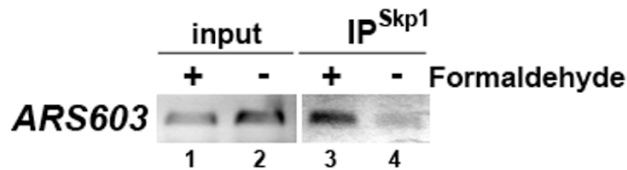
S. Figure 1. The 18Xmyc-tagged Dia2 allele is functional. A) Dia2-18Xmyc rescues the cold-sensitive and HU-sensitive defects of the *dia2* allele. Serial dilutions of the indicated diploid strains were spotted on rich media containing the indicated amounts of HU and were incubated at 25°C. B) Expression of the 18Xmyc-tagged Dia2 protein. Whole cell extracts of Y80 and the Dia2-18Xmyc strain were subjected to immunoblotting using anti-Myc antibodies. The 18Xmyc tagged Dia2 protein exists as two major forms. Anti-Pgk1 antibodies were used as a loading control. C) The Dia2 F-box deletion mutant does not bind Skp1. Skp1 was immunoprecipitated as described in the Materials and Methods section from cells expressing either wildtype Dia2 or the ΔF-box mutant tagged with 18 myc epitopes.

Koepp et al., Supplemental Figure 2



S. Figure 2. Overexpression of *CLB5* and *CLB6* is toxic to *dia2* cells. WT and *dia2* cells transformed with galactose-inducible vectors expressing *CLB4*, *CLB5* and *CLB6* were grown on selective media containing galactose at 30°C. All strains grew on selective media containing glucose (data not shown).

Koepp et al., Supplemental Figure 3



S. Figure 3. Skp1 associates with *ARS603* in nocodazole-arrested cells. Chromatin immunoprecipitation was performed as described in Materials and Methods.

CHAPTER III

Yra1 Is Required for S Phase Entry and Affects Dia2

Binding to Replication Origins

Chapter Summary

The *Saccharomyces cerevisiae* F-box protein Dia2 is important for DNA replication and genomic stability. Using an affinity approach, we identified Yra1, a transcription-coupled mRNA export protein, as a Dia2 interaction partner. We find that *yra1* mutants are sensitive to *DIA2* expression levels. Like Dia2, Yra1 associates with chromatin and binds replication origins, suggesting that they may function together in DNA replication. Consistent with this idea, Yra1 and Dia2 co-immunoprecipitate with Hys2, a subunit of DNA polymerase δ . The C-terminus of Yra1 is required to interact with Dia2. A *yra1* mutant that lacks this domain is temperature-sensitive yet has no apparent defect in RNA export. Remarkably, this mutant also fails to enter S phase at the non-permissive temperature. Significantly, other mutants in transcription-coupled export do not exhibit S phase entry defects or sensitivity to *DIA2* expression levels. Together, these results indicate that Yra1 has a role in DNA replication distinct from its role in mRNA export. Furthermore, Dia2 binding to replication origins is significantly reduced when association with Yra1 is compromised, suggesting that one aspect of Yra1's role in DNA replication may involve recruiting Dia2 to chromatin.

Introduction

The ubiquitin proteasome system plays an important role in mediating a wide variety of cellular process including cell division and DNA replication and repair. Members of the highly conserved SCF (Skp1/Cdc53/F-box protein) ubiquitin ligase family are involved in controlling cell proliferation by regulating the ubiquitin-mediated proteolysis of key cell cycle regulators (28, 50, 84, 110, 159, 160, 167, 180, 191). SCF complexes are modular ubiquitin ligases whose specificity is determined by individual F-box proteins, which act as substrate-specific adapters (50, 159). Many F-box proteins have been identified in both humans and model eukaryotic systems, suggesting that SCF pathways are a highly conserved mechanism for controlling protein function.

In *Saccharomyces cerevisiae*, the F-box protein Dia2 has been linked to DNA replication and genomic stability. The *dia2Δ* mutant is hypersensitive to DNA damage, exhibits chromosome loss and rearrangement and accumulates DNA damage foci (15, 83, 128). Two large-scale genomic analyses have identified many synthetic interactions between *dia2Δ* and mutants involved in DNA replication, replication checkpoint signaling, DNA damage and DNA repair, suggesting that Dia2 functions in one or more of these pathways (15, 128). The *Schizosaccharomyces pombe* Pof3 protein is structurally and functionally related to Dia2 (76). The *pof3* mutant also exhibits genomic instability, sensitivity to DNA damage and synthetic interactions with checkpoint genes (76, 107), suggesting that the function performed by Dia2 and Pof3 is evolutionarily conserved.

The mechanistic role that Dia2 performs in DNA replication is not known. We have found that Dia2 associates with origins of replication in a cell cycle-dependent manner,

suggesting that Dia2 may regulate DNA replication as a chromatin-bound protein (83).

Recent work suggests that Dia2 may play a role in helping replication complexes traverse the replication fork barrier at the rDNA locus (15). A third possibility is that Dia2 may link DNA replication with sister chromatid cohesion as Dia2 shows genetic interactions with the anaphase inhibitor Pds1 and Ctf4, a protein that binds DNA polymerase and is important for sister chromatid cohesion (128, 148). Intriguingly, Pof3 interacts with Mcl1, the *S. pombe* homolog of Ctf4 (107).

Dia2 is a *bona fide* F-box protein in that it assembles with Skp1, Cdc53 and Rbx1 into a functional SCF ubiquitin ligase complex (66, 83, 84, 88). Presumably the role of Dia2 in DNA replication involves targeting a substrate protein for ubiquitination, but no replication-specific targets have been identified. Indeed, little is known about Dia2 interaction partners in general, regardless of whether they might be ubiquitination targets. A large-scale proteomic analysis identified a few replication proteins and a large number of proteins involved in ribosome biogenesis as interaction partners of Dia2 (66), but the relevance of these interactions has recently been called into question (15).

Using an affinity-based approach, we have identified Yra1 as a new Dia2 interaction partner. We demonstrate that endogenous Yra1 and Dia2 co-immunoprecipitate, confirming the validity of the affinity screen. Furthermore, we find that a fraction of both Yra1 and Dia2 protein populations behave as classically defined chromatin-bound proteins. Although Yra1 has been extensively studied for its role in transcription-coupled mRNA export [TREX] (65, 69, 94, 95, 165, 168, 194, 195), we present evidence that Yra1 also has a role in DNA replication. Previous studies have found that *yra1* mutants are sensitive to the DNA replication inhibitor hydroxyurea (75) and that Yra1 contributes

to the genomic stability of transcribed sequences (142), but it is not clear if these observations are the result of a direct role in DNA replication or are secondary effects of Yra1's function in mRNA export. We find that Yra1 binds replication origins and a subunit of DNA polymerase δ . The association of Yra1 with origins occurs even after treatment with RNase A/T1 and inhibition of transcription. Importantly, we show that a *yra1* mutant that lacks 17 amino acids at the C-terminus, which has been shown to be competent for mRNA export (194), is defective in S phase entry. Significantly, other TREX mutants do not exhibit S phase entry defects or sensitivity to *DIA2* overexpression. Together, these results indicate that Yra1's role in DNA replication is distinct from its role in mRNA export. In addition, the *yra1* C-terminal truncation mutant is defective in binding Dia2. Furthermore, Dia2 association with replication origins is severely compromised in this mutant, suggesting that Yra1 may recruit Dia2 to chromatin.

Materials and Methods

Generation of strains and constructs

Saccharomyces cerevisiae strains used in this study are described in Table 1.

Yeast were maintained and cultured according to standard methods (Rose, 1990).

Plasmids *yra1-1* (gift of Ed Hurt, Heidelberg University), *HA-YRA1*, *HA-yra1 Δ ARB* and *HA-yra1-210* (gifts of Françoise Stutz, University of Geneva) were transformed into *yra1 Δ* (DKY456) and *dia2 Δ yra1 Δ* (DKY460) strains carrying a *CEN URA3 YRA1* plasmid. The transformants were then incubated on 5-FOA plates to generate DKY457, DKY458, DKY 459, DKY479 and DKY480 respectively. The strains OAY535 (*HA-MCM4*) and OAY617 (*HA-CDC45*) were provided by Anja K. Bielinsky (University of Minnesota). The pRS404-3HA-*HYS2* plasmid (gift of Anja K. Bielinsky, University of Minnesota) was linearized with EcoRI, gel purified and transformed into DKY456 and DKY408 to generate DKY473 and DKY505, respectively. The *HYS2-HA* integration and expression was verified by western blotting. The *sub2* alleles were provided by Christine Guthrie (University of California, San Francisco). The *CLB2-HA* construct was obtained from Mike Tyers (Samuel Lunenfeld Research Institute). The *DIA2* overexpression construct, pACK123, was generated by PCR amplification using primers LM31 and DK96 (Table 2) and digested with Sal I and Bam HI. The resulting fragment was cloned into the Sal I and Bam HI sites of p1223 (100).

Protein purification and mass spectrometry

The GST-Dia2 expression vector was generated by moving the Nde I – Bam HI insert from pDMK107 (83) into p1205 (100). Protein was expressed in the *E. coli* strain BL21 (DE3). Cells were grown in 4 L of LB at 37°C until O.D.600 of 0.7 and then

induced with 0.5 mM IPTG at 25°C overnight. Cells were lysed by sonication in lysis buffer (100 mM NaCl, 50 mM Tris-HCl pH 8.0, 2.5 mM EDTA, 0.1% Tween-20, 1 mM PMSF with CompleteTM protease inhibitors (Roche)). Lysed cells were centrifuged at 10,000 rpm in a Sorvall SS-34 rotor for 30 min at 4°C. Supernatant was incubated for 4 hours at 4°C with rotation with 1 mL GT-Sepharose (Amersham Pharmacia) equilibrated with lysis buffer. GT-Sepharose was washed three times with 10 volumes of lysis buffer prior to elution. GST-Dia2 was eluted in three successive incubations with 1 vol each of lysis buffer containing 15 mM glutathione. Eluted GST-Dia2 was desalted on a BioGel-P6 column (3 vol, BioRad) using 50 mM HEPES/KOH pH 7.6, 0.5 mM KCl. The GST-Dia2 protein was coupled to Affigel-10 (BioRad) according to the manufacturer's instructions.

To prepare yeast extracts, 2 L of logarithmically growing yeast cells were incubated overnight at 30°C. Cells were treated with 100 mM Tris-HCl pH 9.2, 10 mM DTT for 15 min at 30°C prior to spheroplasting. Spheroplasts were generated by incubating cells in 1 M sorbitol, 50 mM Tris-HCl pH 7.5, 50 mM MgCl₂, 50 mM CaCl₂ and 1.1 mg zymolyase 100T per g of wet cells for 30 min at 30°C. Spheroplasts were washed once in 1 M sorbitol and then centrifuged through a cushion of 2 M sorbitol at 3500xg for 15 min at 4°C. Spheroplasts were resuspended in 125 mM KOAc, 30 mM HEPES/KOH pH 7.2, 3 mM EDTA, 3 mM EGTA, 2 mM DTT, 0.5 mM PMSF and 10 µg each of pepstatin, aprotinin and leupeptin and then dropped into liquid nitrogen in a pre-cooled mortar. Cells were ground with a pestle while in liquid nitrogen. Lysed cells were thawed and centrifuged at 100,000xg for 45 min at 4°C. The supernatant was desalted on

a Biogel-P6 column (BioRad) using 50 mM Tris-HCl pH 8.0, 150 mM KCl, 0.5 mM DTT and 0.5 mM PMSF.

The GST-Dia2 column was equilibrated with 10 vol of 50 mM Tris-HCl pH 8.0, 150 mM KCl, 0.5 mM DTT and then loaded with the yeast extract. After binding, the column was washed with 10 vol of 50 mM Tris-HCl pH 8.0, 150 mM KCl, 0.5 mM DTT. Bound proteins were eluted using a step gradient of KCl, beginning at 0.2 M. Eluted proteins were precipitated with 3% TCA and resuspended in loading buffer prior to resolution by SDS-PAGE. Gels were stained with Coomassie Blue and proteins were prepared for mass spectrometry as described (186).

Co-Immunoprecipitations

Preparation of lysates was adapted from Ricke and Bielinsky, 2004. 50 ml of logarithmically growing yeast culture was harvested and cells were lysed in ChIP lysis buffer (50 mM HEPES-KOH pH 7.5, 140 mM NaCl, 1 mM EDTA, 1% Triton X100, 0.1% sodium deoxycholate, protease inhibitors (1mM PMSF and CompleteTM protease inhibitors (Roche)) by vortexing with glass beads for 40-60 minutes at 4°C. After the addition of 1mM PMSF, the samples were subjected to sonication 3 times for 10 seconds each. The lysates were recovered after 2 centrifugation steps, one for 20,000xg for 10 minutes at 4°C followed by 20,000xg for 15 minutes at 4°C. For DNase treatment of lysates, samples were incubated with 100 KU of DNase I for 45 min on ice. Anti-Myc (9E10) antibodies (Covance Research Products, Inc., Berkeley, CA), anti-HA (HA.11) antibodies (Covance Research products, Inc., Berkeley, CA) and IgG sepharose beads (Amersham) were used for immunoprecipitation. For experiments with HA-Hys2 and ProteinA-Yra1 from non-crosslinked samples, lysates were desalted on a Centricon-10

column (Millipore) using NETN (100 mM NaCl, 1 mM EDTA, 20 mM Tris-HCl, pH 8.0, 0.5% Ige-pal plus 1 mM PMSF, Complete[™] protease inhibitors (Roche), 10 mM NaF, 25 mM β -glycerophosphate). Immunoprecipitates were incubated 4 h to overnight at 4°C with rotation and then washed three times with 10 vol of NETN. For experiments with cross-linked proteins, samples were treated with formaldehyde and lysed as described for chromatin immunoprecipitations. Immunoprecipitates from formaldehyde-treated samples were washed twice in ChIP lysis Buffer, once with ChIP lysis buffer containing 500 mM NaCl and once with 10mM Tris pH 8.0, 0.25M LiCl, 0.5% Igepal, 0.5% sodium deoxycholate. Anti-Myc (9E10) and anti-HA (HA.11) antibodies (Covance Research Products, Inc., Berkeley, CA) and HRP-conjugated anti-mouse antibodies (Jackson Immunoresearch, Inc. West Grove, PA) were used for immunoblotting.

Chromatin Fractionation Assay

Chromatin fractionation was performed as described (98), with the following modifications. Strains were grown to $\sim 2 \times 10^7$ cells/ml and 1×10^9 total cells were collected. Cells were washed twice with 1X phosphate buffered saline (137 mM NaCl, 2.7 mM KCl, 10 mM Na₂HPO₄, 2 mM KH₂PO₄, pH 7.4) and incubated in 1 ml SNH buffer (400 mM Sorbitol, pH 7.5, 150 mM NaCl, 50 mM HEPES) with 10 mM DTT for 10 minutes. Cells were resuspended in 2 ml SNH + 10 mM DTT and spheroplasted with 1 mg Zymolyase -20T (ICN Biomedicals, Inc). Spheroplasting was complete when a 1:100 dilution in water at OD₆₀₀ was less than 10% of original value. Spheroplasts were washed with 1 ml SNH + 2.5 mM MgCl₂, then resuspended in SNH pre-lysis buffer (SNH +50 mM NaF, 1X Complete Protease Inhibitor Cocktail (Roche), 1mM PMSF, 2.5 mM MgCl₂). Spheroplasts were lysed by addition of Triton X-100 to 0.5% final

concentration, and incubated on ice with gentle agitation for 10 minutes to generate the whole cell extract (WCE). WCE was separated into supernatant and pellet by microcentrifugation at 12,000 rpm for 10 min at 4°C to generate soluble protein and crude chromatin pellet. The pellet was washed and resuspended to a volume equal to the supernatant with SNH lysis buffer (SNH pre-lysis + 0.5% Triton X-100). For micrococcal nuclease (MNase) treatment, the pellet from WCE centrifugation was resuspended to half volume with SNH lysis buffer. The suspension was then incubated at 37°C for 2 min, after which 1 unit MNase (Sigma) and CaCl₂ to 1 mM were added and the incubated at 37°C for an additional 1 minute. EGTA was added to a final concentration of 1 mM to halt the reaction, and the reaction microcentrifuged at 10,000 rpm for 2 min at 4°C. The pellet was digested once more as above, with 0.2 units MNase. Supernatants were combined and mixed and the pellet was resuspended to starting volume with SNH lysis buffer. Half of the MNase supernatant was centrifuged at 100,000 x g in a Beckman TLA-100.3 rotor for 1 hour at 4°C to generate high speed fractions. The supernatant was removed and the pellet resuspended with SNH lysis buffer. All pellet and supernatant fractions were brought to same cell equivalents by addition of SNH lysis buffer, and 1 volume of 2X Laemmli loading buffer added. Samples were boiled for 5 min and then microcentrifuged for 1 min prior to resolution by SDS-PAGE.

Histone association assay

Extraction and immunoprecipitation (anti-Histone H3 (Abcam) of proteins for histone association assay was performed as described (140). Proteins resolved by SDS-PAGE immunoblots were probed with anti-HA (HA.11) antibodies (Covance Research

Products, Inc., Berkeley, CA) and HRP-conjugated anti-mouse antibodies (Jackson Immunoresearch, Inc. West Grove, PA).

Chromatin Immunoprecipitation

Cultures of 50 mL logarithmically growing cells were harvested after cross-linking with 1.35 mL of 37% formaldehyde for 15 minutes. Cross-linking was quenched by the addition of glycine to 125mM. The whole cell extract was prepared for chromatin immunoprecipitation in ChIP lysis buffer as described for Co-IPs (141). Anti-HA (HA.11) antibodies (Covance Research Products, Inc., Berkeley, CA) and IgG sepharose beads (Amersham) were used for immunoprecipitation. The samples were washed twice in ChIP lysis Buffer, once with ChIP lysis buffer containing 500 mM NaCl, once with 10 mM Tris pH 8.0, 0.25 M LiCl, 0.5% Igepal, 0.5% sodium deoxycholate and finally with 1xTE. Formaldehyde cross-linking was reversed by heating the samples at 65°C for 6-12 hours followed by phenol/chloroform extraction of DNA. *ARS1*, *ARS305*, *ARS603* primers (4), Intergenic and *PMA1* promoter primers (adapted from (195) were used to amplify the immunoprecipitated DNA (Table 2). RNase (RNaseA/T1 Cocktail, Ambion) treatment of samples for the ChIP protocol was performed as described (1). Logarithmically growing yeast cells were treated with 1,10-phenanthroline (100 µg/ml final conc) for 2 h, to inhibit transcription before performing ChIP. Cell cycle arrest was induced by the addition of alpha factor, hydroxyurea (200mM), and nocadazole (15µg/ml) respectively. Cells were harvested when 90% of cells exhibited appropriate arrest.

RNA extraction and RT-PCR

Total RNA from exponentially growing cells was isolated using RNeasy® Midi kit (Qiagen Ltd). Total RNA was incubated with RQ1 Rnase-free DNase (Promega) at 37°C for 15 minutes. DNase-treated total RNA was recovered by acid phenol/chloroform (Ambion) extraction followed by ethanol precipitation. The RNA concentration and purity was calculated by measuring the absorbance at 260 and 280 nm before and after DNase treatment.

1-2 µg of total RNA was reverse transcribed using Oligo dT primers and Superscript II RT (Invitrogen) by incubating at 42°C for 1h. The reaction was terminated by incubation at 70°C for 15 minutes and then used as a template for PCR amplification.

Flow cytometry

Cells were collected and fixed in 70% ethanol for at least 30 minutes and then resuspended in PBS (140 mM NaCl, 3 mM KCl, 5 mM Na₂HPO₄, 2 mM KH₂PO₄, pH7.4) + 0.02% sodium azide. To prepare for flow cytometry, fixed cells were treated with FACS buffer (200 mM Tris-HCl, 20 mM EDTA + 0.1% RNase A) overnight at 37°C and then stained in 50 µg/ml propidium iodide in PBS. Prior to analysis, cells were diluted 10-fold in PBS and sonicated for 5 sec at 15% efficiency using a Sonic Dismembrator (Fisher Scientific, Pittsburgh, PA). Data analysis was performed with the FlowJo v6.3.3 software and graphs generated using Deltagraph 5.0.

Results

Dia2 interacts with Yra1 physically and genetically

To identify Dia2 interacting proteins, we used a biochemical affinity column approach. We generated a recombinant GST-Dia2 fusion protein construct for expression in *E. coli*. The purified GST fusion protein was coupled to Affi-gel-10 matrix and used as an affinity column for proteins extracted from a *dia2Δ* strain (Figure 1). After washing in low salt buffer, proteins were eluted from the column with increasing amounts of KCl. Eluted proteins were TCA precipitated, resuspended in loading buffer and resolved by SDS-PAGE. At 500 mM KCl, a number of proteins were observed to elute from the column. We used mass spectrometry to identify some of these proteins (186). One of the most prominent bands migrated just above the 25 kD marker (Figure 1) and was identified as Yra1 by three peptides, “LNLIVDPNQRPVK”, “EFFASQVGGVQR”, and “GQSTGMANITFK”.

To confirm that Dia2 and Yra1 interact with each other, we performed co-immunoprecipitation experiments using our 18xMyc -tagged version of Dia2 (83) and an HA-tagged allele of *YRA1* (194). As shown in Figure 1B, HA-Yra1 co-immunoprecipitates with Dia2-18xMyc. Likewise, the reciprocal immunoprecipitation indicates that Dia2-18xMyc co-immunoprecipitates with HA-Yra1. The interaction is specific as no purification is observed when mock immunoprecipitations with normal IgG are performed. The larger Dia2 form, which is close to the predicted size, interacts preferentially with Yra1 in this assay. We have observed a similar preference for interaction with the larger Dia2 form in anti-Skp1 immunoprecipitates (16). To determine whether DNA mediates the interaction between Dia2 and Yra1, we treated protein

extracts with DNase I prior to co-immunoprecipitation. As shown in Figure 1C, HA-tagged Yra1 still co-immunoprecipitates with myc-tagged Dia2 in extracts treated with DNase I. We conclude that Dia2 and Yra1 physically interact, although whether this interaction is direct or is mediated by an intermediary protein remains to be established.

A straightforward explanation for the Dia2-Yra1 interaction is that Yra1 might be a substrate of the SCF^{Dia2} complex. To test this possibility, we examined Yra1 protein turnover in wildtype and *dia2Δ* cells using a protein stability assay (Figure 1D).

Cycloheximide was added to the cells expressing HA-tagged Yra1 (165) at time 0 to stop protein synthesis. The abundance of the Yra1 protein was determined by immunoblotting protein samples collected at 30-minute intervals for 2 hours. Under these conditions we observe no change in the abundance of the Yra1 protein in either wildtype or *dia2Δ* cells. As a control, we used the mitotic cyclin Clb2. As expected, HA-tagged Clb2 was unstable in both wildtype and *dia2Δ* cells. We also examined Protein A-tagged Yra1 abundance in cells in G1, S or M phase by immunoblotting samples from wildtype and *dia2Δ* cells arrested with alpha factor, hydroxyurea or nocodazole, respectively (Figure 1E). We observe no change in Yra1 abundance under these conditions as well, suggesting that Yra1 is not a proteolytic target of the SCF^{Dia2} complex.

As Yra1 has well-documented roles in transcription-coupled mRNA export (69, 94, 95, 165, 168, 194, 195) and Dia2 has been linked to DNA replication (15, 83, 128), we were puzzled as to why they might be in a complex together. To investigate the potential role of the Dia2-Yra1 interaction, we used a number of available *yra1* mutants that exhibited different phenotypes (Figure 2A). The temperature-sensitive *yra1-1* allele exhibits an mRNA export defect as measured by an *in situ* hybridization assay for poly

A+ RNA (165). The *yra1-1* mutant carries five point mutations, two of which are in the conserved central RBD domain and two of which are in a C-terminal motif called the C-box (165). The RBD motif, also called a RRM domain, is found in many RNA-binding proteins (108). The ability of Yra1 to bind RNA *in vitro* has been mapped to two domains, an N-terminal region following the N-box and a C-terminal region upstream of the C-box (194). The *yra1 ΔRBD* mutant has the RBD domain deleted in frame whereas the C-box is deleted in the temperature-sensitive *yra1 1-210* mutant. The *yra1 ΔRBD* mutant and the *yra1 1-210* mutant exhibit indistinguishable binding to RNA *in vitro* and to an mRNA export partner protein, Mex67, when compared to wildtype Yra1 (194). However, they exhibit striking differences in growth at 37°C and in the export of poly A+ RNA from the nucleus (194). The *yra1 ΔRBD* mutant exhibits an mRNA export defect at 37°C but is viable at this temperature, whereas the *yra1 1-210* strain shows a dramatic growth phenotype but does not exhibit an mRNA export defect (194). These observations suggested that Yra1 might have an additional function.

We crossed the *yra1* mutants with a *dia2Δ* strain covered by a *DIA2 URA3* plasmid, induced sporulation of the resulting diploid, dissected tetrads and recovered the appropriate double mutant strains. We then tested these strains for growth on media containing 5-FOA to examine what happened to the cells when both *DIA2* and *YRA1* were mutated. We observed that the *dia2Δ yra1-1* and the *dia2Δ yra1 1-210* strains were inviable (Figure 2B). The *dia2Δ yra1 ΔRBD* strain was viable but exhibited slower growth than the *yra1 ΔRBD* strain alone. We also overexpressed *DIA2* in each of the *yra1* mutants. We found that overexpression of *DIA2* induced lethality in the *yra1-1* and *yra1 1-210* strains at their permissive temperature, whereas the effect of overexpression

of *DIA2* in the *yra1* Δ *RBD* strain was only moderate (Figure 2C). Thus, the strongest genetic interactions were observed between the *dia2* Δ and the *yra1-1* and *yra1 1-210* mutants. Both of these mutants are temperature-sensitive, but they exhibit different effects on mRNA export, suggesting that the role of Yra1 shared with Dia2 does not involve mRNA export.

Yra1 associates with chromatin and replication origins

As Dia2 is linked to DNA replication and genomic stability, it is possible that the Dia2-Yra1 interaction is important for these pathways. There are a number of reports that suggest Yra1 can bind chromatin in chromatin immunoprecipitation assays (1, 95) and since Dia2 binds replication origins (83), the interaction between these proteins might involve chromatin. To verify that Yra1 is chromatin-bound, we used two assays: a histone association assay (141) and a classic chromatin fractionation assay (98). The histone association assay is similar to chromatin immunoprecipitation, such that cross-linked proteins are immunoprecipitated with anti-histone H3 antibodies. After reversal of the crosslinks, immunoprecipitated proteins are resolved by SDS-PAGE and immunoblotted. As shown in Figure 3A, HA-Yra1 is efficiently immunoprecipitated in this assay as is myc-tagged Dia2. The results of the chromatin fractionation are shown in Figure 3B. As expected, a substantial amount of both Yra1 and the positive control protein Mcm4, a component of the Mcm2-7 replicative helicase complex, are released into the supernatant upon micrococcal nuclease treatment and then found in the chromatin pellet fraction after ultracentrifugation. Similar results are observed with the Dia2 protein. Together, our results confirm that Yra1 and Dia2 associate with chromatin.

We used chromatin immunoprecipitation to determine whether Yra1 binds replication origins as Dia2 does. We found that Yra1 binds *ARS305*, *ARS1* (early-firing) and *ARS603* (late-firing) sequences in a crosslinker-dependent manner (Figure 4A). As has been previously shown, Yra1 does not co-precipitate with DNA sequences from the *PMA1* promoter or an intergenic region from chromosome IV (195), indicating that the interaction with replication origins is specific.

As Yra1 has been previously shown to immunoprecipitate with the 3' end of actively transcribed genes in preparation for RNA processing and export (95) and since many origins of replication are in highly transcribed areas of the genome, we sought to determine whether Yra1 association with origins was dependent on transcription. Using an assay described by Abruzzi et al., 2004, we determined that the binding of Yra1 to *ARS305* and *ARS603* is resistant to RNase A/T1 treatment (Figure 4B). We examined Yra1 association with origins in the presence of 1,10-phenanthroline, a metal ion chelator that inhibits RNA polymerases in *S. cerevisiae* (56). As shown in Figure 4C, treatment of cells with 1,10-phenanthroline has no effect on the binding of Yra1 to *ARS1* and *ARS603* sequences (Figure 4C, top panel). To verify that the 1,10-phenanthroline inhibited transcription as reported (56), we assayed the abundance of the unstable *RPL8B* transcript by reverse transcription-PCR, using the *ACT1* transcript (actin) as a control (Figure 4C, bar graph). We quantified the results of these experiments, expressing the abundance of the *RPL8B* transcript as a percentage where the untreated sample is arbitrarily set to 100%. By this analysis, we observe a four-fold decrease in the abundance of the *RPL8B* transcript after treatment with 1,10-phenanthroline, which is similar to the decrease previously described (56). Together, these results suggest the Yra1 association with

origins is not simply a mere coincidence due to its recruitment to transcriptionally active genes.

We examined Yra1 association with origins during G1, S and M phases using chromatin immunoprecipitation from cells arrested with alpha factor, hydroxyurea or nocodazole, respectively. Yra1 showed association with the early origin *ARS305* and the late origin *ARS603* in cells arrested in all three phases, although binding during G1 may be reduced (Figure 4D). Similar results were observed with early origin *ARS607* and late origin *ARS501* (data not shown). Interestingly, the association of Dia2 with origins is strongest in M phase (83), indicating that Dia2 and Yra1 may interact on chromatin at this time.

A role for Yra1 in DNA replication

Given the association of Yra1 with Dia2 and replication origins, we asked whether Yra1 might bind other origin-binding proteins involved in DNA replication. We generated strains co-expressing Protein A-tagged Yra1 with either HA-tagged Cdc45, required for DNA replication initiation, or HA-tagged Hys2, a component of DNA polymerase δ , to use in co-immunoprecipitation experiments (5). We performed these co-immunoprecipitation experiments using protein samples from either untreated (Figure 5A) or formaldehyde-crosslinked cells (Figure 5B). We observed immunoprecipitation of HA-Hys2 with Protein A-Yra1 purified with IgG sepharose in both crosslinked and non-crosslinked samples (Figure 5A and 5B). HA-Hys2 did not independently bind to the IgG sepharose in either situation, indicating that this reaction was dependent on Yra1. Furthermore, we observed no interaction between Cdc45 and Yra1 in either situation (Figure 5A, results from crosslinked samples not shown), suggesting that Yra1 does not

promiscuously interact with HA-tagged proteins. We also examined whether Dia2 might interact with Hys2 using co-immunoprecipitation (Figure 5C). Intriguingly, a fraction of the Dia2 protein population also co-purified with HA-Hys2, suggesting that Yra1, Dia2 and Hys2 may function together in a complex.

To determine if *yra1* mutants exhibited defects in DNA replication, we performed two types of synchronization experiments. In the first, we arrested cells in late G1 phase by alpha factor treatment, released the cells from the arrest at 36°C and examined samples at 30-minute intervals by flow cytometry to assay entry into S phase. As shown in Figure 6A, both *yra1-1* and *yra1 1-210* mutants exhibit defects in S phase entry whereas the *yra1 ΔRBD* mutant enters S phase indistinguishably from wildtype cells. No obvious defects in S phase entry were observed at the permissive temperature in any of the mutants (data not shown). To determine if the *yra1* mutants were also defective for S phase progression, we released alpha-factor arrested cells into media containing hydroxyurea at the permissive temperature to allow them to enter early S phase. After 2 hours, the cells were released from HU arrest at 36°C and samples collected at 30-minute intervals were prepared for flow cytometry. In this case, all four strains renewed progression through S phase at approximately the same rate (Figure 6B). As a comparison, we performed the same experiments with the *dia2Δ* strain and observed no defects in S phase entry or progression. These results suggest that Yra1 has a role in S phase initiation but not in S phase progression.

To determine if the role of Yra1 in DNA replication was linked to the function of the TREX complex, we examined conditional alleles of another TREX subunit, Sub2 (69, 80, 166, 195). The *sub2-1* allele is temperature-sensitive and cold-sensitive, whereas the

sub2-5 allele is cold-sensitive (80). Unlike *yra1* mutants, neither *sub2* allele was sensitive to the overexpression of *DIA2* (Figure 7A). Furthermore, neither *sub2* mutant exhibited S phase entry (Figure 7B) or S phase progression defects (Figure 7C). These results strongly suggest that Yra1's role in DNA replication is independent of the role of the TREX complex.

Yra1 is important for Dia2 origin association

Intriguingly, the two *yra1* mutants that are defective in S phase entry have mutations at the C-terminus of the Yra1 protein, in the C-box. In addition, these mutants exhibit the most sensitivity to *DIA2* expression levels. We thus sought to determine if the C-box is important for binding to Dia2. We generated strains expressing Dia2-18xMyc and the HA-tagged *yra1* mutant alleles and used them in co-immunoprecipitation experiments. The protein levels of the *yra1 1-210* and *yra1 ΔRBD* mutants are indistinguishable from wildtype HA-Yra1 (194). The *yra1 1-210* mutant is severely compromised in binding myc-tagged Dia2 whereas the *yra1 ΔRBD* mutant still binds Dia2, although perhaps not quite as well as wildtype Yra1 (Figure 8B). Similar results are observed in both asynchronous and nocodazole-arrested cultures. We observe no difference in the ability of the HA-tagged proteins to be immunoprecipitated with anti-HA antibodies, indicating that the failure to co-purify Dia2 is a result of impaired binding to the Yra1 1-210 protein. These results indicate that the C-box is important in Yra1 association with Dia2.

Finally, we examined whether Dia2 could still bind replication origins when Yra1 association is compromised. We performed chromatin immunoprecipitation of myc-tagged Dia2 in the *yra1 1-210* mutant using both asynchronous and nocodazole-arrested cultures. As shown in Figure 8C, Dia2 origin association is compromised in the *yra1 1-*

210 mutant background in both asynchronous and nocodazole-arrested cells, although it is competent to bind in the *yra1* Δ *RBD* mutant background under these conditions.

Together, these results suggest that Yra1 is required to recruit Dia2 to replication origins.

Discussion

The results of our study support two main conclusions: 1) Yra1 has a role in DNA replication that is distinct from its role in mRNA export, and 2) Yra1 binding to Dia2 is important for Dia2 association with replication origins.

Yra1 functions in DNA replication

Previous work has suggested the possibility of a role for Yra1 in S phase but it has been difficult to determine whether the results observed were an indirect result of Yra1's role in mRNA export. For example, the *yra1-2* mutant has been shown to be sensitive to hydroxyurea (75). Yra1 is part of the TREX complex, which bridges transcription and mRNA export (166). TREX subunits have been shown to be important for the maintenance of genomic stability of transcribed sequences (142). Recent work indicates that mutants in the TREX subunit called Hpr1 lead to disrupted transcription and mRNP biogenesis that inhibits the movement of replication forks through areas of the genome undergoing transcription during S phase (190). As Yra1 is a member of the TREX complex, it is possible that *yra1* mutants could also lead to defective mRNP biogenesis that disrupts DNA replication. This might explain the replication defects that we observe in *yra1* mutants. However, we show that mutants in another TREX subunit, Sub2, do not exhibit S phase entry defects. Moreover, in such a role, we predict that Yra1 would be important for S phase progression and not necessarily S phase entry. Rather, our results suggest that the opposite is the case; that Yra1 is important for S phase entry but is not essential for S phase progression. Therefore, we think this possibility is unlikely.

All evidence to date suggests that the *yra1 1-210* mutant is competent for mRNA export, yet we observe an S phase entry phenotype with this mutant. The *yra1 1-210*

mutant does not accumulate poly A+ RNA in the nucleus at the non-permissive temperature (194). In addition, the *yra1 1-210* mutant behaves indistinguishably from wildtype Yra1 in its ability to bind RNA *in vitro* and to associate with the Mex67 mRNA export protein (194). In principle, it is possible that the *yra1 1-210* mutant is defective in the export of a subset of mRNAs at sufficiently low abundance that they cannot be detected by *in situ* hybridization and that this defect causes the S phase entry phenotype that we observe. However, in this situation we would expect the C-box to be important for binding such RNAs and no RNA-binding activity has been identified for the C-box domain (194).

A simpler interpretation of our results is that the functions of Yra1 in mRNA export and DNA replication are genetically separable. We demonstrate that two *yra1* temperature-sensitive mutants, *yra1-1* and *yra1 1-210*, with distinct mRNA export phenotypes exhibit defects in S phase entry from an alpha factor arrest. Intriguingly, both mutants have mutations in the C-box. The *yra1 1-210* mutant is a complete deletion of the C-box and the *yra1-1* mutant has two point mutations in this domain. Interestingly, these mutations in *yra1-1* appear to be largely responsible for the temperature-sensitive phenotype (165), which is consistent with the severe growth defect of the *yra1 1-210* mutant (194). Indeed, these results suggest that the essential function of Yra1 may be in DNA replication.

Other RNA-binding proteins have been suggested to play roles in DNA synthesis and S phase. In humans, the DNA- and RNA helicase UPF1 has shown to function in maintaining genomic stability by contributing to DNA replication and cell cycle

progression (6). In addition, transcriptional complexes are suggested to be critical determinants in proper initiation and progression of DNA replication (171).

The results presented here likely provide clues to the specific role Yra1 plays in DNA replication. Our results suggest that Yra1 functions on chromatin at replication origins. The observation that Yra1 associates with Hys2, a component of DNA pol δ , coupled with the requirement for Yra1 for S phase entry suggests that Yra1 may function at the transition from initiation to DNA synthesis. Since Yra1 still binds origins after treatment of lysates with RNaseA/T1, it is unlikely that RNA serves as an intermediate for the association with chromatin, although we cannot rule out the possibility that an RNA transcript is protected from digestion by blocking proteins. As Yra1 does not appear to associate with Cdc45, a helicase co-factor important for loading DNA polymerases α and ϵ at the origin (12), it is possible that Yra1 interacts with only a subset of proteins found at the origin during the transition to DNA synthesis.

Yra1 is important for Dia2 origin association

Our data imply that Dia2 and Yra1 function in the same pathway. Mutants in *YRA1* and *DIA2* exhibit synthetic defects, which is typically associated with function in the same or parallel pathways. Since Yra1 and Dia2 physically interact, they likely function together in the same pathway. As both proteins associate with chromatin and with replication origins, it is probable that they function together on chromatin. We demonstrate that the C-box of Yra1 is required to interact efficiently with Dia2 and that when Dia2 binding to Yra1 is compromised so is its ability to bind replication origins. Thus, Yra1 may have a role in recruiting Dia2 to replication origins.

One possibility is that Yra1 might recruit SCF^{Dia2} to replication origins to target an unknown substrate for ubiquitination. Yra1 itself is unlikely to be a substrate of SCF^{Dia2} as we observe no changes in Yra1 protein stability in *dia2Δ* mutants nor do we observe any obvious modified forms of Yra1. Finding common interaction partners of Dia2 and Yra1 may be key to determining how they function together. Large-scale proteomic analyses have not yet identified any common interaction partners of Dia2 and Yra1, but we find that both can immunoprecipitate with Hys2 (66, 86). We look forward to future studies examining further the composition of Dia2 and Yra1 complexes.

The roles that Dia2 and Yra1 play in DNA replication do not appear to be equivalent as the *yra1* temperature-sensitive mutants and the *dia2Δ* strain exhibit different S phase entry phenotypes. We show here that *yra1* mutants are defective for S phase entry. In contrast, *dia2Δ* mutants have been suggested to prematurely enter S phase (83) or to be defective in replication fork progression through the replication fork barrier at the rDNA locus (15). Thus, the role Yra1 plays in DNA replication encompasses functions in addition to recruiting Dia2 to replication origins.

Chromatin structure is likely to have a significant impact on DNA replication and a number of chromatin-remodeling complexes have been suggested to play a role in DNA replication (reviewed in (49)). We show here that a fraction of both the Yra1 and Dia2 protein populations behave as classically defined chromatin proteins. Furthermore, Yra1 has been shown to associate with chromatin at locations other than replication origins (1, 95, 195). In addition, a large scale proteomic screen has identified a number of proteins involved either in chromatin modification or DNA replication as interaction partners of Yra1 (86). Perhaps Yra1 has a general role in the assembly of complexes on chromatin

that may explain its function in DNA replication. Future work will be necessary to mechanistically define the role of Yra1 in DNA replication.

In conclusion, we have identified Yra1 as a protein that interacts both physically and genetically with the F-box protein Dia2. We demonstrate that both Dia2 and Yra1 are chromatin-associated proteins that bind replication origins. Importantly, we find that Yra1 has a novel role in DNA replication distinct from its role in mRNA export. Yra1 and Dia2 bind to a DNA pol δ subunit and *yra1* mutants are defective for S phase entry, including a temperature-sensitive allele that is competent for mRNA export. Significantly, other TREX mutants do not exhibit S phase entry defects or sensitivity to *DIA2* overexpression. Yra1 may recruit Dia2 to chromatin as the *yra1* C-terminal truncation mutant exhibits reduced binding to Dia2 and Dia2 origin association is compromised in this mutant. Together, these results broaden our understanding of S phase entry and the dynamics of chromatin-associated proteins.

Table 1. Strains used in this study

Strain	Genotype	Source
DKY194 (<i>dia2Δ</i>)	<i>dia2Δ::kanMX can1-100 ade2-1 his3-11,15 leu2-3,112 trp1-1 ura3-1 MATa</i>	Koepp et al., 2001
DKY315 (<i>yra1-1</i>)	<i>yra1Δ::HIS3 ura3 leu2 his3 trp1 ade2 MAT a</i> , carries <i>CEN TRP1 yra1-1</i>	Derived from Strasser and Hurt, 2000
DKY389 (<i>ProtA-YRA1</i>)	<i>yra1Δ::HIS3 ura3 leu2 his3 trp1 ade2 MAT a</i> , carries <i>CEN LEU2 ProtA-YRA1</i>	Derived from Strasser and Hurt, 2000
DKY390 (<i>dia2Δ ProtA-YRA1</i>)	<i>dia2Δ::kanMX yra1Δ::HIS3 ura3 leu2 his3 trp1 ade2 MAT a</i> , carries <i>CEN LEU2 ProtA-YRA1</i>	This study
DKY408 (<i>DIA2-18xMyc</i>)	<i>DIA2::DIA2-18Xmyc-HIS3 can1-100 ade2-1 his3-11,15 leu2-3,112 trp1-1 ura3-1 MATa</i>	Koepp et al., 2006
DKY410 (<i>dia2Δ yra1-1</i>)	<i>dia2Δ::kanMX yra1Δ::HIS3 ura3 leu2 his3 trp1 ade2 MAT a</i> , carries <i>CEN TRP1 yra1-1, CEN URA3 DIA2</i>	This study
DKY456 (<i>yra1Δ/YRA1</i>)	<i>yra1Δ::HIS3 ura3 leu2 his3 trp1 ade2 MAT a</i> , carries <i>CEN URA3 YRA1</i>	Derived from Strasser and Hurt, 2000
DKY457 (<i>HA-YRA1</i>)	<i>yra1Δ::HIS3 ura3 leu2 his3 trp1 ade2 MAT a</i> , carries <i>CEN TRP1 HA-YRA1</i>	Derived from Zenklusen et al., 2002
DKY458 (<i>HA-yra1ΔRBD</i>)	<i>yra1Δ::HIS3 ura3 leu2 his3 trp1 ade2 MAT a</i> , carries <i>CEN TRP1 HA-yra1ΔRBD</i>	Derived from Zenklusen et al., 2002
DKY459 (<i>HA-yra1-210</i>)	<i>yra1Δ::HIS3 ura3 leu2 his3 trp1 ade2 MAT a</i> , carries <i>CEN TRP1 HA-yra1-210</i>	Derived from Zenklusen et al., 2002
DKY460 (<i>dia2Δ yra1Δ/YRA1</i>)	<i>dia2Δ::kanMX yra1Δ::HIS3 ura3 leu2 his3 trp1 ade2 MAT a</i> , carries <i>CEN URA3 YRA1</i>	This study
DKY464 (<i>dia2Δ HA-yra1-210</i>)	<i>dia2Δ::kanMX yra1Δ::HIS3 ura3 leu2 his3 trp1 ade2 MAT a</i> , carries <i>CEN TRP1 HA-yra1-210, CEN URA3 YRA1</i>	This study
DKY472 (<i>DIA2-18xMyc yra1Δ/YRA1</i>)	<i>DIA2-18xMyc::HIS3 yra1Δ::HIS3 ura3 leu2 his3 trp1 ade2 MAT a</i> , carries <i>CEN URA3 YRA1</i>	This study
DKY473 (<i>yra1Δ/YRA1 HA-HYS2</i>)	<i>HYS2-3HA::TRP1 yra1Δ::HIS3 ura3 leu2 his3 trp1 ade2 MAT a</i> , carries <i>CEN URA3 YRA1</i>	This study
DKY479 (<i>dia2Δ HA-YRA1</i>)	<i>dia2Δ::kanMX yra1Δ::HIS3 ura3 leu2 his3 trp1 ade2 MAT a</i> , carries <i>CEN TRP1 HA-YRA1</i>	This study

DKY480 (<i>dia2Δ HA-yra1ΔRBD</i>)	<i>dia2Δ::kanMX yra1Δ::HIS3 ura3 leu2 his3 trp1 ade2 MAT a</i> , carries <i>CEN TRP1 HA-yra1ΔRBD</i>	This study
DKY482 (<i>DIA2-18xMyc HA-YRA1</i>)	<i>DIA2-18xMyc::HIS3 yra1Δ::HIS3 ura3 leu2 his3 trp1 ade2 MAT a</i> , carries <i>CEN TRP1 HA-YRA1</i>	This study
OAY535 (<i>HA-MCM4</i>)	<i>MCM4-3HA::TRP1 ura3-1 leu2-3,112 his3-11,15 trp1-1 ade2-1 can1-100 MATa bar1::hisG</i>	Aparicio et al., 1997
DKY484 (<i>HA-MCM4 ProtA-YRA1</i>)	<i>MCM4-3HA::TRP1 yra1Δ::HIS3 ura3 leu2 his3 trp1 ade2</i> , carries <i>CEN LEU2 ProtA-YRA1</i>	This study
OAY617 (<i>HA-CDC45</i>)	<i>CDC45-3HA::TRP1 ura3-1 leu2-3,112 his3-11,15 trp1-1 ade2-1 can1-100 MATa bar1::hisG</i>	Aparicio et al., 1997
DKY486 (<i>HA-CDC45 ProtA-YRA1</i>)	<i>CDC45-3HA::TRP1 yra1Δ::HIS3 ura3 leu2 his3 trp1 ade2</i> , carries <i>CEN LEU2 ProtA-YRA1</i>	This study
DKY487 (<i>HA-HYS2 ProtA-YRA1</i>)	<i>HYS2-3HA::TRP1 yra1Δ::HIS3 ura3 leu2 his3 trp1 ade2 MAT a</i> , carries <i>CEN LEU2 ProtA-YRA1</i>	This study
DKY505 (<i>DIA2-18xMyc HA-HYS2</i>)	<i>DIA2-18xMyc::HIS3 HYS2-3HA::TRP1 ura3 leu2 his3 trp1 ade2 MAT a</i>	This study
DKY506 (<i>DIA2-18xMyc HA-yra1ΔRBD</i>)	<i>DIA2-18xMyc::HIS3 yra1Δ::HIS3 ura3 leu2 his3 trp1 ade2 MAT a</i> , carries <i>CEN TRP1 HA-yra1ΔRBD</i>	This study
DKY507 (<i>DIA2-18xMyc HA-yra1 1-210</i>)	<i>DIA2-18xMyc::HIS3 yra1Δ::HIS3 ura3 leu2 his3 trp1 ade2 MAT a</i> , carries <i>CEN TRP1 HA-yra1 1-210</i>	This study
DKY508 (<i>DIA2-18xMyc HA-yra1-1</i>)	<i>DIA2-18xMyc::HIS3 yra1Δ::HIS3 ura3 leu2 his3 trp1 ade2 MAT a</i> , carries <i>CEN TRP1 HA-yra1-1</i>	This study
DKY509 (<i>SUB2</i>)	<i>sub2Δ::kanMX ura3 leu2 his3 MAT a</i> , carries <i>CEN URA3 SUB2</i>	Derived from Kistler and Guthrie, 2001
DKY510 (<i>sub2-1</i>)	<i>sub2Δ::kanMX ura3 leu2 his3 MAT a</i> , carries <i>CEN HIS3 sub2-1</i>	Derived from Kistler and Guthrie, 2001
DKY511 (<i>sub2-5</i>)	<i>sub2Δ::kanMX ura3 leu2 his3 MAT a</i> , carries <i>CEN HIS3 sub2-5</i>	Derived from Kistler and Guthrie, 2001

Table 2. Primers used in this study

Name	Sequence (5'-3')
SS-PMA1promoter-Forward	GTTACTCTCACACTCTTAGTTTCG
SS-PMA1promoter-Reverse	TTTATCAACGAGGTTGATAGAAAA
SS-Intergenic-Forward	GTGCCTGCTAGTGAAGAATACA
SS-Intergenic-Reverse	CAAGCAAGCCTTGTGCATAAGA
DK167	CATATGGCTCCAGGTAAGAAAG
DK168	GGATCCTTAAGCGAGTCGGAAGTC
DK424	GACTGACTACTTGATGAAGA
LM16	TTAGAAACACTTGTGGTGAACGATAG
LM31	GGAGTCGACGACGATGTCTATAAATTTATTACCAAGAAC
DK96	CGGGATCCCTATGAGTATGAATATGA

Swaminathan et al., Figure 1

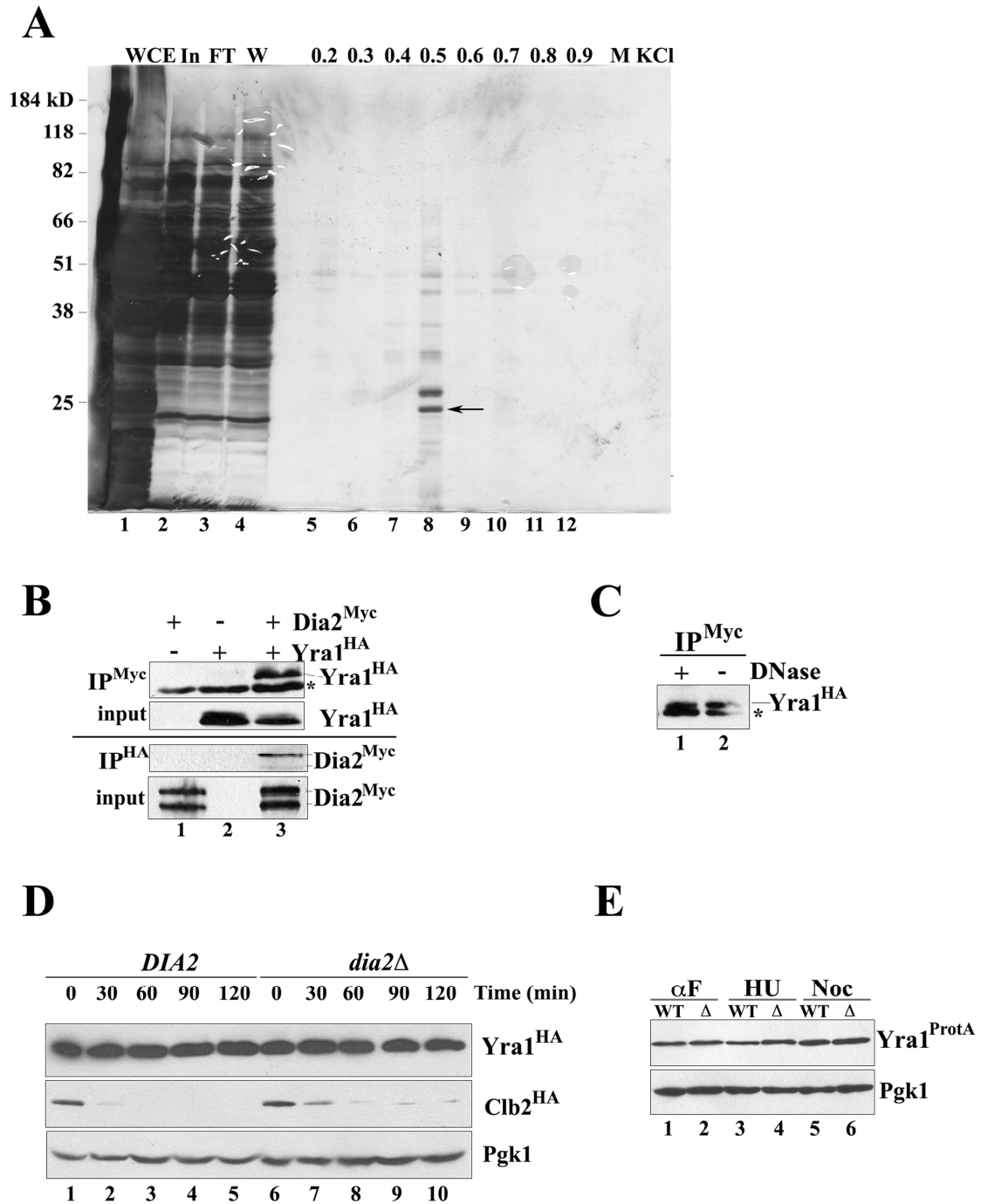


Figure 1. Dia2 binds Yra1. A) Yra1 binds a GST-Dia2 affinity column and elutes at 0.5M KCl. Recombinant GST-Dia2 was purified from *E. coli* and coupled to Affigel-10 to generate an affinity column. An extract from *dia2Δ* cells was passed over the affinity column and proteins that bound were eluted using a KCl step gradient. Eluted proteins were TCA precipitated and resolved by SDS-PAGE. The arrow indicates the Yra1 band identified by mass spectrometry. WCE=whole cell extract, In=input, FT=flow-through, W=wash. B) HA-tagged Yra1 co-immunoprecipitates with Dia2-18xMyc. Dia2-18xMyc was immunoprecipitated from lysates of the indicated strains with anti-myc antibodies and the immunoprecipitates were probed with anti-HA antibodies (top panel). The * indicates the IgG light chain. HA-Yra1 was immunoprecipitated from lysates of the indicated strains with anti-HA antibodies and the immunoprecipitates were probed with anti-myc antibodies (bottom panel). C) Yra1 and Dia2 association is resistant to DNase treatment. Immunoprecipitations were performed as in (B) except that lysates were pretreated with DNase I. D) Yra1 is a stable protein and its stability is unchanged in *dia2Δ* cells. Cycloheximide was added to the indicated strains expressing HA-tagged Yra1 and HA-tagged Clb2 at time 0. Samples were collected at the indicated time points and lysates were prepared for immunoblotting with anti-HA antibodies. The same blot was probed with antibodies against Pgk1 as a loading control. E) The abundance of Yra1 is unchanged during the cell cycle. The indicated cells were arrested with alpha factor (α F), hydroxyurea (HU) or nocodazole (Noc) and lysates prepared for immunoblotting with anti-Protein A antibodies. The same blot was probed with anti-Pgk1 antibodies as a loading control. WT=wildtype, Δ =*dia2Δ*.

Swaminathan et al., Figure 2

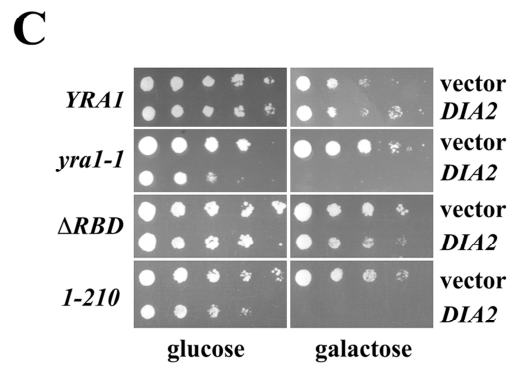
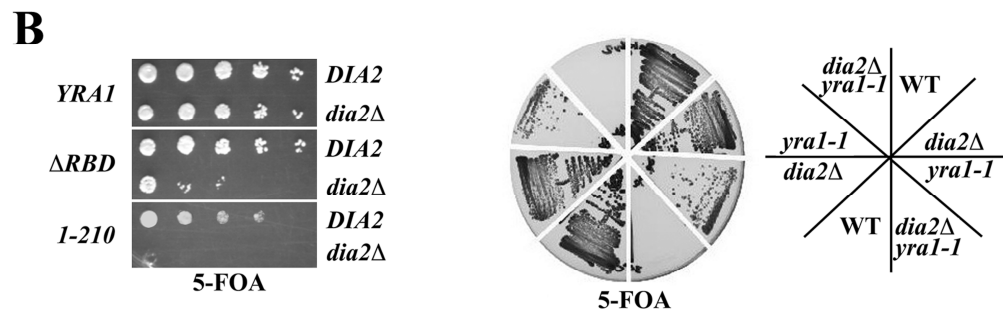
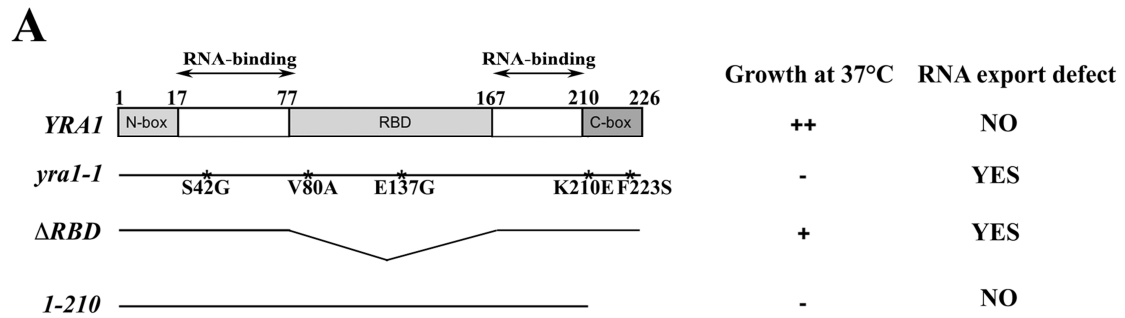


Figure 2. Dia2 interacts genetically with Yra1. A) Diagram of Yra1 domain structure and mutants used in this study. The diagram shows the changes in each mutant and indicates their growth and mRNA export phenotypes (adapted from (165, 195)). B) *dia2Δ* is synthetically lethal with *yra1-210* and *yra1-1* mutants and synthetically sick with *yra1 ΔRBD*. The indicated double mutant strains were generated by standard genetics. Either a *CEN URA3 DIA2* or *CEN URA3 YRA1* plasmid was maintained in each cross. The indicated strains were then incubated on media containing 5-FOA. The left panel shows a ten-fold dilution series of the indicated strains. The right panel shows streaks of colonies from two complete tetrads from the *dia2Δ yra1-1* cross. C) Overexpression of Dia2 from a galactose-inducible promoter is lethal to *yra1-1* and *yra1-210* mutants. The indicated strains were transformed with either an empty vector or a *DIA2* overexpression construct. Serial dilutions of cultures at equal densities were spotted on media containing glucose (as a control) or galactose to induce expression at the permissive temperature.

Swaminathan et al., Figure 3

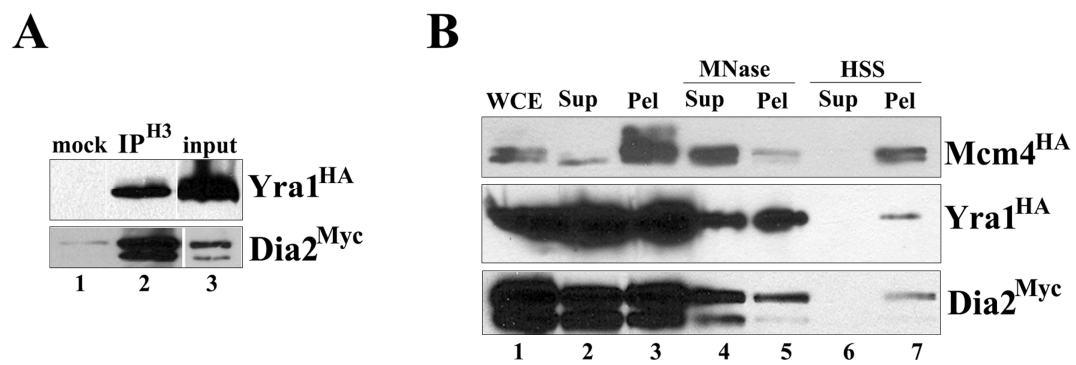


Figure 3. Yra1 and Dia2 associate with chromatin. A) HA-Yra1 (top panel) and Dia2-18xMyc (bottom panel) co-immunoprecipitate with histone H3 in a histone association assay (141). Mock immunoprecipitations were used as negative controls (lane 1). B) Yra1 and Dia2 fractionate with chromatin. Chromatin was fractionated from the indicated strains as described (98). HA-Mcm4 was used a control chromatin-bound protein. WCE=whole cell extract, Sup=supernatant, Pel=pellet, MNase=micrococcal nuclease, HSS=high-speed spin.

Swaminathan et al., Figure 4

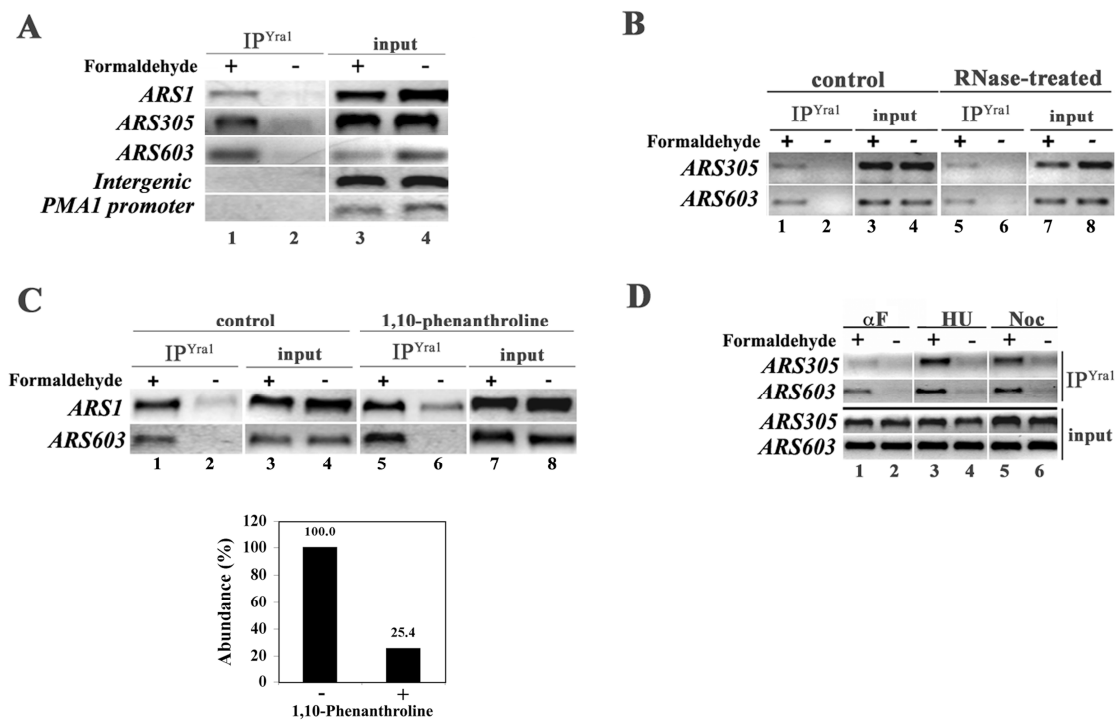


Figure 4. Yra1 associates with replication origins. A) Yra1 binds origins *ARS1*, *ARS305*, *ARS603* but not non-origin regions (intergenic and *PMA1* promoter). Chromatin immunoprecipitation was performed using either the HA-tagged Yra1 strain or the Protein A-tagged Yra1 strain. After formaldehyde crosslinking, cells were harvested and lysates prepared. Equal amounts of total protein were immunoprecipitated with anti-HA antibodies or IgG-sepharose. Chromatin was isolated and cross-links were reversed before PCR analysis. B) Yra1 origin association is not sensitive to RNase treatment. Samples were prepared as in (A) except that lysates were treated with an RNase A/T1 cocktail prior to immunoprecipitation. C) Yra1 still associates with origins after treatment with 1,10-phenanthroline (top panel). Cells were treated with 1,10-phenanthroline (100 $\mu\text{g/ml}$) or ethanol (control) for 2 hours prior to harvesting and then samples were prepared as in (A). 1,10-phenanthroline treatment leads to reduction of the unstable *RPL8B* transcript (bottom panel). Quantitation of the relative abundance, as measured by RT-PCR, of the unstable *RPL8B* transcript relative to the stable *ACT1* transcript in the presence or absence of 1,10-phenanthroline. Results are expressed as a percentage where the abundance from the untreated sample is arbitrarily set to 100%. D) Yra1 origin association in cells arrested with alpha-factor (αF), hydroxyurea (HU) or nocodazole (Noc). Cells were arrested with alpha factor, hydroxyurea or nocodazole and samples were prepared as in (A).

Swaminathan et al., Figure 5

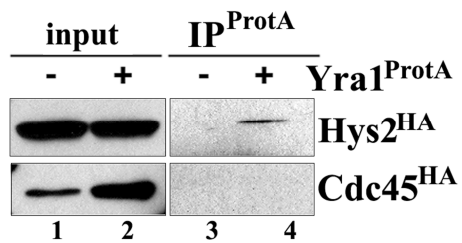
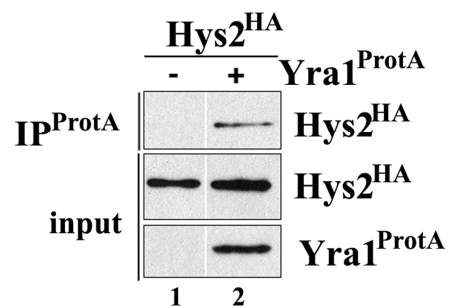
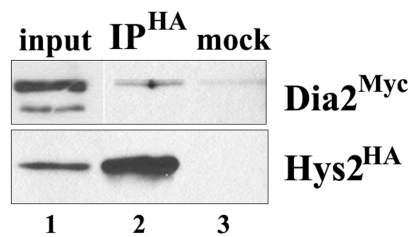
A**B****C**

Figure 5. Yra1 interacts with Hys2. A) HA-Hys2 co-purifies with Protein A-tagged Yra1 from non-crosslinked protein extracts. Protein extracts were prepared from the indicated strains and incubated with IgG-sepharose. Precipitates were immunoblotted with anti-HA antibodies. B) HA-Hys2 co-purifies with Protein A-tagged Yra1 from formaldehyde-crosslinked extracts. Protein extracts from the indicated strains were prepared as for chromatin immunoprecipitation and incubated with IgG-sepharose. Prior to resolution by SDS-PAGE and immunoblotting with anti-HA antibodies, samples were incubated at 100°C for 30 min to reverse crosslinks. C) Dia2-18xMyc copurifies with HA-Hys2 in non-crosslinked protein extracts. Protein extracts were prepared from a strain expressing both Dia2-18xMyc and HA-Hys2 and incubated with anti-HA antibodies. Precipitates were immunoblotted with anti-Myc and anti-HA antibodies.

Swaminathan et al., Figure 6

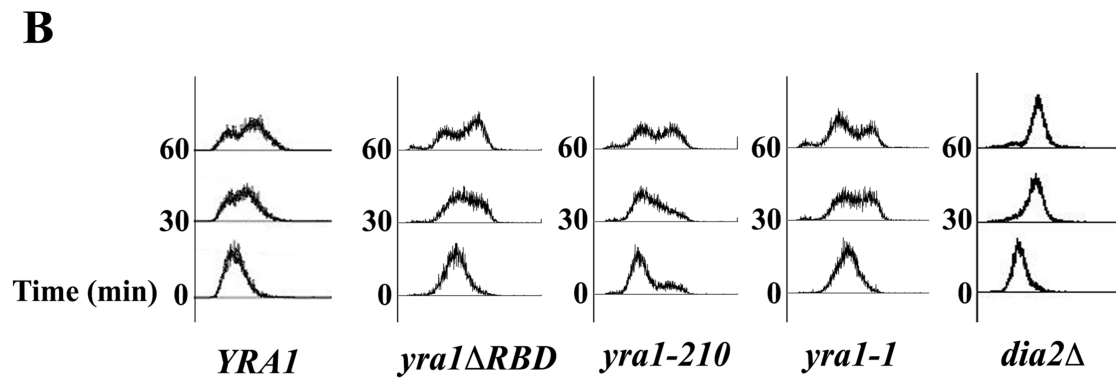
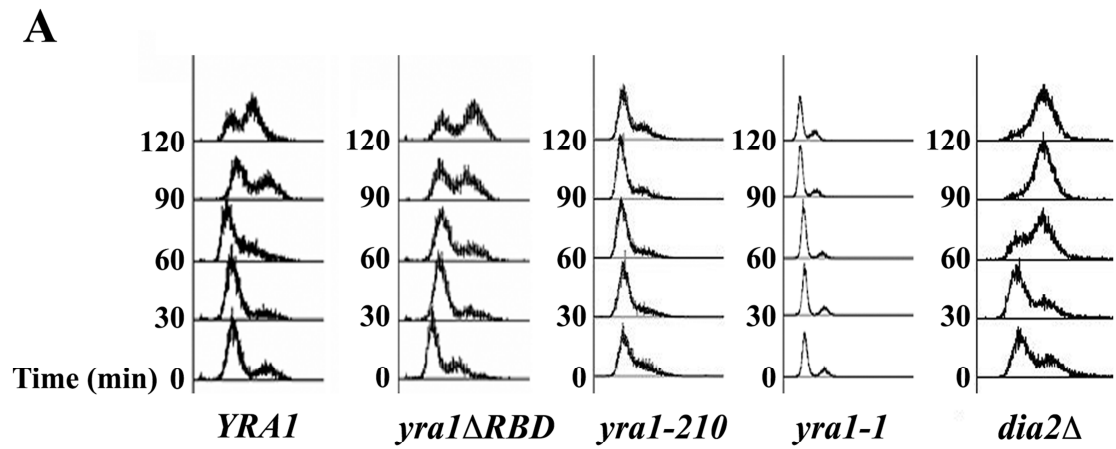


Figure 6. *yrp1* mutants are defective for S phase entry. A) The indicated strains were arrested in G1 using alpha factor at 25°C and then released at 36°C. Samples were taken at the indicated time points and prepared for flow cytometry. B) The indicated strains were first arrested in G1 with alpha factor at 25°C, then released into media containing 200 mM HU at 25°C to synchronize in early S phase. After 2 hours, the cells were released at 36°C. Samples were taken at the indicated time points and prepared for flow cytometry.

Swaminathan et al., Figure 7

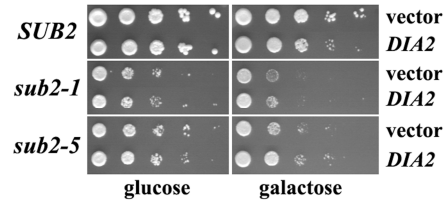
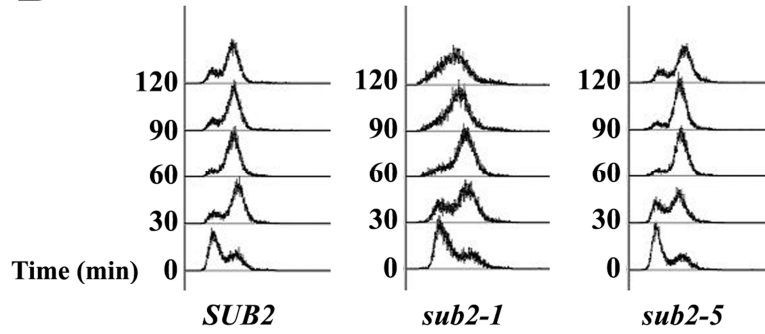
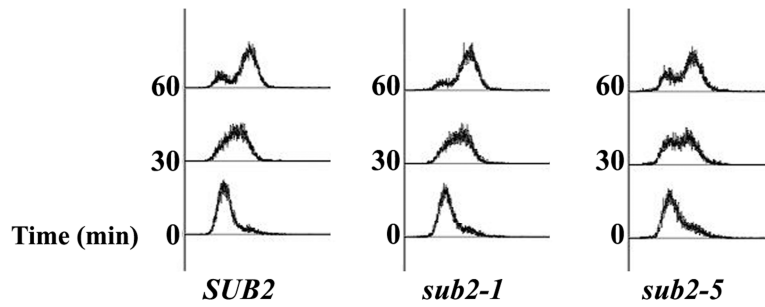
A**B****C**

Figure 7. *sub2* mutants are competent in S phase entry. A) The indicated strains were transformed with either an empty vector or a *DIA2* overexpression construct. Serial dilutions of cultures at equal densities were spotted on media containing glucose (as a control) or galactose to induce expression at the permissive temperature. B) The indicated strains were arrested in G1 using alpha factor at 30°C and then released at 36°C. Samples were taken at the indicated time points and prepared for flow cytometry. C) The indicated strains were first arrested in G1 with alpha factor at 30°C, then released into media containing 200 mM HU at 30°C to synchronize in early S phase. After 2 hours, the cells were released at 36°C. Samples were taken at the indicated time points and prepared for flow cytometry.

Swaminathan et al., Figure 8

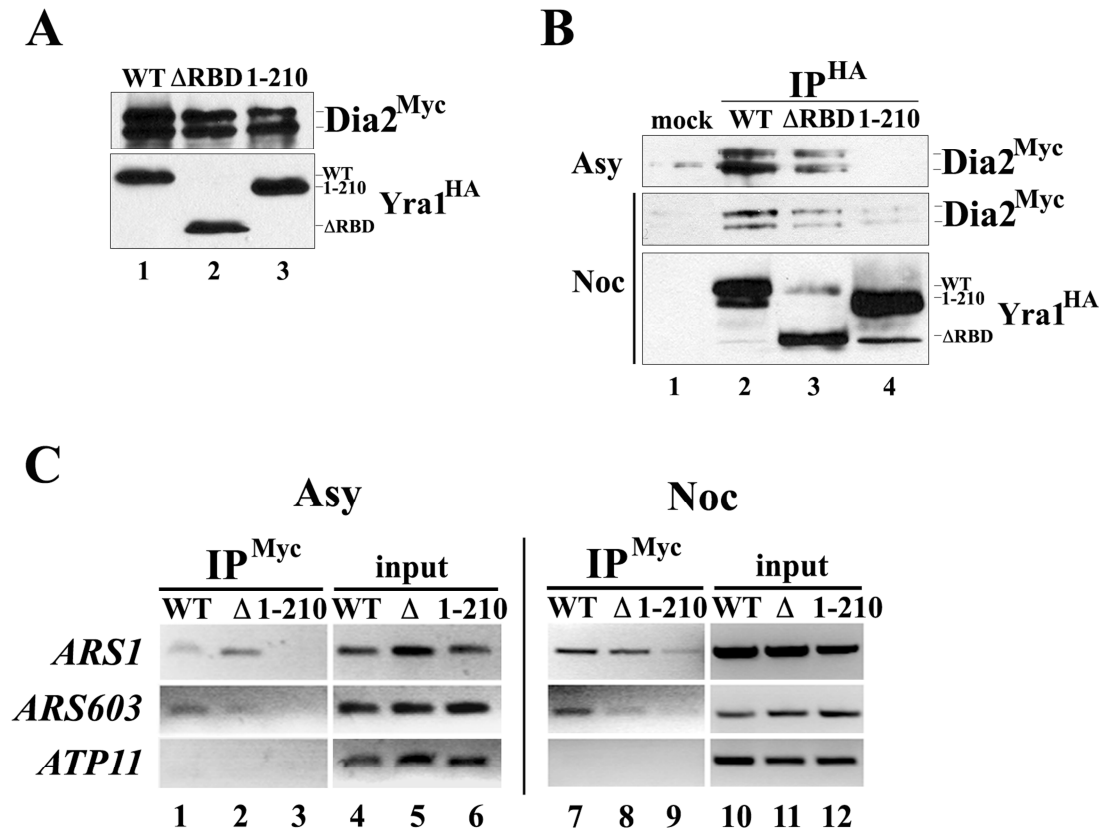


Figure 8. Binding to Yra1 is important for Dia2 origin association. A) Protein expression in the double-tagged Dia2-18xMyc HA-Yra1 strains is equivalent. Protein extracts from the indicated strains were blotted with anti-Myc (top panel) or anti-HA (bottom panel) antibodies. B) The C-box in Yra1 is important in Dia2 binding. HA-Yra1 was immunoprecipitated from lysates of the indicated strains with anti-HA antibodies and the immunoprecipitates (IP) were probed with anti-myc antibodies or anti-HA antibodies. Extracts from both asynchronous (Asy) and nocodazole-arrested (Noc) cultures were used. Mock reactions were incubated with normal IgG. Two different blots using the same samples are shown in the middle and bottom panels. C) Dia2 origin association is compromised in the *yra1 1-210* mutant. Chromatin immunoprecipitation was performed using the indicated strains as in Figure 4 except that anti-Myc antibodies were used. Extracts from both asynchronous (Asy) and nocodazole-arrested (Noc) cultures were used. WT = wildtype, Δ = *yra1* Δ RBD, 1-210 = *yra1 1-210*, IP = immunoprecipitate.

CHAPTER IV

Activation of the S-phase checkpoint inhibits degradation of the F-box protein Dia2

Chapter Summary

A stable genome is critical to cell viability and proliferation. During DNA replication, the S-phase checkpoint pathway responds to replication stress. In budding yeast, the chromatin-bound F-box protein Dia2 is required to maintain genomic stability and may help replication complexes overcome sites of damaged DNA and natural fragile regions. SCF (Skp1/Cul1/F-box protein) complexes are modular ubiquitin ligases. We show here that Dia2 is itself targeted for ubiquitin-mediated proteolysis and activation of the S-phase checkpoint pathway inhibits Dia2 protein degradation. S-phase checkpoint mutants fail to stabilize Dia2 in response to replication stress. Deletion of *DIA2* from these checkpoint mutants exacerbates their sensitivity to hydroxyurea, suggesting that stabilization of Dia2 contributes to the replication stress response. Unlike other F-box proteins, deletion of the F-box domain in Dia2 does not stabilize the protein. Rather, an N-terminal domain that is also required for nuclear localization is necessary for degradation. When a strong NLS is added to *dia2* mutants lacking this domain, the Dia2 protein is both stable and nuclear. Together, our results suggest that Dia2 protein turnover does not involve an autocatalytic mechanism and that Dia2 proteolysis is inhibited by activation of the replication stress response.

Introduction

Maintenance of genomic integrity is required for cellular viability and proliferation. During S-phase, problems during DNA synthesis or the presence of genotoxic stress activate conserved checkpoint responses (2, 18, 20, 123, 174). These pathways promote cell viability by mediating a transcriptional response (3), stabilizing replication forks (2, 77, 101, 125), suppressing late-firing origins of replication (147, 155), and slowing S-phase progression (18, 123, 133, 147). In budding yeast, sensing and activation of the S-phase checkpoint response is dependent on many proteins. Sensing of DNA damage or stalled replication forks relies on the Rad24-dependent loading of the heterotrimeric Rad17-Mec3-Ddc1 (9-1-1 complex) sliding clamp onto DNA (61, 106, 181). This leads to Mec1 kinase activation followed by the downstream activation of the primary signaling kinase Rad53 (18, 123, 174). Mec1 dependent activation of the replication checkpoint also requires the adaptor Mrc1, the *S. cerevisiae* homolog of human Claspin that forms a complex to stabilize replication forks at sites of replication stress (2, 77, 101, 125). Additionally, although Chk1 is activated by Mec1 to promote anaphase arrest following DNA damage, it has also been proposed to play a role in response to hydroxyurea (HU)-induced replication blocks (25, 146, 149).

The ubiquitin proteasome system controls a wide variety of cellular processes including cell division and DNA replication and repair. Members of the highly conserved SCF (Skp1/Cdc53/F-box protein) ubiquitin ligase family are involved in controlling cell proliferation by regulating the ubiquitin-mediated proteolysis of key cell cycle regulators (28, 50, 84, 110, 159, 160, 167, 180, 191). SCF complexes are modular ubiquitin ligases whose specificity is determined by individual F-box proteins, which act as substrate-

specific adapters (50, 159). Many F-box proteins have been identified in both humans and model eukaryotic systems, indicating that SCF complexes and their associated roles are highly conserved.

The *Saccharomyces cerevisiae* F-box protein Dia2 is important for DNA replication and genomic stability. The *dia2Δ* mutant is hypersensitive to DNA damage, exhibits chromosome loss and rearrangement and accumulates DNA damage foci (15, 83, 128). Dia2 is a *bona fide* F-box protein in that it assembles with Skp1, Cdc53 and Rbx1 into a functional SCF ubiquitin ligase complex (66, 83, 84, 88). The *dia2Δ* strain progresses more slowly through S phase than wildtype cells when challenged with the DNA-damaging agent MMS, suggesting that Dia2 promotes passage of replication complexes through areas of damaged DNA (15).

F-box proteins are key to the assembly of substrate proteins with a complete SCF ubiquitin ligase complex. There is evidence that the abundance of individual F-box proteins may be regulated to control the ubiquitination of specific target proteins. For example, some F-box proteins have been shown to be targeted for ubiquitin-mediated destruction via an auto-ubiquitination mechanism (52, 197). Conversely, loss of SCF components appears to negatively affect the stability of some F-box proteins (51, 109, 132, 162). Alternatively, F-box proteins may be targeted for destruction by non-SCF ubiquitin ligases. The human F-box protein Skp2 is a target of the APC/C ubiquitin ligase in a cell cycle-dependent manner (10). In addition, the nuclear localization of yeast Cdc4 has been shown to be important in the turnover of one of its targets, Far1 (16).

The mechanistic role that Dia2 performs in DNA replication is not known. To gain a better understanding of the activity of an SCF^{Dia2} complex throughout the cell cycle, we

examined the regulation of the Dia2 protein. Here we demonstrate that Dia2 protein abundance is controlled by ubiquitin-mediated degradation and is independent of an autocatalytic mechanism. Importantly, we find that Dia2 protein turnover is blocked by activation of the S-phase checkpoint, suggesting that SCF^{Dia2} activity is required for the cellular response to replication stress.

Materials and Methods

Plasmid and Strain Construction

Dia2 expression constructs were generated by PCR amplification of the *DIA2* coding region with SpeI and BamHI ends using oligonucleotides AK34 and DK96 (Full length), AK40 and DK96 (Δ N214), AK41 and DK96 (LRR), AK34 and AK43 (TPR), AK51 and DK96 (Δ N 189), AK62 and DK96 (Δ N149), AK72 and DK96 (SVFL), and AK73 and DK96 (SV Δ N214). The *DIA2* mutant lacking the NLS region (Δ NLS) was generated using oligonucleotides AK68 and AK69 using the PCR stitching method. The SV Δ NLS variant was generated by amplification of the Δ NLS mutant with primers AK72 and DK96. PCR products were digested with SpeI and BamHI and ligated into the p1219 vector (100) to generate galactose-inducible proteins with 9 myc epitopes at the N-termini. The p1219-myc9 Dia2- Δ F construct was generated by replacing the MluI/NotI fragment from p1219-myc9-Dia2 with a MluI/NotI fragment from pDMK289 (83). To generate the panel of 9MYC-*DIA2* integration vectors, a 1 kb KpnI/XhoI fragment of *DIA2* 5' untranslated sequence was ligated with an XhoI/NotI fragment from the generated p1219-9MYC-*DIA2* plasmids, and ligated into the pRS406 vector with KpnI/NotI ends. Constructs were integrated using BclI and transformed into *dia2* Δ cells using established techniques (143). Integration was monitored by PCR using primers AK44 and AK45 or AK60 and AK61, and protein expression determined by western blotting.

Yeast Cell Culture and Treatments

Yeast were maintained and cultured according to standard methods (143).

For α -factor arrests, cultures were grown in liquid minimal media or YPD and pulsed with 4 μ g alpha factor peptide (α F; Genscript) every hour for 2 hours. Hydroxyurea (HU; US Biological Corp.) treated cells were grown in minimal or YPD media with a final concentration of 200 mM HU for 2 hours. Cells arrested with nocodazole (Noc; Sigma) were incubated in minimal or YPD media at a final concentration of 15 μ g/mL for 2 hours. Arrests were monitored by cell morphology and flow cytometry as previously described (169). For proteasome inhibition experiments, the *9MYC-DIA2 rpn4 Δ pdr5 Δ* strain was grown overnight at 30°C in YPD. Cultures were diluted mid-log phase and incubated for 90 minutes with a final concentration of 50 μ M MG132 (Sigma) or dimethyl sulfoxide (DMSO, drug vehicle).

Reverse Transcription PCR

Cells were grown in 10 mL YPD media to 2×10^7 cells/ml and collected by centrifugation at 4000 rpm at 4°C. Cells were processed and total RNA collected using the “PureLink” micro-to-midi kit (Invitrogen). Following RNA elution, DNase I treatment was performed and the RNA was precipitated. Reverse transcription of 2 micrograms of total RNA was performed using Superscript II (Invitrogen) with oligo dT50 primer. The cDNA was used in PCR reactions with primers DK96 and AK18 or primers LM16 and DK424. Products were analyzed using on 2% agarose gels.

Stability Assays

Cells were grown at 30°C in 5mL YPD overnight, diluted to 1×10^7 cells/mL and regrown for 90 minutes. Cell densities of approximately 2×10^7 cells/mL were then used for cell

cycle arrest with appropriate chemicals as noted above. Cycloheximide (CHX; Sigma) was added to log phase cultures at a final concentration of 100 μ g/mL. Cells were collected at the indicated time points. The *9MYC-DIA2 cdc15-2* strain was shifted to 37°C for 2 hours prior to addition of CHX. Cells were collected at indicated time points and processed to extract protein using the trichloroacetic acid (TCA) precipitation method described below. Samples were resolved by SDS-PAGE and immunoblotted with anti-myc (9E10, Covance Research) and anti-Pgk1 (Molecular Probes) primary antibodies, followed by anti-mouse HRP (horse radish peroxidase) secondary antibodies. Protein abundance was quantified using Image J software and corrected against the Pgk1 loading control of the same sample. Quantifications were analyzed on images representative of abundance based upon linear film exposure times.

Immunofluorescence

Cells were prepared as described (143) and incubated with 1:500 anti-myc (9E10, Covance Research) primary antibody followed by 1:1000 FITC (fluorescein isothiocyanate)-conjugated anti-mouse antibodies. Cells were treated with 1:1000 DAPI (4',6'-diamidino-2-phenylindole) for nuclear staining. Cells were visualized using a Zeiss Axioscop 2 microscope equipped with a Zeiss AxioCam R2 digital camera and 100X objective with DIC (differential interference contrast), FITC, and DAPI filters. Images were captured using Zeiss Axiovision software release 3.1 (Carl Zeiss, Thornwood, NY).

Immunoprecipitation Experiments

For cells harboring a plasmid under galactose control, the cells were induced for 1 hour with 2% galactose at 30°C. Cell pellets were resuspended in NETN lysis buffer (20 mM Tris, pH 8.0, 100 mM NaCl, 1 mM EDTA, 0.5% Igepal, 10 mM NaF, 25 mM β -glycerophosphate, 1mM PMSF, 1mM pepstatin, plus Complete Protease inhibitor cocktail (Roche Applied Science). Cells were vortexed for 10 minutes at 4°C with glass beads. Lysates were microcentrifuged at 10000 rpm at 4°C and the cleared supernatant was transferred to new tubes. 1mg of lysate was incubated with 1:200 anti-Myc or 1:200 anti-Skp1 antibodies (a generous gift from J. Wade Harper, Harvard Medical School) (159). The samples were then incubated with protein A/G agarose for two hours at 4°C (Santa Cruz Biotechnology). Agarose beads were washed three times with NETN lysis buffer and then boiled in 1X Laemmli loading dye prior to SDS-PAGE.

Trichloroacetic Acid (TCA) Protein Precipitation

Cells pellets were lysed by vortexing in 20% trichloroacetic acid (TCA) for 2 minutes with glass beads, and microcentrifuged at 3000 RPM for 10 minutes. The precipitated protein was resuspended in 1X Laemmli loading dye and neutralized with Tris Base. Samples were boiled 5 minutes, and centrifuged at 3000 RPM for 10 minutes. Protein concentration was determined using the RCDC kit (Biorad).

Results

Dia2 is an unstable protein

We investigated Dia2 protein abundance during cell division using a strain that expresses a 9myc-tagged allele of *DIA2*. The Dia2^{Myc} strain is indistinguishable from a wildtype strain in terms of sensitivity to hydroxyurea, MMS, and growth at room temperature (Figure S1A). Additionally, Dia2^{Myc} interacts with Skp1 (Figure S1B) and chromatin (Figure S1C) as expected (169).

We monitored Dia2 protein levels in cells synchronized with alpha factor. Cells were released from an alpha factor arrest at 30°C and then alpha factor was added back at 60 minutes after entry into S phase to capture a single cell division cycle. As shown in Figure 1A, Dia2 protein abundance is initially low in late G1 but increases at 15 minutes after release, as cells move into S phase (lanes 1 and 2). The protein levels remain high until the 120-minute timepoint, after cells have returned to G1. We conclude that Dia2 protein abundance is low in late G1 and is higher during the rest of the cell cycle. A similar profile is observed when cells are synchronized using an early G1 arrest, indicating that this is not a specific response to mating pheromone (data not shown). These results are consistent with a requirement for SCF^{Dia2} activity during S phase and indeed we observe that SCF^{Dia2} complex formation occurs in cells arrested in S phase with hydroxyurea as measured by Skp1 co-immunoprecipitation (Figure 1B, lane 6). As previously reported, we observe no obvious change in mRNA transcript levels (Figure 1C) at different points in the cell cycle (31, 163). These results suggest Dia2 protein levels are modulated through a post-transcriptional mechanism.

We hypothesized that if control of Dia2 protein levels were required for normal cellular function, then we would observe a cell growth phenotype when the Dia2 protein is overexpressed. Thus, we transformed wildtype cells with a *DIA2* galactose-inducible expression vector. When Dia2 expression is induced on galactose-containing media, we find that cells exhibit a mild growth defect. Since Dia2 is important for genomic stability, we tested growth of cells overexpressing *DIA2* in the presence of the DNA damaging agent MMS. In this case we find that cells exhibit a strong growth defect (Figure 1D). These results suggest that regulation of Dia2 protein abundance is required for normal cellular function and are consistent with a proposed role for Dia2 in genomic maintenance.

We tested whether proteolysis controls Dia2 protein levels. An asynchronous culture expressing Dia2^{Myc} was grown to log phase, translation was inhibited by the addition of cycloheximide and samples were collected every 30 minutes for 150 minutes. As shown, Dia2 protein abundance decreased during the time course (Figure 1E), indicating that the Dia2 protein is unstable, with a half-life of approximately 60 minutes.

The ubiquitin-dependent proteasome pathway is a major regulatory system for proteolysis within cells. We investigated the possibility that Dia2 was targeted for destruction by the ubiquitin proteasome system by treating cells with the proteasome inhibitor MG132. The abundance of Dia2 protein increased in MG132-treated cells (Figure 1F, compares lanes 2 and 4), consistent with Dia2 proteolysis via the ubiquitin proteasome system. If Dia2 is targeted for ubiquitin-mediated proteolysis, it should be poly-ubiquitinated. To test this, 9myc-tagged Dia2 was immunoprecipitated from MG132-inhibited cells and immunoblotted using anti-myc or anti-ubiquitin antibodies.

As shown, higher molecular weight species of Dia2 accumulate in the presence of MG132, which cross-react with anti-ubiquitin antibodies (Figure 1F, lane 6 vs. 8). No ubiquitin conjugates are observed in an anti-myc immunoprecipitation from an untagged strain, indicating that the conjugates we observe are specific for Dia2. Together, our data provide evidence that the ubiquitin-proteasome pathway controls Dia2 protein turnover.

Dia2 turnover in G1 is not controlled by the SCF pathway

We next investigated which regions of Dia2 are important for regulating its turnover. A panel of domain and deletion mutants was engineered with an N-terminal 9myc epitope tag and integrated into the endogenous *DIA2* locus (Figure 2A). Protein expression was determined by western blot (Figure 2B). Each mutant protein was tested for competence in forming an SCF complex by co-immunoprecipitation with anti-Skp1 antibodies (Figure 2C). As expected, full-length Dia2 bound to Skp1, and a strong interaction was seen with the $\Delta N214$ mutant (lanes 6 and 8). We did not observe any co-immunoprecipitation of the ΔF , TPR (tetatricopeptide repeats), or LRR (leucine rich repeats) domain mutants with Skp1 (lanes 7, 9,10), which do not contain the F-box domain required for binding Skp1. None of the Dia2 deletions complement the *dia2 Δ* strain and mutant cells exhibited similar sensitivity to HU, MMS, and low temperatures (Figure 2D).

To examine the stability of the Dia2 deletion mutants, we performed stability assays in alpha-factor arrested cells. Translation was inhibited by the addition of cycloheximide and Dia2 protein abundance followed for three hours at one-hour intervals. Strikingly, both full-length Dia2 and the ΔF -box mutant exhibited similar half-lives (Figure 3A, lanes 1-4,5-8). This suggests that the previously reported *in vitro*

autoubiquitination of SCF^{Dia2} (88) does not control Dia2 protein stability *in vivo*, at least during G1. When the other mutants were analyzed it was clear that both the Δ N214 mutant and the LRR domain fragment remain stable during the time course of the experiment, whereas the TPR domain was turned over with a rate similar to wildtype (Figure 3A, lanes 9-20). This suggests that Dia2 protein turnover requires the N-terminal domain, deletion of which generates a stabilized form of Dia2.

To further examine whether Dia2 protein was turned over in an autoubiquitination pathway, we performed stability assays in SCF mutants. We determined the stability of Dia2^{Myc} in temperature-sensitive *skp1-11*, *cdc53-1*, and *cdc34-2* mutants. Cells were shifted to the non-permissive temperature of 37°C for 2 hours followed by addition of cycloheximide. Samples were collected at one-hour intervals. As shown, none of the SCF pathway mutants displayed any detectable stabilization of Dia2 (Figure 3B). Rather, the *skp1-11* and *cdc53-1* mutants appeared to increase the turnover rate of Dia2, as has been observed for the Grr1 and Met30 F-box proteins (51, 109, 132, 162). Similar results were observed in the *skp1-12* temperature sensitive strain (data not shown). By contrast, a known SCF ubiquitination target, the CDK inhibitor Sic1, was stabilized in SCF pathway mutants (Figure S2). We conclude that Dia2 proteolysis occurs independently of an autocatalytic mechanism.

Dia2 turnover requires a 20 amino acid N-terminal domain

We characterized the domain mutants for possible changes in localization (Figure 3C). Using immunofluorescence, we observed that full-length Dia2 strongly localized to the nucleus at all points in the cell cycle as expected (15). The F-box domain mutant, and the N-terminal TPR region also localized to the nucleus, suggesting that sufficient

information for nuclear targeting resides prior to the F-box domain in Dia2. Moreover, Dia2 is not required to interact with Skp1 via the F-box domain for nuclear localization to occur. By contrast, both the $\Delta N214$ mutant and leucine-rich repeat domain were mislocalized throughout the cell. However, these mutants did not appear to be excluded from the nucleus.

We considered whether Dia2 trafficking to the nucleus influenced the rate of protein turnover. To test this possibility, we sought to restore the nuclear localization of the stable, mislocalized *DIA2* mutants. Three predicted nuclear localization signals (NLS) exist in Dia2 in a cluster just upstream of the F-box domain (93). The $\Delta N214$ and LRR mutants lack all three, and are mislocalized. We therefore generated several mutants to probe the requirement for the NLS-containing region (Figure 4A). These mutants included two additional N-terminal deletions that begin before the NLS region ($\Delta N189$ and $\Delta N149$) and an in-frame deletion of the entire 20 amino acid NLS region (ΔNLS). Both the $\Delta N149$ and the $\Delta N189$ mutants localized to nucleus, whereas the ΔNLS mutant was localized throughout the cell, similar to the $\Delta N214$ mutant (Figure 4B). These results indicate that the 20 amino acid NLS domain is important for nuclear targeting and encodes at least one functional NLS.

The N-terminal mutants exhibited varying growth phenotypes. Both the $\Delta N189$ and $\Delta N149$ mutants exhibited less sensitivity to HU and MMS than *dia2* Δ cells, with the $\Delta N149$ mutant approaching near-wildtype levels of sensitivity (Figure 4C, left panel). In addition, the ΔNLS mutant is indistinguishable from wildtype under these conditions

(Figure 4C, right panel). These results indicate that the residues between 149 and 189 are critical for Dia2 protein function.

We then tested protein stability of these mutants in G1-arrested cells (Figure 4D). Interestingly, we found that the Δ NLS protein is stable, but the nuclear-localized Δ N189 and Δ N149 mutants are unstable, with turnover rates similar to wildtype Dia2. These results may be explained by a requirement for the 20-amino acid domain in both protein turnover and nuclear localization or a requirement for Dia2 to be localized to the nucleus for degradation.

To distinguish between these possibilities, we added the strong NLS sequence from the SV40 T antigen (Tag) to stable Dia2 mutants (SV Δ N214 and SV Δ NLS) and full-length Dia2 as a control (SVFL), as shown in Figure 4A. As expected, all three of these proteins localized to the nucleus by immunofluorescence (Figure 5A) and exhibited growth phenotypes nearly identical to their counterparts lacking the exogenous SV40 Tag NLS (data not shown). When we performed stability assays in G1-arrested cells with these mutants, we found that the mutants lacking the 20 amino acid NLS region are still stable, despite being localized to the nucleus via the added SV40 Tag NLS (Figure 5B). The full-length Dia2 protein with the added SV40 Tag NLS exhibited protein turnover with similar kinetics as wildtype Dia2, indicating that the addition of the exogenous NLS does not interfere with normal Dia2 protein turnover. We conclude that the N-terminal 20 amino acid region contains residues required for Dia2 protein degradation as well as nuclear trafficking.

We investigated whether overexpression of stable, nuclear forms of Dia2 interfered with cell cycle dynamics in wildtype cells. We examined the cell cycle

distribution of wildtype cells overexpressing SVFL, SV Δ N214 and SV Δ NLS from a galactose-inducible promoter using flow cytometry. Cells expressing full-length Dia2 exhibited a slight increase in the percentage of G1 cells (Figure 5C) coincident with a decrease in cells in G2/M, similar to cells overexpressing full-length Dia2 lacking this NLS (data not shown). Interestingly, cells expressing the stable, nuclear forms of Dia2 (SV Δ N214 and SV Δ NLS) exacerbated this phenotype, showing significantly increased numbers of cells in G1 and a reduced number in G2/M. These results suggest that excess Dia2 that cannot be efficiently degraded may interfere with either G1 progression or the G1-to-S phase transition.

Checkpoint activation blocks Dia2 turnover in response to HU treatment

We compared Dia2 protein stability in G1-arrested cells to cells blocked at other stages of the cell cycle. As predicted from the low abundance of Dia2 in G1 cells, we found that Dia2 protein turnover was most rapid in cells arrested with alpha factor (Figure 6A, top). Interestingly, Dia2 was also unstable in cells arrested in late M using the *cdc15-2* allele and in cells arrested prior to anaphase using the drug nocodazole (Figure 6A, lower panels). However, in hydroxyurea-arrested cells we detected very little Dia2 proteolysis under the same conditions (Figure 6A).

Because Dia2 is stable in HU-arrested cells, we considered whether activation of the S-phase checkpoint response inhibits Dia2 protein turnover. To test this, we examined Dia2 protein turnover in S-phase checkpoint mutants. If Dia2 turnover is inhibited by the S-phase checkpoint, we predicted Dia2 to be unstable in mutants that are checkpoint-defective. We inserted the 9MYC-DIA2 allele in *chk1 Δ* , *rad17 Δ* , *rad24 Δ* , *rad53-21*, and

mrc1Δ strains. Cells were treated with HU and Dia2 protein stability was assayed as previously described. Cell cycle arrest was monitored by flow cytometry (data not shown). As shown in Figure 6B, the Dia2 protein was not stabilized in any mutant (Figure 6B, top lanes 5-24). A requirement for Chk1 was unexpected, as the *chk1Δ* strain is not sensitive to HU treatment and no defect in the S-phase checkpoint response has been previously described without the presence of other mutated checkpoint genes (146, 149). To rule out an indirect effect of checkpoint mutants on Dia2 protein turnover, we examined Dia2 protein stability in these strains in G1-arrested cells and observed similar rates of turnover as in wildtype cells (Figure S3).

We furthered this analysis by testing Dia2 stability during an intra-S DNA damage checkpoint. Alpha-factor arrested cells were released into media containing MMS to activate the checkpoint and cycloheximide was added to inhibit translation. In wildtype cells, the Dia2 protein was stabilized under these conditions, whereas in the checkpoint mutant *rad53-21*, the Dia2 protein was degraded (Figure 6C, lanes 7-12). These results suggest that inhibition of Dia2 protein turnover is dependent on functional DNA damage and replication checkpoint pathways.

If Dia2 stabilization is required for the cellular response to replication stress, then removal of *DIA2* should exacerbate the phenotypes of S-phase checkpoint mutants. We and others have shown that *dia2Δ* cells exhibit synthetic growth phenotypes on normal media in combination with checkpoint mutants (15, 83, 128, 177). We tested a series of these double mutants for their sensitivity to HU, which induces replication stress. We find that deletion of *DIA2* increased sensitivity to HU in *chk1Δ*, *rad17Δ*, *rad24Δ*, and

mrc1Δ (Figure 6D). Thus, we conclude that blocking Dia2 protein turnover contributes to the cellular response to replication stress.

Altogether our results support a model (Figure 7) in which the ubiquitin-mediated destruction of Dia2 is inhibited by induction of the S-phase checkpoint. Dia2 protein levels are low in G1 due to ubiquitin-mediated turnover. This is not the result of an autoubiquitination or SCF-dependent reaction and is dependent on a 20 amino acid N-terminal domain in Dia2. These findings are consistent with previous data that suggests a role for Dia2 in DNA and genomic maintenance.

Discussion

In this study, we have found that Dia2 is an unstable protein and that it is targeted for ubiquitin-mediated proteolysis and that an N-terminal domain that is important for both degradation and nuclear localization. The turnover of the Dia2 protein does not seem to be the sole result of an auto-ubiquitination mechanism as deletion of the F-box domain does not stabilize the protein, despite the SCF^{Dia2} complex exhibiting auto-ubiquitination activity *in vitro* (88). Additionally, other F-box proteins are stabilized in SCF pathway mutants, however this is not the case for Dia2 (52, 197). Rather, Dia2 is even less stable in *skp1-11* and *cdc53-1* mutants, consistent with the observation that other F-box proteins are destabilized when core SCF components are defective (51, 109, 132, 162). Some F-box proteins are targets of other ubiquitin ligases, such as the APC/C. We anticipate that Dia2 is also the target of a non-SCF ubiquitin ligase and we look forward to future studies that identify such a ubiquitin ligase.

The observation that the same 20 amino acid domain is required for both nuclear localization and protein degradation is interesting. NLS sequences are rich in positively charged residues and the region in Dia2 contains 9 lysine residues but no arginines. It may simply be a coincidence that the NLS sequences in Dia2 could also potentially serve as ubiquitination sites. Alternatively, the regulation of Dia2 localization and ubiquitination may be intertwined. Further studies will be necessary to determine whether nuclear localization and degradation of Dia2 are linked and to dissect critical residues for each in the relevant 20 amino acid domain.

The inhibition of Dia2 protein turnover by the S-phase checkpoint is consistent with the role of Dia2 in genome maintenance and DNA replication. It has been proposed

that Dia2 may regulate the activity of replisome complexes as they move through areas of the genome that are difficult to replicate and prone to DNA damage (15). The accumulation of the Dia2 protein as cells enter S and the stabilization of the Dia2 protein in response to replication stress fit this model nicely. Our results suggest that stabilization of Dia2 occurs downstream of either Rad53 or Chk1 activation. We do not know how the S-phase checkpoint interfaces with the Dia2 protein turnover pathway. Two obvious possibilities exist: 1) Dia2 itself could be a target of the S-phase checkpoint pathway or 2) the ubiquitination pathway that controls Dia2 turnover may be regulated by the S-phase checkpoint. Regardless of the mechanism, cells are clearly sensitive to Dia2 protein levels. In the absence of Dia2, cells are hypersensitive to replication block by HU and in wildtype cells, these same conditions lead to a stabilization of Dia2 protein levels. Moreover, overexpression of Dia2 in wildtype cells leads to increased sensitivity to MMS. Together, these observations suggest that during times of replication stress, SCF^{Dia2} activity is maintained to promote genomic integrity but that there is an optimal level of SCF^{Dia2} activity. One mechanism used to control SCF^{Dia2} activity appears to be regulation of the abundance of the Dia2 protein itself.

In summary, by studying the regulation of the F-box protein Dia2, we have found that it is targeted for proteolysis by a ubiquitin-mediated pathway. The turnover of Dia2 is distinct from other F-box proteins in that it is independent of an auto-ubiquitination mechanism. Dia2 protein turnover is inhibited by the activation of the S-phase checkpoint and we propose that SCF^{Dia2} activity is required for the cellular response to replication stress.

Table 1. Strains used in this study

Strain	Description	Source
Y80	<i>MATa can1-100 ade2-1 his3-11,15 leu2-3,112 trp1-1 ura3-1</i>	Bai et al. (1996)
DKY194	as Y80 but <i>dia2Δ::kanMX</i>	Koepp et al. (2001)
AKY149	as DKY194 but <i>dia2Δ::kanMX::9MYC-DIA2 URA3</i>	This Study
AKY182	as AKY149 but <i>cdc15-2</i>	This Study
AKY184	as AKY149 but <i>MCM4::MCM4-3HA TRP1</i>	This Study
AKY168	as AKY149 but <i>rpn4Δ::HIS3 pdr5Δ::LEU2</i>	This Study
AKY188	as AKY149 but <i>DIA2-ΔF</i> (bp Δ670-792)	This Study
AKY189	as AKY149 but <i>DIA2-ΔN214</i> (bp 640-2241)	This Study
AKY190	as AKY149 but <i>DIA2-LRR</i> (bp 793-2241)	This Study
AKY192	as AKY149 but <i>DIA2-TPR</i> (bp 1-669)	This Study
AKY193	as AKY149 but <i>DIA2-ΔN189</i> (bp 565-2241)	This Study
AKY199	as AKY149 but <i>DIA2-ΔN149</i> (bp 447-2241)	This Study
AKY238	as DKY194 but <i>dia2Δ::kanMX::9MYC-SV40NLS-DIA2 URA3</i>	This Study
AKY239	as AKY149 but <i>DIA2-ΔNLS</i> (bp Δ580-639)	This Study
AKY240	as AKY238 but <i>DIA2-ΔNLS</i> (bp Δ580-639)	This Study
AKY241	as AKY238 but <i>DIA2-ΔN214</i> (bp 640-2241)	This Study
DKY404	as Y80 but <i>dia2Δ::kanMX chk1Δ::HIS3</i>	Koepp et al. (2006)
DKY405	as Y80 but <i>dia2Δ::kanMX mrc1Δ::HIS3</i>	Koepp et al. (2006)
DKY449	as Y80 but <i>dia2Δ::kanMX rad17Δ::kanMX</i>	Koepp et al. (2006)
DKY450	as Y80 but <i>dia2Δ::kanMX rad24Δ::kanMX</i>	Koepp et al. (2006)
AKY203	as DKY404 but <i>dia2Δ::kanMX::9MYC-DIA2 URA3</i>	Koepp et al. (2006)
AKY204	as DKY449 but <i>dia2Δ::kanMX::9MYC-DIA2 URA3</i>	This Study
AKY205	as DKY450 but <i>dia2Δ::kanMX::9MYC-DIA2 URA3</i>	This Study
AKY206	<i>rad53-21</i> but <i>DIA2::9MYC-DIA2 URA3</i>	This Study
AKY207	as DKY405 but <i>dia2Δ::kanMX::9MYC-DIA2 URA3</i>	This Study
AKY170	as AKY149 but <i>skp1-11</i>	This Study
AKY174	as AKY149 but <i>cdc53-1</i>	This Study
AKY180	as AKY149 but <i>cdc34-2</i>	This Study

Table 2. Plasmids used in this study

Plasmid	Relevant Features	Source
p1219	<i>GAL1,10 promoter CEN TRP1 AMP^R</i>	Liu et al., 1998
pACK135	<i>GAL1,10 promoter 9MYC-DIA2 CEN TRP1 AMP^R</i>	This Study
pACK136	<i>GAL1,10 promoter 9MYC-DIA2-ΔF CEN TRP1 AMP^R</i>	This Study
pACK137	<i>GAL1,10 promoter 9MYC-DIA2-ΔN214 CEN TRP1 AMP^R</i>	This Study
pACK138	<i>GAL1,10 promoter 9MYC-DIA2-LRR CEN TRP1 AMP^R</i>	This Study
pACK140	<i>GAL1,10 promoter 9MYC-DIA2-TPR CEN TRP1 AMP^R</i>	This Study
pACK154	<i>GAL1,10 promoter 9MYC-DIA2-ΔN189 CEN TRP1 AMP^R</i>	This Study
pACK171	<i>GAL1,10 promoter 9MYC-DIA2-ΔN149 CEN TRP1 AMP^R</i>	This Study
pACK176	<i>GAL1,10 promoter 9MYC-SV40NLS-DIA2 CEN TRP1 AMP^R</i>	This Study
pACK177	<i>GAL1,10 promoter 9MYC-DIA2-ΔNLS CEN TRP1 AMP^R</i>	This Study
pACK178	<i>GAL1,10 promoter 9MYC-SV40NLS-DIA2-ΔNLS CEN TRP1 AMP^R</i>	This Study
pACK179	<i>GAL1,10 promoter 9MYC- SV40NLS-DIA2-ΔN CEN TRP1 AMP^R</i>	This Study
pACK142	pRS406 1kb 5' <i>DIA2 UTR 9MYC-DIA2 URA3 AMP^R</i>	This Study
pACK143	pRS406 1kb 5' <i>DIA2 UTR 9MYC-ΔF-DIA2 URA3 AMP^R</i>	This Study
pACK144	pRS406 1kb 5' <i>DIA2 UTR 9MYC-ΔN214-DIA2 URA3 AMP^R</i>	This Study
pACK145	pRS406 1kb 5' <i>DIA2 UTR 9MYC-DIA2-LRR URA3 AMP^R</i>	This Study
pACK147	pRS406 1kb 5' <i>DIA2 UTR 9MYC-DIA2-TPR URA3 AMP^R</i>	This Study
pACK155	pRS406 1kb 5' <i>DIA2 UTR 9MYC- DIA2-ΔN189 URA3 AMP^R</i>	This Study
pACK174	pRS406 1kb 5' <i>DIA2 UTR 9MYC- DIA2-ΔN149 URA3 AMP^R</i>	This Study
pACK181	pRS406 1kb 5' <i>DIA2 UTR 9MYC- SV40NLS-DIA2 URA3 AMP^R</i>	This Study
pACK182	pRS406 1kb 5' <i>DIA2 UTR 9MYC- DIA2- ΔNLS URA3 AMP^R</i>	This Study
pACK183	pRS406 1kb 5' <i>DIA2 UTR 9MYC- SV40NLS-DIA2-ΔNLS URA3 AMP^R</i>	This Study
pACK184	pRS406 1kb 5' <i>DIA2 UTR 9MYC- SV40NLS-DIA2-ΔN URA3 AMP^R</i>	This Study

Table 3. Oligonucleotides used in this study

Oligo	Sequence 5' → 3'
LM16	<i>TTAGAAACACTTGTGGTGAACGATAG</i>
DK424	<i>GACTGACTACTTGATGAAGA</i>
AK34	<i>GCGACTAGTATGTCGTATAAATTT</i>
DK96	<i>CGGGATCCCTATGAGTATGAATATGA</i>
AK40	<i>GGACTAGTACCAAGAAAAC</i>
AK41	<i>GGACTAGTTTCAACTTGGCACCA</i>
AK43	<i>CCGGATCCCTAATTGCCAACTAAATC</i>
AK44	<i>AAACGGATTCATCATGAG</i>
AK45	<i>GCCACGCCTGAATTCCCTG</i>
AK51	<i>GGACTAGTGAGACCAAAATAGCA</i>
AK60	<i>TTGTTCACTACTAGCCATGG</i>
AK61	<i>GCAGTACGATATCACCAACGG</i>
AK68	<i>GAGGAGACCAAAATAAGTACCAAGAAAAC</i>
AK69	<i>AGTTTTCTTGGTACTTATTTTGGTCTCCTC</i>
AK70	<i>TGTTCTCGTGGACTGGAGGAGACCAAAATA</i>
AK71	<i>TATTTTGGTCTCCTCCAGTCCACGAGAACA</i>
AK72	<i>GGACTAGTCCGAAGAAGAAACGGAAGGGTATGTCGTATAAATTT</i>
AK73	<i>GGACTAGTCCGAAGAAGAAACGGAAGGGTAGTACCAAGAAAAC</i>

Kile and Koepf, Figure 1

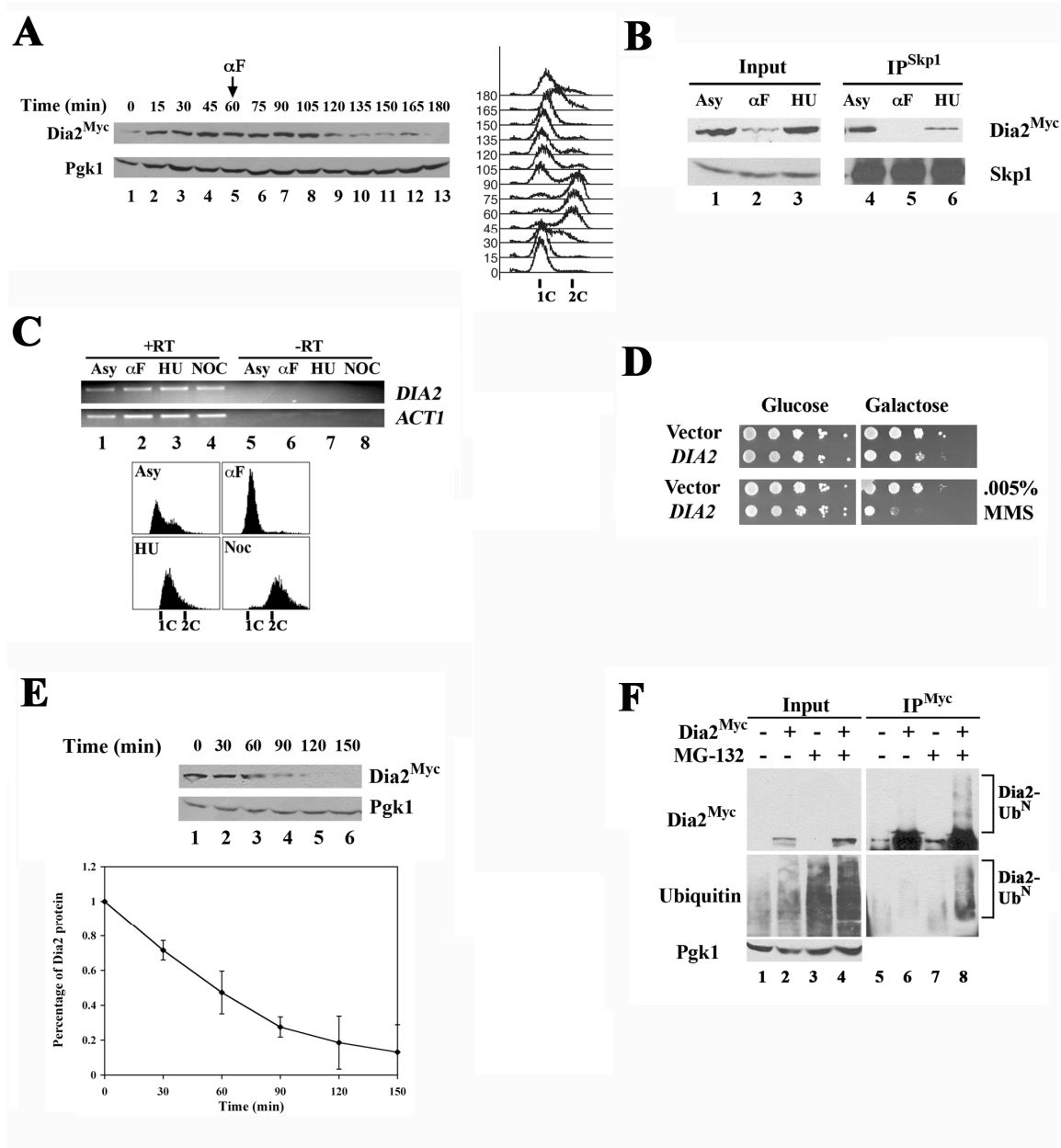


Figure Legends

Figure 1. Dia2^{Myc} protein abundance fluctuates throughout the cell cycle. A) Dia2 protein levels in synchronized cells. The *9MYC-DIA2* strain was synchronized in G₁ with alpha-factor pheromone and released into rich media at 30°C. After 60 minutes α F was added back to the media for re-arrest in G₁. Immunoblots were probed with anti-myc or anti-Pgk1 antibodies (as a loading control). Cell cycle progression was monitored by flow cytometry. B) Dia2^{Myc} associates with Skp1 during S-phase. Skp1 was immunoprecipitated with anti-Skp1 antibodies (159) from Dia2^{Myc} lysates from asynchronous (Asy), alpha-factor (α F), or HU-arrested cultures. Immunoblots were probed with anti-myc or anti-Skp1 antibodies. C) *DIA2* transcript abundance does not fluctuate. Total RNA was extracted and RT-PCR was performed as described in Materials and Methods. *ACT1* was monitored as a control. Cell cycle stage was monitored by flow cytometry. D) *DIA2* overexpression leads to a growth defect in the presence of MMS. Wildtype cells containing empty vector or *DIA2* under the control of the *GAL1,10* promoter were spotted in 10-fold serial dilutions to minimal media with 2% glucose or 2% galactose. Plates were incubated at room temperature. MMS was included at the indicated amount. E) Dia2 is an unstable protein. Dia2^{Myc} cells were treated with 100 μ g/mL CHX and samples taken every 30 minutes. Samples were immunoblotted with anti-Myc antibodies and anti-Pgk1 antibodies were used to control for loading. Quantitation of three independent experiments is shown on the graph. F) Dia2^{Myc} is ubiquitinated. WT or Dia2^{Myc} cells were treated with DMSO (lanes 1-2) or MG132 (lanes 3-4) for 90 minutes and immunoprecipitated with anti-myc antibodies (lanes 5-8)

and immunoblotted with anti-myc or anti-ubiquitin antibodies. Pgk1 was monitored as a loading control.

Kile and Koepp, Figure 2

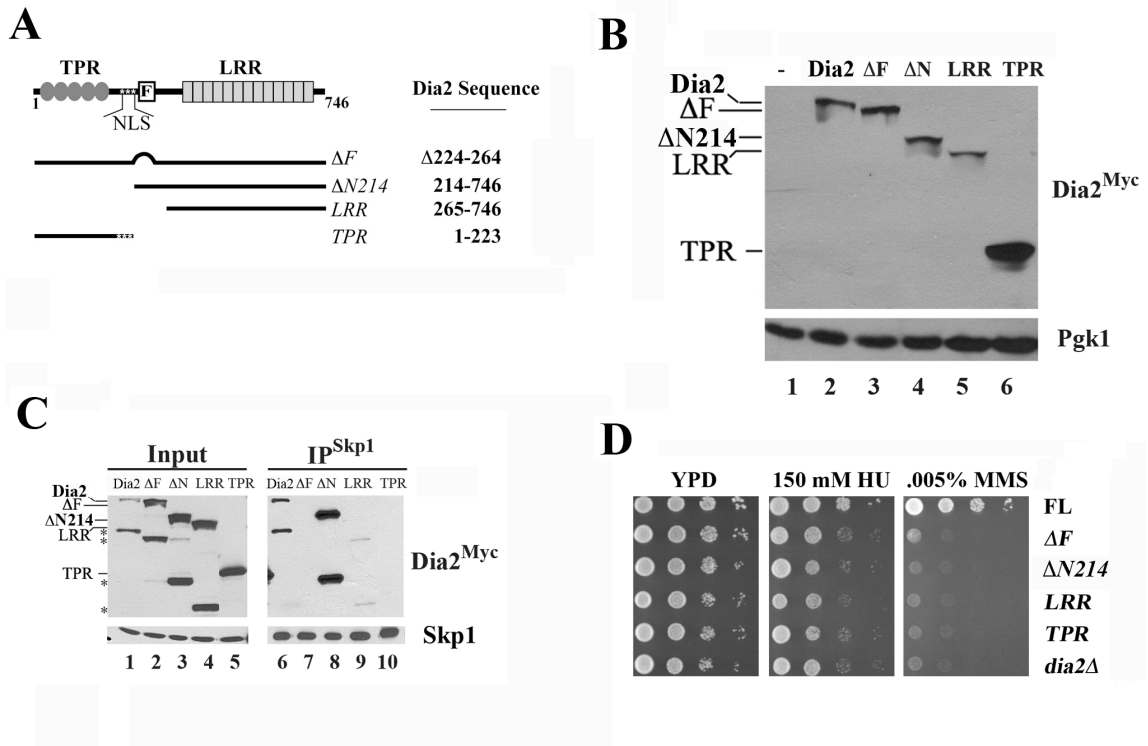


Figure 2. Analysis of Dia2 mutants. A) Diagram of Dia2 domains and mutants used in this study. Relevant amino acid residues or changes are indicated. TPR = Tetratricopeptide repeats, F = F-box domain, LRR = Leucine Rich repeats, NLS = nuclear localization sequence. B) Expression of Dia2 deletion mutants. Asynchronous strains expressing Dia2^{Myc} (lane 2) or the various mutants (lanes 3-6) were grown at 30°C and collected. TCA precipitates were prepared as described in Materials and Methods and immunoblotted with anti-myc or anti-Pgk1 antibodies. Extract from a wildtype strain was included as an untagged control (lane 1). C) Mutants lacking the F-box do not associate with Skp1. Dia2 mutants were expressed from plasmids using the *GALI,10* promoter and co-immunoprecipitated with anti-Skp1 antibodies. Immunoblots were probed with anti-myc or anti-Skp1 antibodies. The identity of the protein in each band is indicated. Asterisks (*) indicate breakdown products. D) Dia2 mutants do not rescue *dia2Δ* phenotypes. Strains expressing integrated Dia2^{Myc} and variants were spotted to YPD plates containing the indicated amounts of hydroxyurea (HU) or MMS in 10-fold dilution series. Plates were grown at room temperature.

Kile and Koepp, Figure 3

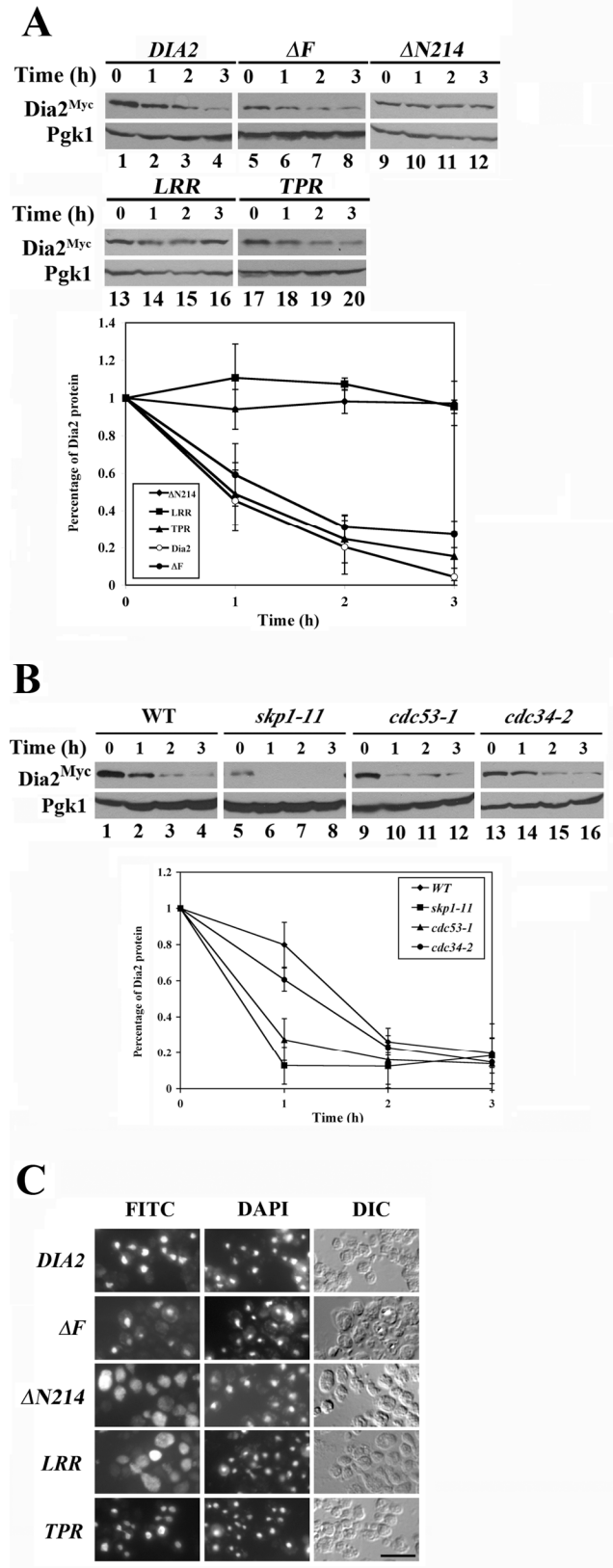


Figure 3. Dia2 protein turnover is not controlled by the SCF pathway. A) N-terminal deletion mutants of Dia2 are stabilized. Dia2^{Myc} strains were treated with alpha-factor for 2 hours and translation inhibited by CHX. The indicated time points (h=hours) were collected after inhibition and protein samples were resolved on SDS-PAGE prior to immunoblotting with anti-myc antibodies. Pgk1 was monitored as a loading control. Quantitation of three independent experiments is shown on the graph. B) Turnover of Dia2 does not require the SCF pathway. The 9MYC-DIA2 allele was inserted into *skp1-11*, *cdc53-1*, and *cdc34-2* strains. Cultures were grown in YPD at 25°C and shifted to 37°C for 2 hours prior to the addition of CHX. Samples were collected at the indicated times and immunoblotted with anti-myc or anti-Pgk1 antibodies. Quantitation of three independent experiments is shown on the graph. C) Deletion of the N-terminal region mislocalizes Dia2. Dia2 variants were expressed in *dia2Δ* cells and protein was visualized by immunofluorescence as described in Materials and Methods. Scale bar, 5μm.

Kile and Koepf, Figure 4

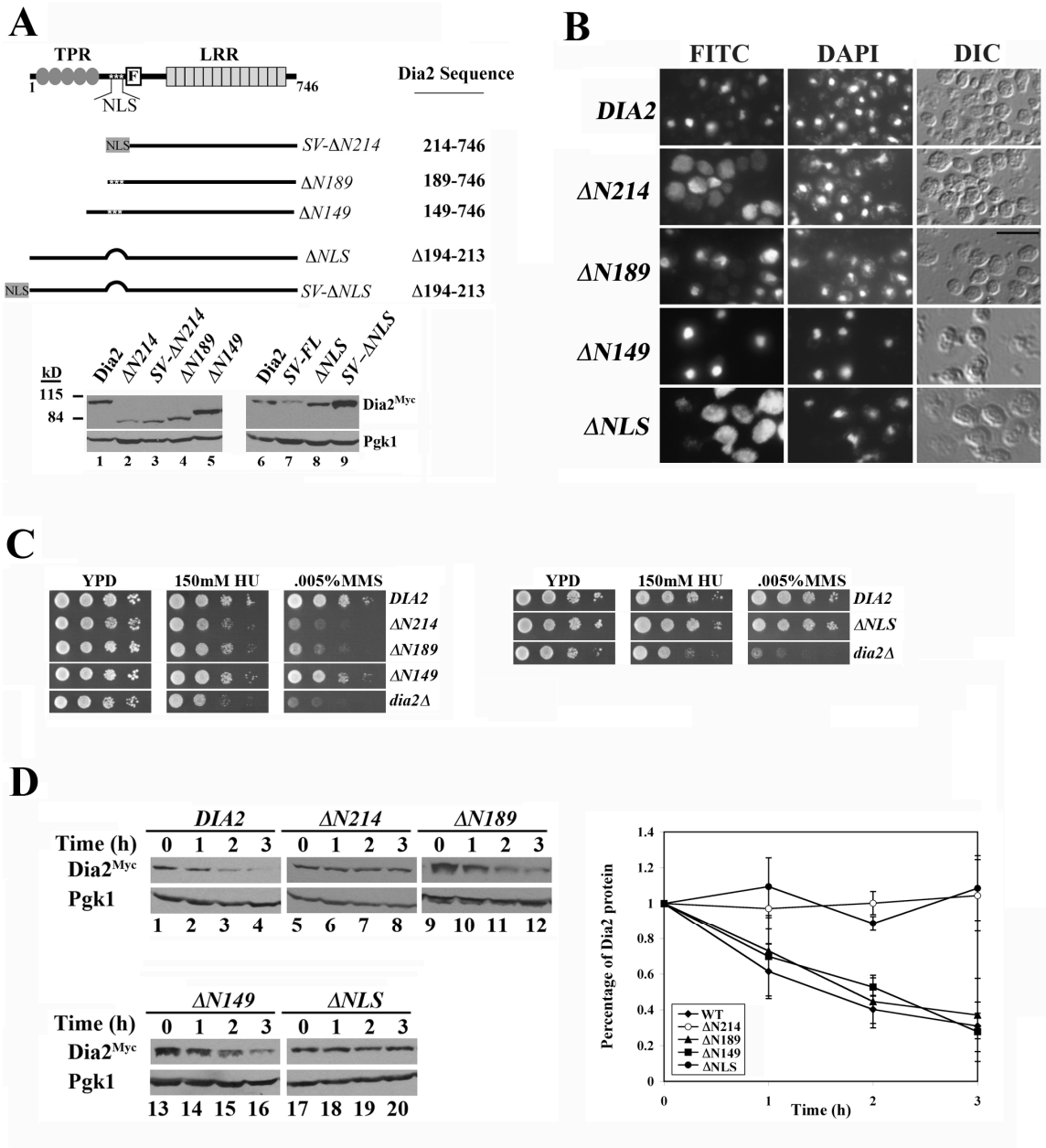


Figure 4. Dia2 degradation requires an NLS-containing domain. A) Diagram of N-terminal Dia2 deletion mutants used in this study. Expression of the mutant proteins is shown in the lower panel. Samples were prepared and blotted as described in Figure 2B. B) Dia2 mutants lacking the NLS region are mislocalized. Immunofluorescence was performed as in Figure 3. Scale bar, 5 μ m. C) Growth phenotypes of Dia2 N-terminal deletions. Indicated strains were spotted to YPD with the indicated amounts of hydroxyurea or MMS-containing media in 10-fold dilution series and grown at room temperature. D) Nuclear-localized Dia2 mutants are susceptible to proteolysis. Dia2 mutants were subjected to stability assays as described in Figure 3. Quantitation of three independent experiments is shown on the graph.

Kile and Koepp, Figure 5

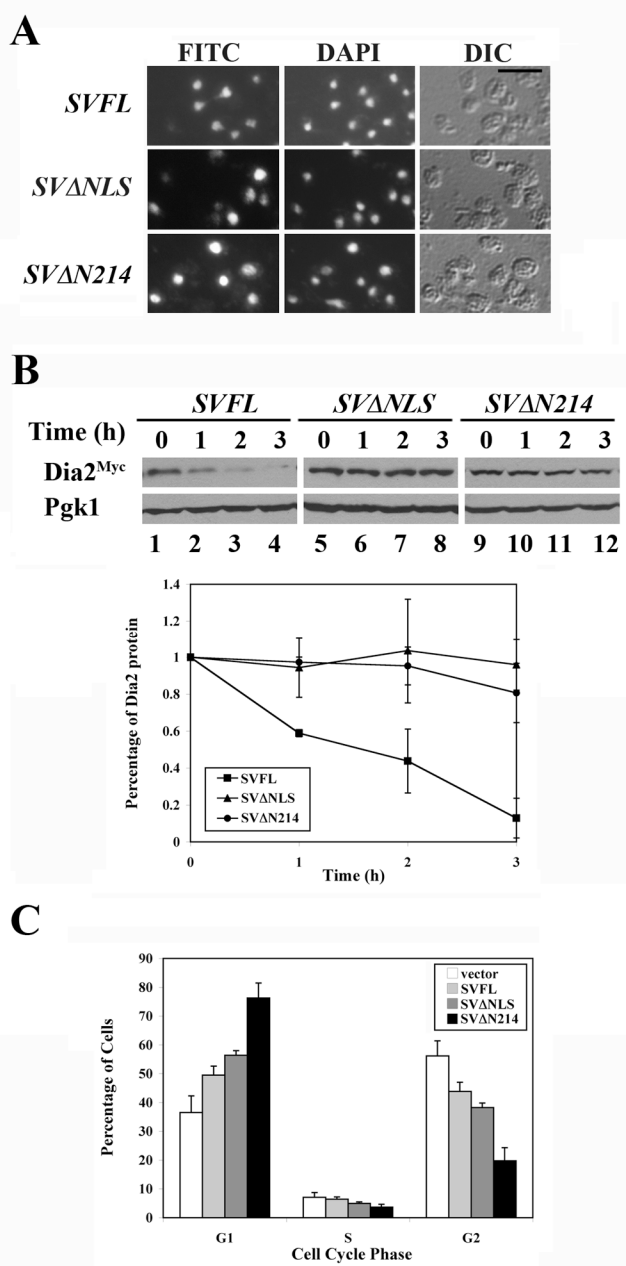
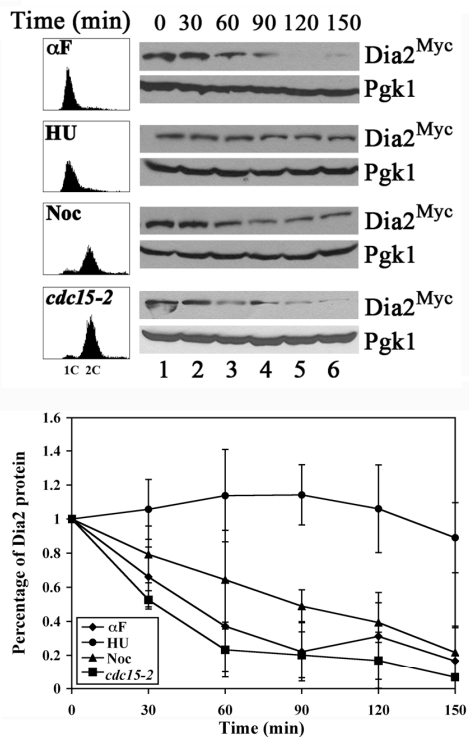


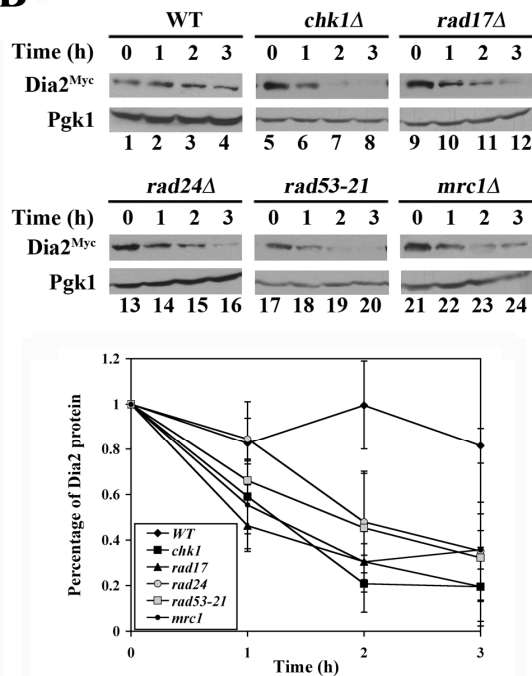
Figure 5. An N-terminal domain required for Dia2 protein turnover overlaps the NLS region. A) Addition of the SV40 T antigen NLS to Dia2 N-terminal deletions restores nuclear localization. Immunoflorescence was performed as in Figure 3. Scale bar, 5 μ m. B) Nuclear, N-terminal Dia2 deletions are stable. Dia2 mutants were subjected to stability assays as described in Figure 3. Quantitation of three independent experiments is shown on the graph. C) Overexpression of stable, nuclear forms of Dia2 alters cell cycle distribution. Wildtype cells expressing the indicated *DIA2* alleles from a galactose-inducible promoter were grown to log phase in galactose-containing media. DNA content was measured by flow cytometry. Quantitation of three independent experiments in shown in the graph.

Kile and Koepp, Figure 6

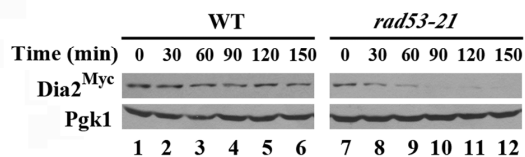
A



B



C



D

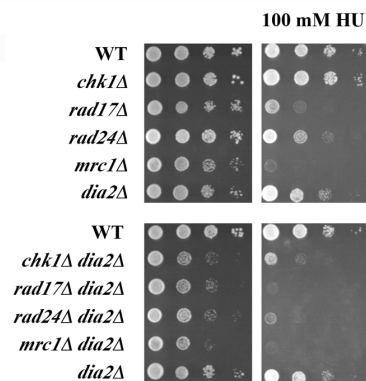


Figure 6. Checkpoint proteins inhibit Dia2 turnover in response to replication stress. A) Dia2 proteolysis is cell cycle regulated. Cells were arrested as described in Materials and Methods, and indicated time points (lanes 1-6) were taken after addition of CHX. The *9MYC-DIA2 cdc15-2* strain was shifted to the non-permissive temperature for 2 hours prior to the addition of CHX. The T=0 timepoint of each arrest was monitored by flow cytometry. Quantitation of three independent experiments is shown on the graph. B) Checkpoint pathway mutants fail to stabilize Dia2 in response to HU treatment. *9MYC-DIA2* alleles were generated in the indicated checkpoint mutants and arrested with HU as described above. Dia2 protein turnover was monitored for the indicated time after the addition of CHX and immunoblotted with anti-myc and anti-Pgk1 antibodies (upper panel). Quantitation of three independent experiments is shown on the graph. C) *rad53-21* mutants fail to stabilize Dia2 during replication stress caused by MMS. *9MYC-DIA2* or *9MYC-DIA2 rad53-21* cultures were arrested in G1 with alpha-factor for 2 hours. Cultures were washed and released into fresh media containing 0.033% MMS. Protein synthesis was halted after 60 minutes by the addition of CHX and the indicated time points were collected. Dia2 was monitored with anti-myc antibodies and anti-Pgk1 antibodies were used as a loading control. D) *dia2Δ* and checkpoint mutants show synthetic growth defects in response to HU. The specified strains were spotted in 10-fold serial dilutions on YPD plates containing the indicated amount of HU and grown at room temperature.

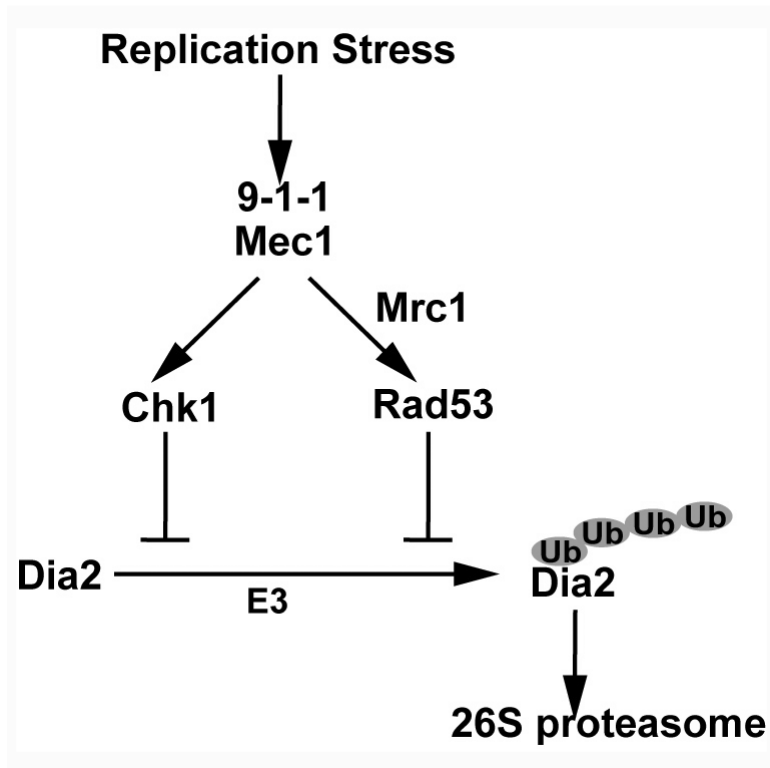
Kile and Koepp, Figure 7

Figure 7. Model for S-phase checkpoint regulation of Dia2. Dia2 is targeted for ubiquitin-mediated destruction by the 26S proteasome and an unknown E3 ligase. Replication stress activates S-phase checkpoints and leads to stabilization of Dia2.

Kile and Koepp, Supplementary Figure S1

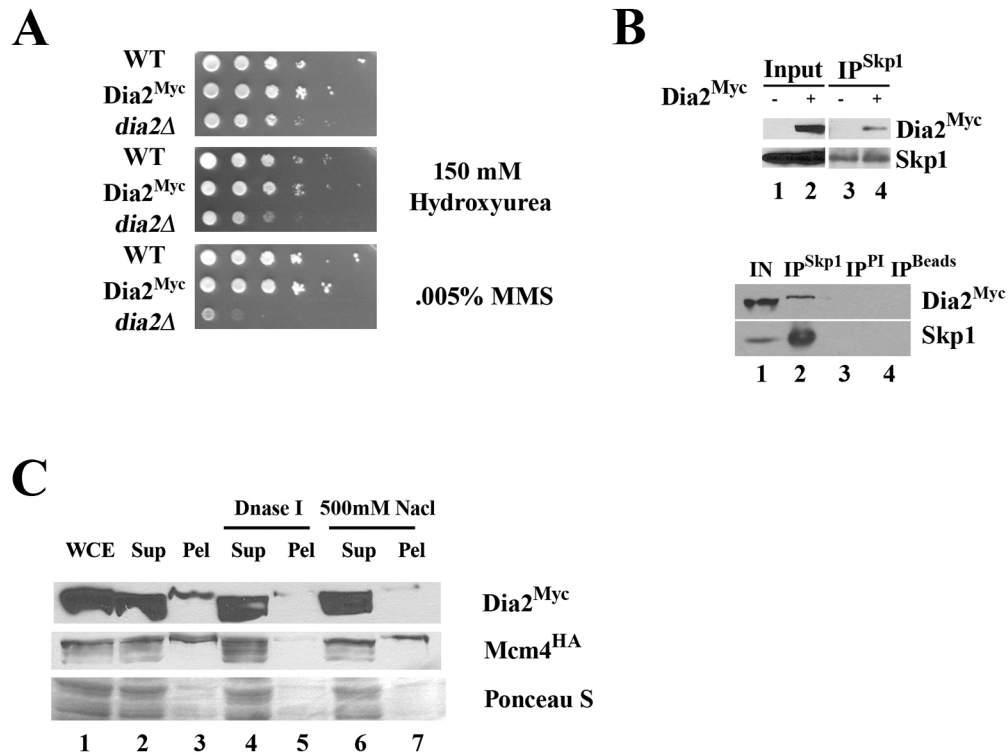


Figure S1. *9MYC-DIA2* behaves as wildtype. A) Growth of the Dia2^{Myc} strain is indistinguishable from wildtype on rich media with the indicated amounts of HU or methyl methanesulfonate (MMS) at room temperature. Ten-fold serial dilutions are shown. B) Dia2^{Myc} associates with Skp1. Skp1 was immunoprecipitated with anti-Skp1 antibodies (159) from an untagged strain or *9MYC-DIA2* strains (lanes 3 and 4, respectively). Immunoblots were probed with anti-myc or anti-Skp1 antibodies. The bottom panel shows Dia2^{Myc} is immunoprecipitated (IP) with anti-Skp1 antibodies, but not with preimmune serum (PI) or protein A/G beads (Beads) in the absence of antibody. C) A fraction of Dia2^{Myc} is chromatin-bound. Dia2^{Myc} cells were fractionated as described (141). Crude pellet-associated Dia2^{Myc} is released with DNase I (compare lane 3 vs. 5) or high salt treatment (compare lane 3 vs. 7). Mcm4^{HA} was monitored as a positive control. WCE = whole cell extract, Su = supernatant, Pel = pellet. Total protein was stained using Ponceau S to visualize overall protein fractionation from equal loaded volumes.

Kile and Koepf, Supplementary Figure S2

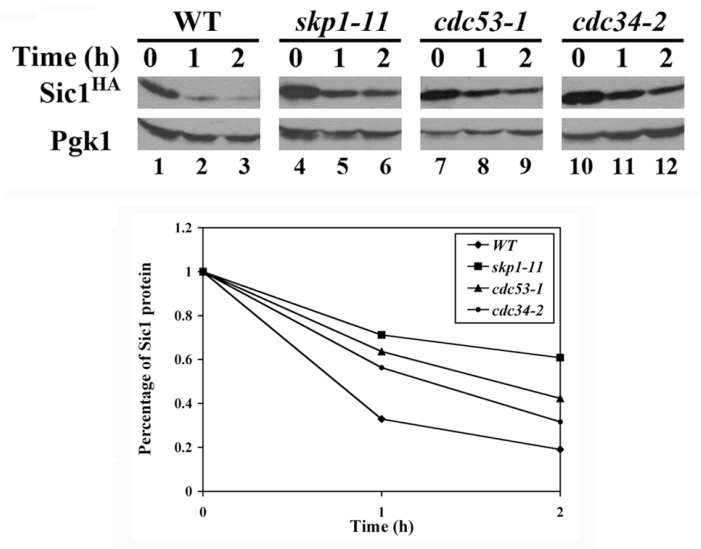


Figure S2. The SCF substrate Sic1 is stabilized in SCF mutants. Stability assays were performed as in Figure 3B except that Sic1 was expressed from a galactose-inducible promoter. Quantitation of the experiment is shown on the graph.

Kile and Koepp, Supplementary Figure S3

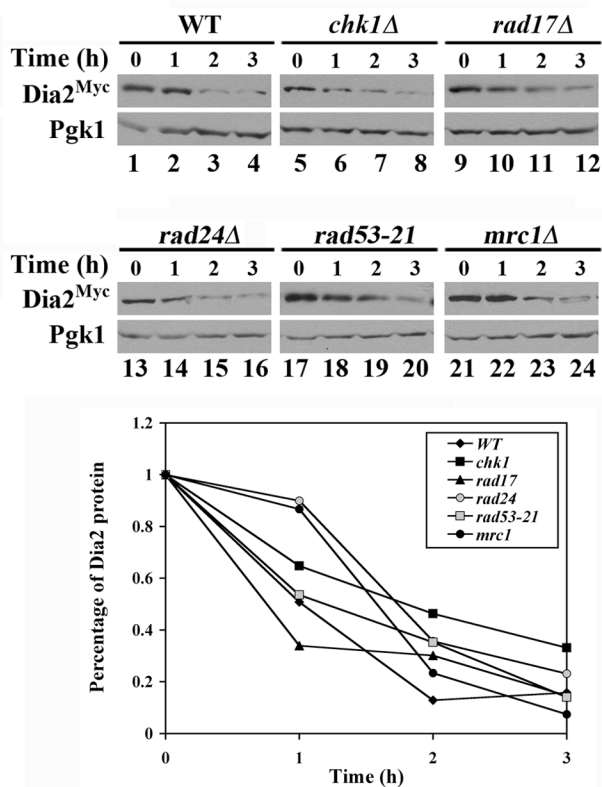


Figure S3. During G1, Dia2 shows turnover rates comparable to wildtype in checkpoint mutants. Stability assays were performed as in Figure 6B except that cells were arrested using alpha factor. Quantitation of a representative experiment is shown on the graph.

CHAPTER V

SUMMARY AND DISCUSSION

DNA replication and maintenance of genome integrity are fundamental processes necessary for the faithful propagation of cells and organisms. Defects in pathways that control these biological activities can result in disastrous outcomes. A prominent hallmark of cancer in humans is often the loss of genomic stability. Genome integrity is threatened when DNA is damaged, and the genome is particularly susceptible during DNA replication (20, 34, 123). As a result, cells have finely tuned processes to replicate and repair DNA. The last decade has brought advancements in understanding the molecular mechanisms involved in genome duplication. Insight into how DNA damage and replication stress are monitored and the cellular responses that follow has also emerged (60). The mechanistic details of these pathways are far from complete, and novel proteins and pathways involved continue to expand our understanding. It is important to further investigate how these processes are regulated to fully understand how genomes are replicated and accurately maintained. Protein turnover mediated by SCF ubiquitin ligases control substrate abundance, and have many established links to cell cycle control and other biological processes (28, 50, 84, 110, 159, 160, 167, 180, 191). F-box proteins provide the critical function of recruiting individual substrates to the core SCF machinery, yet many remain uncharacterized in the particular biological processes they control (50, 159, 192). Therefore, investigation of individual F-box

protein provides further insight into the biological roles that are regulated by SCF-mediated ubiquitination.

We have demonstrated that the F-box protein Dia2 plays a role in DNA replication and genome maintenance in budding yeast. The Dia2 protein physically associates with several origins of replication and *DIA2*-deleted cells are sensitive to replication stress or DNA damage (83). *dia2Δ* cells exhibit a G2/M delay due the loss of genomic integrity and activation of the DNA damage checkpoint, even in the absence of additional replication stress. Yra1 has been identified as a protein interaction partner for Dia2 and affects Dia2 recruitment to replication origins. *yra1* mutants show loss of genome stability, genetically interact with *DIA2*, and are defective in Dia2 protein recruitment to origins (169). These observations suggest that Dia2 and Yra1 are involved in the same pathway that promotes genome maintenance.

Control of Dia2 protein abundance further supports a role for it in DNA replication and genome maintenance. Dia2 becomes more abundant and stable during DNA replication or during periods of replication stress. Control of Dia2 proteolysis is dependent on its N-terminal region, and not via autoubiquitination similar to other F-box proteins (52, 197). Intriguingly, Dia2 stabilization during HU or MMS-induced replication stress requires checkpoint genes, indicating that Dia2's role may intersect with the DNA replication checkpoint. Together, these key findings support the interpretation that Dia2, with Yra1, performs a chromatin-associated role to regulate one or more substrates during DNA replication to promote genomic integrity.

Events such as pre-RC assembly and licensing, replication initiation, and regulation of origin-bound proteins occur at replication origins (12, 17, 152).

Interestingly, Dia2 protein is chromatin-bound and Dia2 associates with origins of replication. We have not experimentally tested if Dia2 affects one or more of these processes, although Dia2 origin association indicate these are intriguing prospects. The premature S-phase in *DIA2* deletion strains suggest that origins may be prematurely firing due to loss of regulatory action by SCF^{Dia2}. This may lead to genome instability followed by activation of the DNA damage checkpoint. Comparing replication intermediates between wild-type and *dia2Δ* cells would help determine if there is such a defect.

Blake and colleagues propose a role for Dia2 in replisome progression in problematic regions of the genome or under general replication stress (15). They have shown that completion of DNA replication is problematic in the presence of replication stress in *dia2Δ* mutants and supports a model for regulating replisome progression (15). Dia2 was not shown to interact with chromatin or replisome components in that study. Origin firing is a point of control during replication stress, and may also result in a failure to complete DNA synthesis (123, 152). Again, inquiry into the role of Dia2 in origin firing may help to distinguish between these possibilities.

Another scenario could be that Dia2 is involved at origins as well as the traveling replisome. Many DNA replication proteins associate with origins as well as travel with the replisome complex (23, 152, 184). We have not investigated if Dia2 travels with the replication fork, but Dia2 could potentially have similar dynamics since Dia2 interacts with replisome proteins that associate with replication origins as well as travel with the replication fork. It would have to be demonstrated that Dia2 associates with additional proteins known to travel with the replication fork by protein interaction. Likewise, it could be formally tested if Dia2 migrates with the replication fork using chromatin

immunoprecipitation to determine if it associates with regions flanking the origin after initiation occurs. These experiments could be very informative to further understand the dynamics of Dia2 chromatin interaction. The current data suggests that Dia2 can at least associate with replication origins, and is supported by its interaction with Yra1(169), but further experiments are required to determine if it associates with the traveling replisome.

An interesting question is whether Dia2 activity is most important at replication origins, additional regions of the genome, or actually travels with the replisome to perform a continuous role during replication progression. While we have shown enrichment of Dia2 at several replication origins, other regions of the genome may also require SCF^{DIA2} function. It has been suggested that Dia2 promotes replisome progression in regions of the genome such as the rDNA locus, as Dia2 can localize in the nucleolus (subnuclear site containing rDNA), and there is an increase of rDNA circles in *dia2Δ* mutants (15). The rDNA locus comprises tandem repeats of elements essential for ribosome biogenesis and is a region of heavy transcriptional activity, which can be troublesome for DNA replication (20, 144, 178, 179). Intriguingly, Dia2 physically associates with this region of the genome as determined by chromatin immunoprecipitation, suggesting a role for Dia2 here as well (A. Ritter and D. Koepp, unpublished observations). Whether this recruitment to rDNA correlates with Dia2's role in genomic integrity remains to be determined, but nevertheless indicates Dia2 can associate with other genomic regions beside origins of replication.

We have shown that Yra1 also is origin-bound and does not appear to be a proteolytic target of SCF^{Dia2}, but instead promotes Dia2 origin association. We propose that Dia2 and Yra1 reside in a complex together to perform a yet undefined mechanistic

role that affects genome maintenance (169). We suspect the C-terminal 17 amino acids of Yra1 specifically recruit Dia2 to promote DNA replication and genome maintenance. It is not yet known if Yra1 and Dia2 directly interact or if other proteins mediate the interaction. The regions within Dia2 that are important for Yra1 binding have not been examined either, however the generation of Dia2 domain mutants now make this analysis possible. Since we detect genetic interaction between *YRA1* and *DIA2*, but not another TREX component, this would further support a role for these proteins in genome maintenance that is distinct from mRNA processing. We have not specifically investigated or observed defects in transcription-coupled export in *dia2* Δ mutants, but our current analysis would indicate that this is unlikely.

Both Yra1 and Dia2 co-purify with Hys2 (a subunit of Pol δ), which provides evidence that both proteins interact with components of the replication fork (169). It would be informative to know if these interactions occur at replication origins, other distinct genomic locations, travel with the replisome, or chromatin in general. Another question is whether Dia2 (or Yra1) interact with other members of the replication fork as stated earlier. Preliminary results suggest that Dia2 can interact with MCM proteins (66, S. Swaminathan and D.Koepp, unpublished observations). Does Yra1 link Dia2 to MCM or are both Yra1 and Dia2 linked through other factors? Indeed, there are many proteins involved in DNA replication and at replication forks and this would likely require extensive analysis. Association of Dia2 and Yra1 with replication proteins is likely to occur with the onset of S phase as well, due to the increase in Dia2 abundance and stabilization.

Dia2 abundance increases upon the onset into S phase and remains high for the rest of the cell cycle until G1 arrest. It is likely that control of Dia2 function is at least partly regulated by its stability, which may be important during periods of replication stress. Replication stress stalls replication forks and induces a replication checkpoint response that stabilizes the fork, inhibits further origin firing, coordinates repair of collapsed forks, as well as other processes (20, 34, 123, 152). Checkpoint-defective strains exposed to replication stress do not block turnover of Dia2. These results suggest that activation of the checkpoint response inhibits turnover of Dia2, which may promote SCF^{DIA2} activity for optimal genome integrity.

An interesting avenue for further investigation will be to understand how control of Dia2 interfaces with the replication checkpoint. While it is certainly possible that checkpoint proteins signal directly to Dia2 and inhibit its turnover, this has not been extensively investigated and several scenarios exist. The replication checkpoint response is mediated by the Mec1 and Rad53 kinases (20, 123). Phosphorylation of Dia2 by these kinases may play a role in its turnover or function, but needs to be more formally examined. Posttranslational modification of Dia2 during the cell cycle or during times of replication stress, such as with hydroxyurea, is not known, but has the potential for controlling Dia2 proteolysis.

It also remains possible that the replication checkpoint affects Dia2 stability by its known downstream effects: stabilizing replication forks to prevent collapse, inhibiting late origins from firing, and preventing the metaphase to anaphase transition (20, 101, 123, 147, 174, 175). It has recently been proposed that preventing replication fork collapse is the critical function of the checkpoint for genome maintenance (60, 101, 152,

175). We have identified links to Dia2 with the replisome as well as replication origins. With these observations in mind, Dia2 stabilization might be promoted by intact replication forks and/or unfired origins. Failure to promote these activities during replication stress could thus expose Dia2 to ubiquitin-mediated destruction, and could be further evidence linking Dia2 stability to DNA replication events.

Alternatively, the replication checkpoint may control the ubiquitin pathway of Dia2 turnover directly. Other ubiquitin ligases may be controlled by the checkpoint, one of which may in turn regulate Dia2. As discussed in more detail below, Dia2 turnover is not dependent on autoubiquitination, suggesting a non-SCF ubiquitin ligase controls its proteolysis. Indeed, many substrates have been recently identified in the mammalian Ubiquitin-Proteasome pathway in the DNA damage response (which shares many of the same replication checkpoint components) (60, 111, 115). It would seem reasonable to assume a similar finding in budding yeast is likely.

A key finding is that proteolysis via autoubiquitination of Dia2 is clearly not the sole mechanism that affects its turnover. Sequences that promote Dia2 nuclear localization interestingly also control turnover of the protein. An outstanding question is whether Dia2 ubiquitination and/or proteolysis occur in the nucleus or cytoplasm. Since deletion of the NLS region contributes to nuclear localization and turnover of Dia2, it is impossible to determine if Dia2 proteolysis normally occurs in the cytoplasm based upon the current data. It may be necessary to further engineer a Dia2 variant driven constitutively into the cytoplasm and compare turnover rates between full length nuclear and non-nuclear Dia2. Dia2 could be nuclear ubiquitinated and destroyed in the nucleus, nuclear ubiquitinated and transported to the cytoplasm for turnover, or transported to the

cytoplasm and ubiquitinated for destruction. We cannot currently distinguish between these possibilities. This could also help determine the localization of a non-SCF ligase that controls Dia2 proteolysis. Thus, nuclear trafficking and turnover of Dia2 may be interrelated, and could be a point of further investigation to understand these dynamics of Dia2 turnover.

As a complement to testing Dia2 protein stability with domain mutants, I also tested these for growth on media containing MMS and HU, which are useful to monitor *DIA2* function. These mutants are the first extensive mutational analysis of Dia2 to dissect overall functional domain relevance. Deletion of the N-terminal TPR domain (Δ N214) displayed equivalent sensitivity to MMS and HU as *dia2* Δ , suggesting this region is also critical for Dia2 function. Not surprisingly, the TPR region or LRR (leucine-rich repeat) regions alone did not show any rescue of *DIA2* function. Several F-box proteins interact with their substrates through LRR motifs (26, 132, 192). It is currently unknown if the TPR region is responsible for substrate binding, or another activity such as recruiting interaction partners such as Yra1. It will be necessary to determine what regions of Dia2 play a role in its function in future studies.

Deletion of the NLS region mislocalizes and stabilizes the Dia2 protein, but paradoxically sensitivity to HU or MMS was not detected. Because Dia2 is nuclear, chromatin and replication origin-bound, and promotes genomic integrity this result would seem to be counter-intuitive to proposed role for Dia2 on chromatin. However, several observations may reconcile these data. First, the Δ NLS mutant is not actually excluded from the nucleus, and residual or lower amounts of Dia2 may be sufficient for genome maintenance. It remains possible one or more unidentified NLS sites remains in Dia2 to

provide this activity. In the same line of reasoning, deletion of the NLS region also increases Dia2 abundance and stability, which may actually suppress nuclear trafficking effects. An interaction partner with Dia2 could also promote nuclear localization, such as Yra1. Lastly, HU and MMS treatment inhibit turnover of Dia2, which in combination with higher Dia2 abundance, may also mask any sensitivity to these agents. The mechanism of Dia2 function in genomic integrity has not yet been directly tied to a chromatin-bound or nuclear localized substrate, so a non-nuclear substrate that affects genome maintenance remains possible. However, given the clear nuclear localization of Dia2, this scenario is seems unlikely.

DIA2 genetically interacts with replication and DNA damage checkpoint genes. As discussed earlier, we observe *dia2Δ* cells are sensitive to additional replication stress and DNA damage by chemical or endogenous insults (15, 83). Synthetic lethal or sick phenotypes of *dia2Δ* in combination with DNA damage checkpoint genes further indicate evidence that *DIA2* is required for proper genome maintenance (83). Indeed, other groups have performed larger whole-genome studies in which *DIA2* has been shown to have synthetic growth defects with numerous other genes, many of which are in genomic integrity or DNA replication pathways (15, 128). Since *dia2Δ* cells exhibit higher endogenous rates of DNA damage and Rad53 activation, it is clear an intact checkpoint response is required for cell viability upon Dia2 loss (15, 83, 128, 148).

Interestingly, HU sensitivity was exacerbated in *dia2Δ* double mutants with checkpoint genes as compared to single mutants. Since Dia2 is stable during HU-induced stress, this indicates SCF^{DIA2} function is required. *dia2Δ* mutants could thus be predicted to be further problematic for the cell and show greater growth defects, which is indeed

what we detect. Perhaps the most striking observation is that *chk1Δ* shows no sensitivity to HU (149), *dia2Δ* is modestly sensitive (15, 83), but the combination of both shows a robust growth defect in response to HU. Additionally, we detect Dia2 protein turnover in *chk1Δ* strains, which is unexpected since Chk1 does not have a defined role in the replication checkpoint in budding yeast. However, links to the replication checkpoint of Chk1 have been made, but require the additional loss of the Dun1 kinase (25, 149). In these studies, it appears that the loss of *DUN1* with *CHK1* results in synthetic lethality in response to replication block/stress by hydroxyurea. Here, Chk1 is proposed to be required for the survival of cells in response to defects in stalled replication forks at early replication origins (25, 149). Since we detect Dia2-binding at early replication origins, it is an intriguing possibility that it may play a role in this pathway.

Regardless, the growth phenotypes of all double mutants genetically support an interpretation that *DIA2* functions within the same or similar genomic integrity pathways, and blocking Dia2 protein turnover may play a role in the replication stress response. However, while it appears that *DIA2* is not required for activation of checkpoints, the interactions uncovered with checkpoint genes as mentioned above require further investigation, as well as identifying the mechanism of checkpoint control of Dia2 turnover and function.

What is the precise role Dia2 plays in S-phase? One possibility could be that SCF^{DIA2} ubiquitinates a substrate (which is then presumably degraded) at origins which is required for a proper “resetting” for the next round of DNA replication. Overabundance of such a substrate could lead to the early S phase we have detected. A premature S-phase has the potential to disrupt the fidelity of DNA replication, decreasing genomic

stability and causing sensitivity to replication stress. Another model could be proposed that Dia2 is at origins and also travels with the replication fork after initiation with similar dynamics as other proteins with known roles in DNA replication. Dia2 could help the replisome move with the replication fork in problematic regions, and may be needed to a greater extent in the presence of replication stress. Here, Dia2 would target a substrate that hinders optimal DNA replication and loss of this turnover leads to genome instability, possibly by fork stalling and collapse. However, we have not directly examined if the “firing” patterns of any origins are altered in *dia2Δ* cells, or if Dia2 moves with the replication fork. These investigations could help elucidate the mechanism for SCF^{DIA2}. Since Dia2 is abundant during S, and is stabilized in the presence of replication stress dependent on checkpoint signaling, this would also indicate a role at origins OR the replisome. As discussed earlier, inhibition of late origin firing and replication fork stabilization occur upon checkpoint activation, and correlates with Dia2 stability. However, since we do not know the exact role for Dia2, stabilization of Dia2 in response to either of these activities is plausible, and will require a more detailed analysis.

A definite substrate for Dia2 that would explain genome integrity defects remains to be identified. It has previously been suggested that Tec1, a transcription factor that affects the budding yeast filamentation pathway, is a substrate of SCF^{DIA2} (8). However, this conclusion is controversial; SCF^{Cdc4} is also implicated in Tec1 ubiquitination and turnover, and direct evidence for SCF^{Dia2} has not been shown (8, 32). Additionally, Tec1 as a substrate for SCF^{DIA2} is not intuitive, as how it could affect genomic integrity is not readily apparent. Nonetheless, a bona fide substrate for Dia2 that explains its role in

genome maintenance remains to be discovered. Determination of one or more Dia2 substrates would clearly help explain the defects that are observed upon *DIA2* deletion.

The aim of this work has been to investigate the function and control of a novel and previously uncharacterized F-box protein Dia2 in *Saccharomyces cerevisiae*. F-box proteins provide the critical function of recruiting specific substrates to the core SCF ubiquitin ligase for ubiquitin modification followed by 26S proteasome-mediated destruction (28, 50, 84, 110, 159, 160, 167, 180, 191). The identification of the cellular roles that F-box proteins regulate continues to expand, and identifying that Dia2 plays a role in genome maintenance significantly advances our knowledge. We detect Dia2 is a chromatin-bound protein and it seems likely that a substrate will also be chromatin bound. It is not yet known whether such a substrate plays a role at replication origins, during replisome progression, or replication stress but such possibilities may not be independent. While a direct mechanistic role or substrate(s) for Dia2 remains unclear, this body of work nonetheless establishes Dia2 as a bona fide F-box protein important in genomic integrity and DNA replication. Budding yeast is often used as a model for DNA replication and genomic stability, with a high degree of conservation of proteins and pathways with humans. Genomic integrity is of critical importance to the cell and organism, and loss of which is strongly correlated with deleterious effects such as cancer. By studying Dia2, we have identified it as a novel factor and a new link between the SCF ubiquitination pathway and its relevance to DNA replication and genome maintenance. It will be exciting to further investigate Dia2 and identify substrates to explain its mechanistic role, which will support a greater understanding of genomic integrity.

Bibliography

1. **Abruzzi, K. C., S. Lacadie, and M. Rosbash.** 2004. Biochemical analysis of TREX complex recruitment to intronless and intron-containing yeast genes. *Embo J* **23**:2620-31.
2. **Alcasabas, A. A., A. J. Osborn, J. Bachant, F. Hu, P. J. Werler, K. Bousset, K. Furuya, J. F. Diffley, A. M. Carr, and S. J. Elledge.** 2001. Mrc1 transduces signals of DNA replication stress to activate Rad53. *Nat Cell Biol* **3**:958-65.
3. **Allen, J. B., Z. Zhou, W. Siede, E. C. Friedberg, and S. J. Elledge.** 1994. The SAD1/RAD53 protein kinase controls multiple checkpoints and DNA damage-induced transcription in yeast. *Genes Dev* **8**:2401-15.
4. **Aparicio, O. M., A. M. Stout, and S. P. Bell.** 1999. Differential assembly of Cdc45p and DNA polymerases at early and late origins of DNA replication. *Proc Natl Acad Sci U S A* **96**:9130-5.
5. **Aparicio, O. M., D. M. Weinstein, and S. P. Bell.** 1997. Components and dynamics of DNA replication complexes in *S. cerevisiae*: redistribution of MCM proteins and Cdc45p during S phase. *Cell* **91**:59-69.
6. **Azzalin, C. M., and J. Lingner.** 2006. The human RNA surveillance factor UPF1 is required for S phase progression and genome stability. *Curr Biol* **16**:433-9.
7. **Bai, C., P. Sen, K. Hofmann, L. Ma, M. Goebel, J. W. Harper, and S. J. Elledge.** 1996. SKP1 connects cell cycle regulators to the ubiquitin proteolysis machinery through a novel motif, the F-box. *Cell* **86**:263-74.
8. **Bao, M. Z., M. A. Schwartz, G. T. Cantin, J. R. Yates, 3rd, and H. D. Madhani.** 2004. Pheromone-dependent destruction of the Tec1 transcription factor is required for MAP kinase signaling specificity in yeast. *Cell* **119**:991-1000.
9. **Bartek, J., C. Lukas, and J. Lukas.** 2004. Checking on DNA damage in S phase. *Nat Rev Mol Cell Biol* **5**:792-804.
10. **Bashir, T., N. V. Dorrello, V. Amador, D. Guardavaccaro, and M. Pagano.** 2004. Control of the SCF(Skp2-Cks1) ubiquitin ligase by the APC/C(Cdh1) ubiquitin ligase. *Nature* **428**:190-3.
11. **Bell, S. P.** 1995. Eukaryotic replicators and associated protein complexes. *Curr Opin Genet Dev* **5**:162-7.
12. **Bell, S. P., and A. Dutta.** 2002. DNA replication in eukaryotic cells. *Annu Rev Biochem* **71**:333-74.
13. **Bell, S. P., and B. Stillman.** 1992. ATP-dependent recognition of eukaryotic origins of DNA replication by a multiprotein complex. *Nature* **357**:128-34.
14. **Bermudez, V. P., L. A. Lindsey-Boltz, A. J. Cesare, Y. Maniwa, J. D. Griffith, J. Hurwitz, and A. Sancar.** 2003. Loading of the human 9-1-1 checkpoint complex onto DNA by the checkpoint clamp loader hRad17-replication factor C complex in vitro. *Proc Natl Acad Sci U S A* **100**:1633-8.
15. **Blake, D., B. Luke, P. Kanellis, P. Jorgensen, T. Goh, S. Penfold, B. J. Breitkreutz, D. Durocher, M. Peter, and M. Tyers.** 2006. The F-box protein

- Dia2 overcomes replication impedance to promote genome stability in *Saccharomyces cerevisiae*. *Genetics*.
16. **Blondel, M., J. M. Galan, Y. Chi, C. Lafourcade, C. Longaretti, R. J. Deshaies, and M. Peter.** 2000. Nuclear-specific degradation of Far1 is controlled by the localization of the F-box protein Cdc4. *Embo J* **19**:6085-97.
 17. **Blow, J. J., and A. Dutta.** 2005. Preventing re-replication of chromosomal DNA. *Nat Rev Mol Cell Biol* **6**:476-86.
 18. **Boddy, M. N., and P. Russell.** 2001. DNA replication checkpoint. *Curr Biol* **11**:R953-6.
 19. **Bonilla, C. Y., J. A. Melo, and D. P. Toczyski.** 2008. Colocalization of sensors is sufficient to activate the DNA damage checkpoint in the absence of damage. *Mol Cell* **30**:267-76.
 20. **Branzei, D., and M. Foiani.** 2005. The DNA damage response during DNA replication. *Curr Opin Cell Biol* **17**:568-75.
 21. **Brewer, B. J., and W. L. Fangman.** 1987. The localization of replication origins on ARS plasmids in *S. cerevisiae*. *Cell* **51**:463-71.
 22. **Brown, E. J., and D. Baltimore.** 2003. Essential and dispensable roles of ATR in cell cycle arrest and genome maintenance. *Genes Dev* **17**:615-28.
 23. **Burgers, P. M.** 2009. Polymerase dynamics at the eukaryotic DNA replication fork. *J Biol Chem* **284**:4041-5.
 24. **Byun, T. S., M. Pacek, M. C. Yee, J. C. Walter, and K. A. Cimprich.** 2005. Functional uncoupling of MCM helicase and DNA polymerase activities activates the ATR-dependent checkpoint. *Genes Dev* **19**:1040-52.
 25. **Caldwell, J. M., Y. Chen, K. L. Schollaert, J. F. Theis, G. F. Babcock, C. S. Newlon, and Y. Sanchez.** 2008. Orchestration of the S-phase and DNA damage checkpoint pathways by replication forks from early origins. *J Cell Biol* **180**:1073-86.
 26. **Cardozo, T., and M. Pagano.** 2004. The SCF ubiquitin ligase: insights into a molecular machine. *Nat Rev Mol Cell Biol* **5**:739-51.
 27. **Carpenter, P. B., P. R. Mueller, and W. G. Dunphy.** 1996. Role for a *Xenopus* Orc2-related protein in controlling DNA replication. *Nature* **379**:357-60.
 28. **Carrano, A. C., E. Eytan, A. Hershko, and M. Pagano.** 1999. SKP2 is required for ubiquitin-mediated degradation of the CDK inhibitor p27. *Nat Cell Biol* **1**:193-9.
 29. **Chen, Z. J., and L. J. Sun.** 2009. Nonproteolytic functions of ubiquitin in cell signaling. *Mol Cell* **33**:275-86.
 30. **Cheng, L., L. Hunke, and C. F. Hardy.** 1998. Cell cycle regulation of the *Saccharomyces cerevisiae* polo-like kinase cdc5p. *Mol Cell Biol* **18**:7360-70.
 31. **Cho, R. J., M. J. Campbell, E. A. Winzler, L. Steinmetz, A. Conway, L. Wodicka, T. G. Wolfsberg, A. E. Gabrielian, D. Landsman, D. J. Lockhart, and R. W. Davis.** 1998. A genome-wide transcriptional analysis of the mitotic cell cycle. *Mol Cell* **2**:65-73.
 32. **Chou, S., L. Huang, and H. Liu.** 2004. Fus3-regulated Tec1 degradation through SCFCdc4 determines MAPK signaling specificity during mating in yeast. *Cell* **119**:981-90.

33. **Ciechanover, A., S. Elias, H. Heller, and A. Hershko.** 1982. "Covalent affinity" purification of ubiquitin-activating enzyme. *J Biol Chem* **257**:2537-42.
34. **Cimprich, K. A., and D. Cortez.** 2008. ATR: an essential regulator of genome integrity. *Nat Rev Mol Cell Biol* **9**:616-27.
35. **Cocker, J. H., S. Piatti, C. Santocanale, K. Nasmyth, and J. F. Diffley.** 1996. An essential role for the Cdc6 protein in forming the pre-replicative complexes of budding yeast. *Nature* **379**:180-2.
36. **Cohen-Fix, O., and D. Koshland.** 1997. The anaphase inhibitor of *Saccharomyces cerevisiae* Pds1p is a target of the DNA damage checkpoint pathway. *Proc Natl Acad Sci U S A* **94**:14361-6.
37. **Connelly, C., and P. Hieter.** 1996. Budding yeast SKP1 encodes an evolutionarily conserved kinetochore protein required for cell cycle progression. *Cell* **86**:275-85.
38. **Cope, G. A., and R. J. Deshaies.** 2003. COP9 signalosome: a multifunctional regulator of SCF and other cullin-based ubiquitin ligases. *Cell* **114**:663-71.
39. **Dahmann, C., J. F. Diffley, and K. A. Nasmyth.** 1995. S-phase-promoting cyclin-dependent kinases prevent re-replication by inhibiting the transition of replication origins to a pre-replicative state. *Curr Biol* **5**:1257-69.
40. **Deshaies, R. J.** 1999. SCF and Cullin/Ring H2-based ubiquitin ligases. *Annu Rev Cell Dev Biol* **15**:435-67.
41. **Detweiler, C. S., and J. J. Li.** 1998. Ectopic induction of Clb2 in early G1 phase is sufficient to block prereplicative complex formation in *Saccharomyces cerevisiae*. *Proc Natl Acad Sci U S A* **95**:2384-9.
42. **Donovan, S., J. Harwood, L. S. Drury, and J. F. Diffley.** 1997. Cdc6p-dependent loading of Mcm proteins onto pre-replicative chromatin in budding yeast. *Proc Natl Acad Sci U S A* **94**:5611-6.
43. **Dowell, S. J., P. Romanowski, and J. F. Diffley.** 1994. Interaction of Dbf4, the Cdc7 protein kinase regulatory subunit, with yeast replication origins in vivo. *Science* **265**:1243-6.
44. **Drury, L. S., G. Perkins, and J. F. Diffley.** 1997. The Cdc4/34/53 pathway targets Cdc6p for proteolysis in budding yeast. *Embo J* **16**:5966-76.
45. **Dutta, A., and S. P. Bell.** 1997. Initiation of DNA replication in eukaryotic cells. *Annu Rev Cell Dev Biol* **13**:293-332.
46. **Ellison, V., and B. Stillman.** 2003. Biochemical characterization of DNA damage checkpoint complexes: clamp loader and clamp complexes with specificity for 5' recessed DNA. *PLoS Biol* **1**:E33.
47. **Emili, A.** 1998. MEC1-dependent phosphorylation of Rad9p in response to DNA damage. *Mol Cell* **2**:183-9.
48. **Escobar-Henriques, M., B. Westermann, and T. Langer.** 2006. Regulation of mitochondrial fusion by the F-box protein Mdm30 involves proteasome-independent turnover of Fzo1. *J Cell Biol* **173**:645-50.
49. **Falbo, K. B., and X. Shen.** 2006. Chromatin remodeling in DNA replication. *J Cell Biochem* **97**:684-9.

50. **Feldman, R. M., C. C. Correll, K. B. Kaplan, and R. J. Deshaies.** 1997. A complex of Cdc4p, Skp1p, and Cdc53p/cullin catalyzes ubiquitination of the phosphorylated CDK inhibitor Sic1p. *Cell* **91**:221-30.
51. **Fey, J. P., and S. Lanker.** 2007. Delayed accumulation of the yeast G1 cyclins Cln1 and Cln2 and the F-box protein Grr1 in response to glucose. *Yeast* **24**:419-29.
52. **Galan, J. M., and M. Peter.** 1999. Ubiquitin-dependent degradation of multiple F-box proteins by an autocatalytic mechanism. *Proc Natl Acad Sci U S A* **96**:9124-9.
53. **Galan, J. M., A. Wiederkehr, J. H. Seol, R. Haguenaer-Tsapis, R. J. Deshaies, H. Riezman, and M. Peter.** 2001. Skp1p and the F-box protein Rcy1p form a non-SCF complex involved in recycling of the SNARE Snc1p in yeast. *Mol Cell Biol* **21**:3105-17.
54. **Garg, P., and P. M. Burgers.** 2005. DNA polymerases that propagate the eukaryotic DNA replication fork. *Crit Rev Biochem Mol Biol* **40**:115-28.
55. **Green, C. M., H. Erdjument-Bromage, P. Tempst, and N. F. Lowndes.** 2000. A novel Rad24 checkpoint protein complex closely related to replication factor C. *Curr Biol* **10**:39-42.
56. **Grigull, J., S. Mnaimneh, J. Pootoolal, M. D. Robinson, and T. R. Hughes.** 2004. Genome-wide analysis of mRNA stability using transcription inhibitors and microarrays reveals posttranscriptional control of ribosome biogenesis factors. *Mol Cell Biol* **24**:5534-47.
57. **Hardy, C. F.** 1996. Characterization of an essential Orc2p-associated factor that plays a role in DNA replication. *Mol Cell Biol* **16**:1832-41.
58. **Hardy, C. F.** 1997. Identification of Cdc45p, an essential factor required for DNA replication. *Gene* **187**:239-46.
59. **Hardy, C. F., O. Dryga, S. Seematter, P. M. Pahl, and R. A. Sclafani.** 1997. *mcm5/cdc46-bob1* bypasses the requirement for the S phase activator Cdc7p. *Proc Natl Acad Sci U S A* **94**:3151-5.
60. **Harper, J. W., and S. J. Elledge.** 2007. The DNA damage response: ten years after. *Mol Cell* **28**:739-45.
61. **Harrison, J. C., and J. E. Haber.** 2006. Surviving the breakup: the DNA damage checkpoint. *Annu Rev Genet* **40**:209-35.
62. **Hartwell, L. H., J. Culotti, and B. Reid.** 1970. Genetic control of the cell-division cycle in yeast. I. Detection of mutants. *Proc Natl Acad Sci U S A* **66**:352-9.
63. **Hershko, A., H. Heller, S. Elias, and A. Ciechanover.** 1983. Components of ubiquitin-protein ligase system. Resolution, affinity purification, and role in protein breakdown. *J Biol Chem* **258**:8206-14.
64. **Hicke, L.** 2001. Protein regulation by monoubiquitin. *Nat Rev Mol Cell Biol* **2**:195-201.
65. **Hieronimus, H., and P. A. Silver.** 2003. Genome-wide analysis of RNA-protein interactions illustrates specificity of the mRNA export machinery. *Nat Genet* **33**:155-61.

66. **Ho, Y., A. Gruhler, A. Heilbut, G. D. Bader, L. Moore, S. L. Adams, A. Millar, P. Taylor, K. Bennett, K. Boutilier, L. Yang, C. Wolting, I. Donaldson, S. Schandorff, J. Shewnarane, M. Vo, J. Taggart, M. Goudreault, B. Muskat, C. Alfarano, D. Dewar, Z. Lin, K. Michalickova, A. R. Willems, H. Sassi, P. A. Nielsen, K. J. Rasmussen, J. R. Andersen, L. E. Johansen, L. H. Hansen, H. Jespersen, A. Podtelejnikov, E. Nielsen, J. Crawford, V. Poulsen, B. D. Sorensen, J. Matthiesen, R. C. Hendrickson, F. Gleeson, T. Pawson, M. F. Moran, D. Durocher, M. Mann, C. W. Hogue, D. Figeys, and M. Tyers.** 2002. Systematic identification of protein complexes in *Saccharomyces cerevisiae* by mass spectrometry. *Nature* **415**:180-3.
67. **Hori, T., F. Osaka, T. Chiba, C. Miyamoto, K. Okabayashi, N. Shimbara, S. Kato, and K. Tanaka.** 1999. Covalent modification of all members of human cullin family proteins by NEDD8. *Oncogene* **18**:6829-34.
68. **Irniger, S., and K. Nasmyth.** 1997. The anaphase-promoting complex is required in G1 arrested yeast cells to inhibit B-type cyclin accumulation and to prevent uncontrolled entry into S-phase. *J Cell Sci* **110 (Pt 13)**:1523-31.
69. **Jimeno, S., A. G. Rondon, R. Luna, and A. Aguilera.** 2002. The yeast THO complex and mRNA export factors link RNA metabolism with transcription and genome instability. *Embo J* **21**:3526-35.
70. **Jin, J., T. Cardozo, R. C. Lovering, S. J. Elledge, M. Pagano, and J. W. Harper.** 2004. Systematic analysis and nomenclature of mammalian F-box proteins. *Genes Dev* **18**:2573-80.
71. **Jonkers, W., and M. Rep.** 2009. Lessons from fungal F-box proteins. *Eukaryot Cell* **8**:677-95.
72. **Kamura, T., D. M. Koepf, M. N. Conrad, D. Skowyra, R. J. Moreland, O. Iliopoulos, W. S. Lane, W. G. Kaelin, Jr., S. J. Elledge, R. C. Conaway, J. W. Harper, and J. W. Conaway.** 1999. Rbx1, a component of the VHL tumor suppressor complex and SCF ubiquitin ligase. *Science* **284**:657-61.
73. **Kanemaki, M., A. Sanchez-Diaz, A. Gambus, and K. Labib.** 2003. Functional proteomic identification of DNA replication proteins by induced proteolysis in vivo. *Nature* **423**:720-4.
74. **Kaplan, K. B., A. A. Hyman, and P. K. Sorger.** 1997. Regulating the yeast kinetochore by ubiquitin-dependent degradation and Skp1p-mediated phosphorylation. *Cell* **91**:491-500.
75. **Kashyap, A. K., D. Schieltz, J. Yates, 3rd, and D. R. Kellogg.** 2005. Biochemical and genetic characterization of Yra1p in budding yeast. *Yeast* **22**:43-56.
76. **Katayama, S., K. Kitamura, A. Lehmann, O. Nikaido, and T. Toda.** 2002. Fission yeast F-box protein Pof3 is required for genome integrity and telomere function. *Mol Biol Cell* **13**:211-24.
77. **Katou, Y., Y. Kanoh, M. Bando, H. Noguchi, H. Tanaka, T. Ashikari, K. Sugimoto, and K. Shirahige.** 2003. S-phase checkpoint proteins Tof1 and Mrc1 form a stable replication-pausing complex. *Nature* **424**:1078-83.

78. **Kesti, T., K. Flick, S. Keranen, J. E. Syvaaja, and C. Wittenberg.** 1999. DNA polymerase epsilon catalytic domains are dispensable for DNA replication, DNA repair, and cell viability. *Mol Cell* **3**:679-85.
79. **Kishi, T., A. Ikeda, N. Koyama, J. Fukada, and R. Nagao.** 2008. A refined two-hybrid system reveals that SCF(Cdc4)-dependent degradation of Swi5 contributes to the regulatory mechanism of S-phase entry. *Proc Natl Acad Sci U S A* **105**:14497-502.
80. **Kistler, A. L., and C. Guthrie.** 2001. Deletion of MUD2, the yeast homolog of U2AF65, can bypass the requirement for sub2, an essential spliceosomal ATPase. *Genes Dev* **15**:42-9.
81. **Kloetzel, P. M.** 2001. Antigen processing by the proteasome. *Nat Rev Mol Cell Biol* **2**:179-87.
82. **Koepp, D. M., J. W. Harper, and S. J. Elledge.** 1999. How the cyclin became a cyclin: regulated proteolysis in the cell cycle. *Cell* **97**:431-4.
83. **Koepp, D. M., A. C. Kile, S. Swaminathan, and V. Rodriguez-Rivera.** 2006. The F-box protein Dia2 regulates DNA replication. *Mol Biol Cell* **17**:1540-8.
84. **Koepp, D. M., L. K. Schaefer, X. Ye, K. Keyomarsi, C. Chu, J. W. Harper, and S. J. Elledge.** 2001. Phosphorylation-dependent ubiquitination of cyclin E by the SCFFbw7 ubiquitin ligase. *Science* **294**:173-7.
85. **Kornitzer, D., and A. Ciechanover.** 2000. Modes of regulation of ubiquitin-mediated protein degradation. *J Cell Physiol* **182**:1-11.
86. **Krogan, N. J., G. Cagney, H. Yu, G. Zhong, X. Guo, A. Ignatchenko, J. Li, S. Pu, N. Datta, A. P. Tikuisis, T. Punna, J. M. Peregrin-Alvarez, M. Shales, X. Zhang, M. Davey, M. D. Robinson, A. Paccanaro, J. E. Bray, A. Sheung, B. Beattie, D. P. Richards, V. Canadien, A. Lalev, F. Mena, P. Wong, A. Starostine, M. M. Canete, J. Vlasblom, S. Wu, C. Orsi, S. R. Collins, S. Chandran, R. Haw, J. J. Rilstone, K. Gandi, N. J. Thompson, G. Musso, P. St Onge, S. Ghanny, M. H. Lam, G. Butland, A. M. Altaf-Ul, S. Kanaya, A. Shilatifard, E. O'Shea, J. S. Weissman, C. J. Ingles, T. R. Hughes, J. Parkinson, M. Gerstein, S. J. Wodak, A. Emili, and J. F. Greenblatt.** 2006. Global landscape of protein complexes in the yeast *Saccharomyces cerevisiae*. *Nature* **440**:637-43.
87. **Kubota, Y., Y. Takase, Y. Komori, Y. Hashimoto, T. Arata, Y. Kamimura, H. Araki, and H. Takisawa.** 2003. A novel ring-like complex of *Xenopus* proteins essential for the initiation of DNA replication. *Genes Dev* **17**:1141-52.
88. **Kus, B. M., C. E. Caldon, R. Andorn-Broza, and A. M. Edwards.** 2004. Functional interaction of 13 yeast SCF complexes with a set of yeast E2 enzymes in vitro. *Proteins* **54**:455-67.
89. **Labib, K., J. F. Diffley, and S. E. Kearsley.** 1999. G1-phase and B-type cyclins exclude the DNA-replication factor Mcm4 from the nucleus. *Nat Cell Biol* **1**:415-22.
90. **Labib, K., and A. Gambus.** 2007. A key role for the GINS complex at DNA replication forks. *Trends Cell Biol* **17**:271-8.
91. **Labib, K., J. A. Tercero, and J. F. Diffley.** 2000. Uninterrupted MCM2-7 function required for DNA replication fork progression. *Science* **288**:1643-7.

92. **Lammer, D., N. Mathias, J. M. Laplaza, W. Jiang, Y. Liu, J. Callis, M. Goebel, and M. Estelle.** 1998. Modification of yeast Cdc53p by the ubiquitin-related protein rub1p affects function of the SCFCdc4 complex. *Genes Dev* **12**:914-26.
93. **Lange, A., R. E. Mills, C. J. Lange, M. Stewart, S. E. Devine, and A. H. Corbett.** 2007. Classical nuclear localization signals: definition, function, and interaction with importin alpha. *J Biol Chem* **282**:5101-5.
94. **Lei, E. P., H. Krebber, and P. A. Silver.** 2001. Messenger RNAs are recruited for nuclear export during transcription. *Genes Dev* **15**:1771-82.
95. **Lei, E. P., and P. A. Silver.** 2002. Intron status and 3'-end formation control cotranscriptional export of mRNA. *Genes Dev* **16**:2761-6.
96. **Lengronne, A., and E. Schwob.** 2002. The yeast CDK inhibitor Sic1 prevents genomic instability by promoting replication origin licensing in late G(1). *Mol Cell* **9**:1067-78.
97. **Liakopoulos, D., G. Doenges, K. Matuschewski, and S. Jentsch.** 1998. A novel protein modification pathway related to the ubiquitin system. *EMBO J* **17**:2208-14.
98. **Liang, C., and B. Stillman.** 1997. Persistent initiation of DNA replication and chromatin-bound MCM proteins during the cell cycle in *cdc6* mutants. *Genes Dev* **11**:3375-86.
99. **Lisby, M., R. Rothstein, and U. H. Mortensen.** 2001. Rad52 forms DNA repair and recombination centers during S phase. *Proc Natl Acad Sci U S A* **98**:8276-82.
100. **Liu, Q., M. Z. Li, D. Leibham, D. Cortez, and S. J. Elledge.** 1998. The univector plasmid-fusion system, a method for rapid construction of recombinant DNA without restriction enzymes. *Curr Biol* **8**:1300-9.
101. **Lopes, M., C. Cotta-Ramusino, A. Pellicoli, G. Liberi, P. Plevani, M. Muzi-Falconi, C. S. Newlon, and M. Foiani.** 2001. The DNA replication checkpoint response stabilizes stalled replication forks. *Nature* **412**:557-61.
102. **Lupardus, P. J., T. Byun, M. C. Yee, M. Hekmat-Nejad, and K. A. Cimprich.** 2002. A requirement for replication in activation of the ATR-dependent DNA damage checkpoint. *Genes Dev* **16**:2327-32.
103. **Lupardus, P. J., and K. A. Cimprich.** 2006. Phosphorylation of *Xenopus* Rad1 and Hus1 defines a readout for ATR activation that is independent of Claspin and the Rad9 carboxy terminus. *Mol Biol Cell* **17**:1559-69.
104. **MacDougall, C. A., T. S. Byun, C. Van, M. C. Yee, and K. A. Cimprich.** 2007. The structural determinants of checkpoint activation. *Genes Dev* **21**:898-903.
105. **Maine, G. T., P. Sinha, and B. K. Tye.** 1984. Mutants of *S. cerevisiae* defective in the maintenance of minichromosomes. *Genetics* **106**:365-85.
106. **Majka, J., and P. M. Burgers.** 2003. Yeast Rad17/Mec3/Ddc1: a sliding clamp for the DNA damage checkpoint. *Proc Natl Acad Sci U S A* **100**:2249-54.
107. **Mamnun, Y. M., S. Katayama, and T. Toda.** 2006. Fission yeast Mcl1 interacts with SCF(Pof3) and is required for centromere formation. *Biochem Biophys Res Commun* **350**:125-130.

108. **Maris, C., C. Dominguez, and F. H. Allain.** 2005. The RNA recognition motif, a plastic RNA-binding platform to regulate post-transcriptional gene expression. *Febs J* **272**:2118-31.
109. **Mathias, N., S. Johnson, B. Byers, and M. Goebel.** 1999. The abundance of cell cycle regulatory protein Cdc4p is controlled by interactions between its F box and Skp1p. *Mol Cell Biol* **19**:1759-67.
110. **Mathias, N., S. L. Johnson, M. Winey, A. E. Adams, L. Goetsch, J. R. Pringle, B. Byers, and M. G. Goebel.** 1996. Cdc53p acts in concert with Cdc4p and Cdc34p to control the G1-to-S-phase transition and identifies a conserved family of proteins. *Mol Cell Biol* **16**:6634-43.
111. **Matsuoka, S., B. A. Ballif, A. Smogorzewska, E. R. McDonald, 3rd, K. E. Hurov, J. Luo, C. E. Bakalarski, Z. Zhao, N. Solimini, Y. Lerenthal, Y. Shiloh, S. P. Gygi, and S. J. Elledge.** 2007. ATM and ATR substrate analysis reveals extensive protein networks responsive to DNA damage. *Science* **316**:1160-6.
112. **Mendenhall, M. D., and A. E. Hodge.** 1998. Regulation of Cdc28 cyclin-dependent protein kinase activity during the cell cycle of the yeast *Saccharomyces cerevisiae*. *Microbiol Mol Biol Rev* **62**:1191-243.
113. **Moir, D., S. E. Stewart, B. C. Osmond, and D. Botstein.** 1982. Cold-sensitive cell-division-cycle mutants of yeast: isolation, properties, and pseudoreversion studies. *Genetics* **100**:547-63.
114. **Moyer, S. E., P. W. Lewis, and M. R. Botchan.** 2006. Isolation of the Cdc45/Mcm2-7/GINS (CMG) complex, a candidate for the eukaryotic DNA replication fork helicase. *Proc Natl Acad Sci U S A* **103**:10236-41.
115. **Mu, J. J., Y. Wang, H. Luo, M. Leng, J. Zhang, T. Yang, D. Besusso, S. Y. Jung, and J. Qin.** 2007. A proteomic analysis of ataxia telangiectasia-mutated (ATM)/ATM-Rad3-related (ATR) substrates identifies the ubiquitin-proteasome system as a regulator for DNA damage checkpoints. *J Biol Chem* **282**:17330-4.
116. **Murakami, Y., and J. Hurwitz.** 1993. DNA polymerase alpha stimulates the ATP-dependent binding of simian virus tumor T antigen to the SV40 origin of replication. *J Biol Chem* **268**:11018-27.
117. **Nakayama, K., H. Nagahama, Y. A. Minamishima, M. Matsumoto, I. Nakamichi, K. Kitagawa, M. Shirane, R. Tsunematsu, T. Tsukiyama, N. Ishida, M. Kitagawa, K. Nakayama, and S. Hatakeyama.** 2000. Targeted disruption of Skp2 results in accumulation of cyclin E and p27(Kip1), polyploidy and centrosome overduplication. *Embo J* **19**:2069-81.
118. **Nakayama, K. I., and K. Nakayama.** 2006. Ubiquitin ligases: cell-cycle control and cancer. *Nat Rev Cancer* **6**:369-81.
119. **Nasmyth, K.** 1996. Viewpoint: putting the cell cycle in order. *Science* **274**:1643-5.
120. **Natale, D. A., C. J. Li, W. H. Sun, and M. L. DePamphilis.** 2000. Selective instability of Orc1 protein accounts for the absence of functional origin recognition complexes during the M-G(1) transition in mammals. *EMBO J* **19**:2728-38.

121. **Nguyen, V. Q., C. Co, K. Irie, and J. J. Li.** 2000. Clb/Cdc28 kinases promote nuclear export of the replication initiator proteins Mcm2-7. *Curr Biol* **10**:195-205.
122. **Nguyen, V. Q., C. Co, and J. J. Li.** 2001. Cyclin-dependent kinases prevent DNA re-replication through multiple mechanisms. *Nature* **411**:1068-73.
123. **Nyberg, K. A., R. J. Michelson, C. W. Putnam, and T. A. Weinert.** 2002. Toward maintaining the genome: DNA damage and replication checkpoints. *Annu Rev Genet* **36**:617-56.
124. **Ohta, T., J. J. Michel, A. J. Schottelius, and Y. Xiong.** 1999. ROC1, a homolog of APC11, represents a family of cullin partners with an associated ubiquitin ligase activity. *Mol Cell* **3**:535-41.
125. **Osborn, A. J., and S. J. Elledge.** 2003. Mrc1 is a replication fork component whose phosphorylation in response to DNA replication stress activates Rad53. *Genes Dev* **17**:1755-67.
126. **Paciotti, V., M. Clerici, G. Lucchini, and M. P. Longhese.** 2000. The checkpoint protein Ddc2, functionally related to *S. pombe* Rad26, interacts with Mec1 and is regulated by Mec1-dependent phosphorylation in budding yeast. *Genes Dev* **14**:2046-59.
127. **Palecek, S. P., A. S. Parikh, and S. J. Kron.** 2000. Genetic analysis reveals that FLO11 upregulation and cell polarization independently regulate invasive growth in *Saccharomyces cerevisiae*. *Genetics* **156**:1005-23.
128. **Pan, X., P. Ye, D. S. Yuan, X. Wang, J. S. Bader, and J. D. Boeke.** 2006. A DNA integrity network in the yeast *Saccharomyces cerevisiae*. *Cell* **124**:1069-81.
129. **Pan, Z. Q., A. Kentsis, D. C. Dias, K. Yamoah, and K. Wu.** 2004. Nedd8 on cullin: building an expressway to protein destruction. *Oncogene* **23**:1985-97.
130. **Parrilla-Castellar, E. R., S. J. Arlander, and L. Karnitz.** 2004. Dial 9-1-1 for DNA damage: the Rad9-Hus1-Rad1 (9-1-1) clamp complex. *DNA Repair (Amst)* **3**:1009-14.
131. **Patton, E. E., A. R. Willems, D. Sa, L. Kuras, D. Thomas, K. L. Craig, and M. Tyers.** 1998. Cdc53 is a scaffold protein for multiple Cdc34/Skp1/F-box protein complexes that regulate cell division and methionine biosynthesis in yeast. *Genes Dev* **12**:692-705.
132. **Patton, E. E., A. R. Willems, and M. Tyers.** 1998. Combinatorial control in ubiquitin-dependent proteolysis: don't Skp the F-box hypothesis. *Trends Genet* **14**:236-43.
133. **Paulovich, A. G., and L. H. Hartwell.** 1995. A checkpoint regulates the rate of progression through S phase in *S. cerevisiae* in response to DNA damage. *Cell* **82**:841-7.
134. **Petroski, M. D., and R. J. Deshaies.** 2005. Function and regulation of cullin-RING ubiquitin ligases. *Nat Rev Mol Cell Biol* **6**:9-20.
135. **Piatti, S., T. Bohm, J. H. Cocker, J. F. Diffley, and K. Nasmyth.** 1996. Activation of S-phase-promoting CDKs in late G1 defines a "point of no return" after which Cdc6 synthesis cannot promote DNA replication in yeast. *Genes Dev* **10**:1516-31.
136. **Pickart, C. M.** 2001. Mechanisms underlying ubiquitination. *Annu Rev Biochem* **70**:503-33.

137. **Pickart, C. M.** 1997. Targeting of substrates to the 26S proteasome. *FASEB J* **11**:1055-66.
138. **Pursell, Z. F., I. Isoz, E. B. Lundstrom, E. Johansson, and T. A. Kunkel.** 2007. Yeast DNA polymerase epsilon participates in leading-strand DNA replication. *Science* **317**:127-30.
139. **Reed, S. I.** 2003. Ratchets and clocks: the cell cycle, ubiquitylation and protein turnover. *Nat Rev Mol Cell Biol* **4**:855-64.
140. **Ricke, R. M., and A. K. Bielinsky.** 2005. Easy detection of chromatin binding proteins by the Histone Association Assay. *Biol Proced Online* **7**:60-9.
141. **Ricke, R. M., and A. K. Bielinsky.** 2004. Mcm10 regulates the stability and chromatin association of DNA polymerase-alpha. *Mol Cell* **16**:173-85.
142. **Rondon, A. G., S. Jimeno, M. Garcia-Rubio, and A. Aguilera.** 2003. Molecular evidence that the eukaryotic THO/TREX complex is required for efficient transcription elongation. *J Biol Chem* **278**:39037-43.
143. **Rose, M. D., F. Winston, and P. Hieter.** 1990. *Methods in Yeast Genetics: A Laboratory Course Manual*. Cold Spring Harbor Laboratory Press, Cold Spring Harbor, NY.
144. **Rothstein, R., B. Michel, and S. Gangloff.** 2000. Replication fork pausing and recombination or "gimme a break". *Genes Dev* **14**:1-10.
145. **Rouse, J., and S. P. Jackson.** 2000. LCD1: an essential gene involved in checkpoint control and regulation of the MEC1 signalling pathway in *Saccharomyces cerevisiae*. *EMBO J* **19**:5801-12.
146. **Sanchez, Y., J. Bachant, H. Wang, F. Hu, D. Liu, M. Tetzlaff, and S. J. Elledge.** 1999. Control of the DNA damage checkpoint by chk1 and rad53 protein kinases through distinct mechanisms. *Science* **286**:1166-71.
147. **Santocanale, C., and J. F. Diffley.** 1998. A Mec1- and Rad53-dependent checkpoint controls late-firing origins of DNA replication. *Nature* **395**:615-8.
148. **Sarin, S., K. E. Ross, L. Boucher, Y. Green, M. Tyers, and O. Cohen-Fix.** 2004. Uncovering novel cell cycle players through the inactivation of securin in budding yeast. *Genetics* **168**:1763-71.
149. **Schollaert, K. L., J. M. Poisson, J. S. Searle, J. A. Schwanekamp, C. R. Tomlinson, and Y. Sanchez.** 2004. A role for *Saccharomyces cerevisiae* Chk1p in the response to replication blocks. *Mol Biol Cell* **15**:4051-63.
150. **Schwob, E., T. Bohm, M. D. Mendenhall, and K. Nasmyth.** 1994. The B-type cyclin kinase inhibitor p40SIC1 controls the G1 to S transition in *S. cerevisiae*. *Cell* **79**:233-44.
151. **Schwob, E., and K. Nasmyth.** 1993. CLB5 and CLB6, a new pair of B cyclins involved in DNA replication in *Saccharomyces cerevisiae*. *Genes Dev* **7**:1160-75.
152. **Sclafani, R. A., and T. M. Holzen.** 2007. Cell cycle regulation of DNA replication. *Annu Rev Genet* **41**:237-80.
153. **Seol, J. H., R. M. Feldman, W. Zachariae, A. Shevchenko, C. C. Correll, S. Lyapina, Y. Chi, M. Galova, J. Claypool, S. Sandmeyer, K. Nasmyth, R. J. Deshaies, A. Shevchenko, and R. J. Deshaies.** 1999. Cdc53/cullin and the essential Hrt1 RING-H2 subunit of SCF define a ubiquitin ligase module that activates the E2 enzyme Cdc34. *Genes Dev* **13**:1614-26.

154. **Sheu, Y. J., and B. Stillman.** 2006. Cdc7-Dbf4 phosphorylates MCM proteins via a docking site-mediated mechanism to promote S phase progression. *Mol Cell* **24**:101-13.
155. **Shirahige, K., Y. Hori, K. Shiraishi, M. Yamashita, K. Takahashi, C. Obuse, T. Tsurimoto, and H. Yoshikawa.** 1998. Regulation of DNA-replication origins during cell-cycle progression. *Nature* **395**:618-21.
156. **Shirayama, M., A. Toth, M. Galova, and K. Nasmyth.** 1999. APC(Cdc20) promotes exit from mitosis by destroying the anaphase inhibitor Pds1 and cyclin Clb5. *Nature* **402**:203-7.
157. **Sidorova, J. M., and L. L. Breeden.** 2003. Precocious G1/S transitions and genomic instability: the origin connection. *Mutat Res* **532**:5-19.
158. **Sidorova, J. M., and L. L. Breeden.** 2002. Precocious S-phase entry in budding yeast prolongs replicative state and increases dependence upon Rad53 for viability. *Genetics* **160**:123-36.
159. **Skowyra, D., K. L. Craig, M. Tyers, S. J. Elledge, and J. W. Harper.** 1997. F-box proteins are receptors that recruit phosphorylated substrates to the SCF ubiquitin-ligase complex. *Cell* **91**:209-19.
160. **Skowyra, D., D. M. Koepp, T. Kamura, M. N. Conrad, R. C. Conaway, J. W. Conaway, S. J. Elledge, and J. W. Harper.** 1999. Reconstitution of G1 cyclin ubiquitination with complexes containing SCFGrr1 and Rbx1. *Science* **284**:662-5.
161. **Smolka, M. B., C. P. Albuquerque, S. H. Chen, and H. Zhou.** 2007. Proteome-wide identification of in vivo targets of DNA damage checkpoint kinases. *Proc Natl Acad Sci U S A* **104**:10364-9.
162. **Smothers, D. B., L. Kozubowski, C. Dixon, M. G. Goebel, and N. Mathias.** 2000. The abundance of Met30p limits SCF(Met30p) complex activity and is regulated by methionine availability. *Mol Cell Biol* **20**:7845-52.
163. **Spellman, P. T., G. Sherlock, M. Q. Zhang, V. R. Iyer, K. Anders, M. B. Eisen, P. O. Brown, D. Botstein, and B. Futcher.** 1998. Comprehensive identification of cell cycle-regulated genes of the yeast *Saccharomyces cerevisiae* by microarray hybridization. *Mol Biol Cell* **9**:3273-97.
164. **Stokes, M. P., J. Rush, J. Macneill, J. M. Ren, K. Sprott, J. Nardone, V. Yang, S. A. Beausoleil, S. P. Gygi, M. Livingstone, H. Zhang, R. D. Polakiewicz, and M. J. Comb.** 2007. Profiling of UV-induced ATM/ATR signaling pathways. *Proc Natl Acad Sci U S A* **104**:19855-60.
165. **Strasser, K., and E. Hurt.** 2000. Yra1p, a conserved nuclear RNA-binding protein, interacts directly with Mex67p and is required for mRNA export. *Embo J* **19**:410-20.
166. **Strasser, K., S. Masuda, P. Mason, J. Pfannstiel, M. Oppizzi, S. Rodriguez-Navarro, A. G. Rondon, A. Aguilera, K. Struhl, R. Reed, and E. Hurt.** 2002. TREX is a conserved complex coupling transcription with messenger RNA export. *Nature* **417**:304-8.
167. **Strohmaier, H., C. H. Spruck, P. Kaiser, K. A. Won, O. Sangfelt, and S. I. Reed.** 2001. Human F-box protein hCdc4 targets cyclin E for proteolysis and is mutated in a breast cancer cell line. *Nature* **413**:316-22.

168. **Stutz, F., A. Bachi, T. Doerks, I. C. Braun, B. Seraphin, M. Wilm, P. Bork, and E. Izaurralde.** 2000. REF, an evolutionary conserved family of hnRNP-like proteins, interacts with TAP/Mex67p and participates in mRNA nuclear export. *Rna* **6**:638-50.
169. **Swaminathan, S., A. C. Kile, E. M. MacDonald, and D. M. Koepp.** 2007. Yra1 is required for S phase entry and affects Dia2 binding to replication origins. *Mol Cell Biol* **27**:4674-84.
170. **Takayama, Y., Y. Kamimura, M. Okawa, S. Muramatsu, A. Sugino, and H. Araki.** 2003. GINS, a novel multiprotein complex required for chromosomal DNA replication in budding yeast. *Genes Dev* **17**:1153-65.
171. **Tan, B. C., C. T. Chien, S. Hirose, and S. C. Lee.** 2006. Functional cooperation between FACT and MCM helicase facilitates initiation of chromatin DNA replication. *Embo J* **25**:3975-85.
172. **Tanaka, S., and J. F. Diffley.** 2002. Interdependent nuclear accumulation of budding yeast Cdt1 and Mcm2-7 during G1 phase. *Nat Cell Biol* **4**:198-207.
173. **Tanaka, S., T. Umemori, K. Hirai, S. Muramatsu, Y. Kamimura, and H. Araki.** 2007. CDK-dependent phosphorylation of Sld2 and Sld3 initiates DNA replication in budding yeast. *Nature* **445**:328-32.
174. **Tercero, J. A., and J. F. Diffley.** 2001. Regulation of DNA replication fork progression through damaged DNA by the Mec1/Rad53 checkpoint. *Nature* **412**:553-7.
175. **Tercero, J. A., M. P. Longhese, and J. F. Diffley.** 2003. A central role for DNA replication forks in checkpoint activation and response. *Mol Cell* **11**:1323-36.
176. **Thrower, J. S., L. Hoffman, M. Rechsteiner, and C. M. Pickart.** 2000. Recognition of the polyubiquitin proteolytic signal. *EMBO J* **19**:94-102.
177. **Tong, A. H., G. Lesage, G. D. Bader, H. Ding, H. Xu, X. Xin, J. Young, G. F. Berriz, R. L. Brost, M. Chang, Y. Chen, X. Cheng, G. Chua, H. Friesen, D. S. Goldberg, J. Haynes, C. Humphries, G. He, S. Hussein, L. Ke, N. Krogan, Z. Li, J. N. Levinson, H. Lu, P. Menard, C. Munyana, A. B. Parsons, O. Ryan, R. Tonikian, T. Roberts, A. M. Sdicu, J. Shapiro, B. Sheikh, B. Suter, S. L. Wong, L. V. Zhang, H. Zhu, C. G. Burd, S. Munro, C. Sander, J. Rine, J. Greenblatt, M. Peter, A. Bretscher, G. Bell, F. P. Roth, G. W. Brown, B. Andrews, H. Bussey, and C. Boone.** 2004. Global mapping of the yeast genetic interaction network. *Science* **303**:808-13.
178. **Torres, J. Z., J. B. Bessler, and V. A. Zakian.** 2004. Local chromatin structure at the ribosomal DNA causes replication fork pausing and genome instability in the absence of the *S. cerevisiae* DNA helicase Rrm3p. *Genes Dev* **18**:498-503.
179. **Torres, J. Z., S. L. Schnakenberg, and V. A. Zakian.** 2004. *Saccharomyces cerevisiae* Rrm3p DNA helicase promotes genome integrity by preventing replication fork stalling: viability of *rrm3* cells requires the intra-S-phase checkpoint and fork restart activities. *Mol Cell Biol* **24**:3198-212.
180. **Tsvetkov, L. M., K. H. Yeh, S. J. Lee, H. Sun, and H. Zhang.** 1999. p27(Kip1) ubiquitination and degradation is regulated by the SCF(Skp2) complex through phosphorylated Thr187 in p27. *Curr Biol* **9**:661-4.

181. **Venclovas, C., and M. P. Thelen.** 2000. Structure-based predictions of Rad1, Rad9, Hus1 and Rad17 participation in sliding clamp and clamp-loading complexes. *Nucleic Acids Res* **28**:2481-93.
182. **Verma, R., R. M. Feldman, and R. J. Deshaies.** 1997. SIC1 is ubiquitinated in vitro by a pathway that requires CDC4, CDC34, and cyclin/CDK activities. *Mol Biol Cell* **8**:1427-37.
183. **Wach, A., A. Brachat, R. Pohlmann, and P. Philippsen.** 1994. New heterologous modules for classical or PCR-based gene disruptions in *Saccharomyces cerevisiae*. *Yeast* **10**:1793-808.
184. **Waga, S., and B. Stillman.** 1998. The DNA replication fork in eukaryotic cells. *Annu Rev Biochem* **67**:721-51.
185. **Wakayama, T., T. Kondo, S. Ando, K. Matsumoto, and K. Sugimoto.** 2001. Pie1, a protein interacting with Mec1, controls cell growth and checkpoint responses in *Saccharomyces cerevisiae*. *Mol Cell Biol* **21**:755-64.
186. **Wang, Y., D. Cortez, P. Yazdi, N. Neff, S. J. Elledge, and J. Qin.** 2000. BASC, a super complex of BRCA1-associated proteins involved in the recognition and repair of aberrant DNA structures. *Genes Dev* **14**:927-39.
187. **Wee, S., R. K. Geyer, T. Toda, and D. A. Wolf.** 2005. CSN facilitates Cullin-RING ubiquitin ligase function by counteracting autocatalytic adapter instability. *Nat Cell Biol* **7**:387-91.
188. **Wei, W., N. G. Ayad, Y. Wan, G. J. Zhang, M. W. Kirschner, and W. G. Kaelin, Jr.** 2004. Degradation of the SCF component Skp2 in cell-cycle phase G1 by the anaphase-promoting complex. *Nature* **428**:194-8.
189. **Weissman, A. M.** 2001. Themes and variations on ubiquitylation. *Nat Rev Mol Cell Biol* **2**:169-78.
190. **Wellinger, R. E., F. Prado, and A. Aguilera.** 2006. Replication fork progression is impaired by transcription in hyperrecombinant yeast cells lacking a functional THO complex. *Mol Cell Biol* **26**:3327-34.
191. **Willems, A. R., S. Lanker, E. E. Patton, K. L. Craig, T. F. Nason, N. Mathias, R. Kobayashi, C. Wittenberg, and M. Tyers.** 1996. Cdc53 targets phosphorylated G1 cyclins for degradation by the ubiquitin proteolytic pathway. *Cell* **86**:453-63.
192. **Willems, A. R., M. Schwab, and M. Tyers.** 2004. A hitchhiker's guide to the cullin ubiquitin ligases: SCF and its kin. *Biochim Biophys Acta* **1695**:133-70.
193. **Zegerman, P., and J. F. Diffley.** 2007. Phosphorylation of Sld2 and Sld3 by cyclin-dependent kinases promotes DNA replication in budding yeast. *Nature* **445**:281-5.
194. **Zenkhusen, D., P. Vinciguerra, Y. Strahm, and F. Stutz.** 2001. The yeast hnRNP-Like proteins Yra1p and Yra2p participate in mRNA export through interaction with Mex67p. *Mol Cell Biol* **21**:4219-32.
195. **Zenkhusen, D., P. Vinciguerra, J. C. Wyss, and F. Stutz.** 2002. Stable mRNP formation and export require cotranscriptional recruitment of the mRNA export factors Yra1p and Sub2p by Hpr1p. *Mol Cell Biol* **22**:8241-53.

196. **Zhang, H., R. Kobayashi, K. Galaktionov, and D. Beach.** 1995. p19Skp1 and p45Skp2 are essential elements of the cyclin A-CDK2 S phase kinase. *Cell* **82**:915-25.
197. **Zhou, P., and P. M. Howley.** 1998. Ubiquitination and degradation of the substrate recognition subunits of SCF ubiquitin-protein ligases. *Mol Cell* **2**:571-80.
198. **Zou, L., and S. J. Elledge.** 2003. Sensing DNA damage through ATRIP recognition of RPA-ssDNA complexes. *Science* **300**:1542-8.
199. **Zou, L., D. Liu, and S. J. Elledge.** 2003. Replication protein A-mediated recruitment and activation of Rad17 complexes. *Proc Natl Acad Sci U S A* **100**:13827-32.
200. **Zou, L., and B. Stillman.** 1998. Formation of a preinitiation complex by S-phase cyclin CDK-dependent loading of Cdc45p onto chromatin. *Science* **280**:593-6.

**AMERICAN SOCIETY FOR MICROBIOLOGY LICENSE
TERMS AND CONDITIONS**

Sep 24, 2009

This is a License Agreement between Andrew C Kile ("You") and American Society for Microbiology ("American Society for Microbiology") provided by Copyright Clearance Center ("CCC"). The license consists of your order details, the terms and conditions provided by American Society for Microbiology, and the payment terms and conditions.

All payments must be made in full to CCC. For payment instructions, please see information listed at the bottom of this form.

License Number 2275550415043

License date Sep 24, 2009

Licensed content publisher American Society for Microbiology

Licensed content publication Microbiology and Cellular Biology

Licensed content title Yra1 Is Required for S Phase Entry and Affects Dia2 Binding to Replication Origins

Licensed content author Swarna Swaminathan, Deanna M. Koepf

Licensed content date Jul 1, 2007

Volume 27

Issue 13

Start page 4674

End page 4684

Type of Use Dissertation/Thesis

Format Electronic

Portion Full article

Order reference number

Title of your thesis /

dissertation

Investigation of function and control of Dia2, a regulator of genomic stability in budding yeast

Expected completion date Nov 2009

Estimated size(pages) 200

Total 0.00 USD

Terms and Conditions

Publisher Terms and Conditions

The publisher for this copyrighted material is the American Society for Microbiology (ASM). By clicking "accept" in connection with completing this licensing transaction, you agree that the following terms and conditions apply to this transaction (along with the Billing and Payment terms

and conditions established by Copyright Clearance Center, Inc. ("CCC"), at the time that you opened your Rightslink account and that are available at any time at

<http://myaccount.copyright.com>).

Rightslink Printable License <https://s100.copyright.com/App/PrintableLicenseFrame.jsp?publish...>

1 of 5 9/24/09 4:13 PM

ASM hereby grants to you a non-exclusive license to use this material. Licenses are for one-time use only with a maximum distribution equal to the number that you identified in the licensing process; any form of republication must be completed within 1 year from the date hereof (although copies prepared before then may be distributed thereafter); any permission for electronic format posting is limited to the edition/volume of that online publication. The copyright of all material specified remains with ASM, and permission for reproduction is limited to the formats and products indicated in your license. The text may not be altered in any way without the express permission of the copyright owners.

1.

The licenses may be exercised anywhere in the world.

2.

You must include the copyright and permission notice in connection with any reproduction of the licensed material, i.e. Journal name, year, volume, page numbers, DOI and reproduced/amended with permission from American Society for Microbiology.

3.

The following conditions apply to photocopies:

- a. The copies must be of high quality and match the standard of the original article.
- b. The copies must be a true reproduction word for word.
- c. No proprietary/trade names may be substituted.
- d. No additional text, tables or figures may be added to the original text.
- e. The integrity of the article should be preserved, i.e., no advertisements will be printed on the article.
- f. The above permission does NOT include rights for any electronic reproduction - CD ROM, diskette or in any other format.

4.

The following conditions apply to translations:

- a. The translation must be of high quality and match the standard of the original article.
- b. The translation must be a true reproduction word for word.
- c. All drug names must be generic; no proprietary/trade names may be substituted.
- d. No additional text, tables or figures may be added to the translated text.
- e. The integrity of the article should be preserved, i.e., no advertisements will be printed on the article.
- f. The permission does NOT include rights for any electronic reproduction - CD - ROM, diskette or in any other format.
- g. The translated version of ASM material must also carry a disclaimer in English and in the language of the translation. The two versions (English and other language) of the disclaimer MUST appear on the inside front cover or at the beginning of the translated material as follows:

The American Society for Microbiology takes no responsibility for the accuracy of the translation from the published English original and is not liable for any errors which may occur. No responsibility is assumed, and responsibility is hereby disclaimed, by

5.

Rightslink Printable License <https://s100.copyright.com/App/PrintableLicenseFrame.jsp?publish...>
2 of 5 9/24/09 4:13 PM

the American Society for Microbiology for any injury and/or damage to persons or property as a matter of product liability, negligence or otherwise, or from any use or operation of methods, products, instructions or ideas presented in the Journal. Independent verification of diagnosis and drug dosages should be made. Discussions, views, and recommendations as to medical procedures, choice of drugs and drug

dosages are the responsibility of the authors.

h. This license does NOT apply to translations made of manuscripts published ahead of print as "[ASM Journal] Accepts" papers. Translation permission is granted only for the final published version of the ASM article. Furthermore, articles translated in their entirety must honor the ASM embargo period, and thus may not appear in print or online until 6 months after the official publication date in the original ASM journal.

E-Books must be password protected. E-Book permission is only granted for those requests that meet ASM's definition of an E-Book, as follows: An E-Book is the electronic version of a textbook that can be ordered on-line and used instead of the printed text. Students are given a pass-code and they are allowed to download it once to their desktop. Restricted access means that students are not permitted to share an account. No other electronic book uses are permitted.

6.

While you may exercise the rights licensed immediately upon issuance of the license at the end of the licensing process for the transaction, provided that you have disclosed complete and accurate details of your proposed use, no license is finally effective unless and until full payment is received from you (either by ASM or by CCC) as provided in CCC's Billing and Payment terms and conditions. If full payment is not received on a timely basis, then any license preliminarily granted shall be deemed automatically revoked and shall be void as if never granted. In addition, permission granted is contingent upon author permission, which you MUST obtain, and appropriate credit (see item number 3 for details). If you fail to comply with any material provision of this license, ASM shall be entitled to revoke this license immediately and retain fees paid for the grant of the license. Further, in the event that you breach any of these terms and conditions or any of CCC's Billing and Payment terms and conditions, the license is automatically revoked and shall be void as if never granted. Use of materials as described in a revoked license, as well as any use of the materials beyond the scope of an unrevoked license, may constitute copyright infringement and ASM reserves the right to take any and all action to protect its copyright in the materials.

7.

ASM reserves all rights not specifically granted in the combination of (i) the license details provided by you and accepted in the course of this licensing transaction, (ii) these terms and conditions and (iii) CCC's Billing and Payment terms and conditions.

8.

ASM makes no representations or warranties with respect to the licensed material and adopts on its own behalf the limitations and disclaimers established by CCC on its behalf in its Billing and Payment terms and conditions for this licensing transaction.

9.

You hereby indemnify and agree to hold harmless ASM and CCC, and their respective

10.

Rightslink Printable License <https://s100.copyright.com/App/PrintableLicenseFrame.jsp?publish...>
3 of 5 9/24/09 4:13 PM

officers, directors, employees and agents, from and against any and all claims arising out of your use of the licensed material other than as specifically authorized pursuant to this license.

This license is personal to you, but may be assigned or transferred by you to a business associate (or to your employer) if you give prompt written notice of the assignment or transfer to the publisher. No such assignment or transfer shall relieve you of the obligation to pay the designated license fee on a timely basis (although payment by the identified assignee can fulfill your obligation).

11.

This license may not be amended except in a writing signed by both parties (or, in the case of ASM, by CCC on ASM's behalf).

12.

Objection to Contrary terms: ASM hereby objects to any terms contained in any purchase order, acknowledgment, check endorsement or other writing prepared by you, which terms are inconsistent with these terms and conditions or CCC's Billing and Payment terms and conditions. These terms and conditions, together with CCC's Billing and Payment terms and conditions (which are incorporated herein), comprise the entire agreement between you and ASM (and CCC) concerning this licensing transaction. In the event of any conflict between your obligations established by these terms and conditions and those established by CCC's Billing and Payment terms and conditions, these terms and conditions shall control.

13.

The following terms and conditions apply to Commercial Photocopy and Commercial Reprint requests and should be considered by requestors to be additional terms. All other ASM terms and conditions indicating how the content may and may not be used also apply.

Limitations of Use:

The Materials you have requested permission to reuse in a commercial reprint or commercial photocopy are only for the use that you have indicated in your request, and they MAY NOT be used for either resale to others or republication to the public. Further, you may not decompile, reverse engineer, disassemble, rent, lease, loan, sell, sublicense, or create derivative works from the Materials without ASM's prior written permission.

14.

Revocation: This license transaction shall be governed by and construed in accordance with the laws of Washington, DC. You hereby agree to submit to the jurisdiction of the federal and state courts located in Washington, DC for purposes of resolving any disputes that may arise in connection with this licensing transaction. ASM or

Copyright Clearance Center may, within 30 days of issuance of this License, deny the permissions described in this License at their sole discretion, for any reason or no reason, with a full refund payable to you. Notice of such denial will be made using the contact information provided by you. Failure to receive such notice will not alter or invalidate the denial. In no event will ASM or Copyright Clearance Center be responsible or liable for any costs, expenses or damage incurred by you as a result of a 15.

Rightslink Printable License <https://s100.copyright.com/App/PrintableLicenseFrame.jsp?publish...>
4 of 5 9/24/09 4:13 PM

denial of your permission request, other than a refund of the amount(s) paid by you to ASM and/or Copyright Clearance Center for denied permissions.

v1.4

Gratis licenses (referencing \$0 in the Total field) are free. Please retain this printable

license for your reference. No payment is required.

If you would like to pay for this license now, please remit this license along with your

payment made payable to "COPYRIGHT CLEARANCE CENTER" otherwise you will be invoiced within 30 days of the license date. Payment should be in the form of a check or

money order referencing your account number and this license number 2275550415043.

If you would prefer to pay for this license by credit card, please go to <http://www.copyright.com/creditcard> to download our credit card payment authorization form.

Make Payment To:

Copyright Clearance Center

Dept 001

P.O. Box 843006

Boston, MA 02284-3006

If you find copyrighted material related to this license will not be used and wish to cancel, please contact us referencing this license number 2275550415043 and noting

the reason for cancellation.

Questions? customer care@copyright.com or +1-877-622-5543 (toll free in the US) or

+1-978-646-2777.

Rightslink Printable License <https://s100.copyright.com/App/PrintableLicenseFrame.jsp?publish...>
5 of 5 9/24/09 4:13 PM

ASM Journals Statement of Authors' Rights**Authors may post their articles to their institutional repositories**

ASM grants authors the right to post their accepted manuscripts in publicly accessible electronic repositories maintained by funding agencies, as well as appropriate institutional or subject-based open repositories established by a government or non-commercial entity. Since ASM makes the final, typeset articles from its primary-research journals available free of charge on the ASM Journals and PMC websites 6 months after final publication, ASM recommends that when submitting the accepted manuscript to PMC or institutional repositories, the author specify that the posting release date for the manuscript be no earlier than 6 months after the final publication of the typeset article by ASM.

Authors may post their articles in full on personal or employer websites

ASM grants the author the right to post his/her article (after publication by ASM) on the author's personal or university-hosted website, but not on any corporate, government, or similar website, without ASM's prior permission, provided that proper credit is given to the original ASM publication.

Authors may make copies of their articles in full

Corresponding authors are entitled to 10 free downloads of their papers. Additionally, all authors may make up to 99 copies of his/her own work for personal or professional use (including teaching packs that are distributed free of charge within your own institution). For orders of 100 or more copies, you should seek ASM's permission or purchase access through Highwire's Pay-Per-View option, available on the ASM online journal sites.

Authors may republish/adapt portions of their articles

ASM also grants the authors the right to republish discrete portions of his/her article in any other publication (including print, CD-ROM, and other electronic formats) of which he or she is author or editor, provided that proper credit is given to the original ASM publication. "Proper credit" means either the copyright lines shown on the top of the first page of the PDF version, or "Copyright © American Society for Microbiology, [insert journal name, volume number, year, page numbers and DOI]" of the HTML version. You may obtain permission from Rightslink. For technical questions about using Rightslink, please contact Customer Support via phone at (877) 622-5543 (toll free) or (978) 777-9929, or e-mail Rightslink customer care at customercare@copyright.com.

Please note that the ASM is in full **compliance with NIH Policy**. Back to [Top](#)^
1752 N Street N.W. • Washington DC 20036 202.737.3600 • 202.942.9355 fax •
journals@asmusa.org

Copyright © 2009 by the American Society for Microbiology. For an alternate

route to Journals.ASM.org, visit: <http://intl-journals.asm.org> | [More Info](#)»